AD-A015 421

MECHANISMS OF MAGNETOPLASMADYNAMIC ARC JET ACCELERATION PROCESSES

Gordon L. Cann, et al

Technion, Incorporated

Prepared for:

Air Force Office of Scientific Research

18 August 1975

AFOSR-TR-75-1.0.2.

288108

INTERIM SCIENTIFIC REPORT NUMBER 2

Contract Number F44620-74-C-0017

Covering Period May 1974- May 1975

TECHNION
INCORPORATED
17751 Sky Park East/Suite F/Irvine, CA 92707/(714) 557-8966

UNCLASSIFIED

SECURITY CLASSIFICATION OF THIS PAGE (When Data Entered)

REPORT DOCUMENTATION PAGE

READ INSTRUCTIONS BEFORE COMPLETING FORM

1. REPORT NUMBER [illegible]	2. GOVT ACCESSION NO.	3. RECIPIENT'S CATALOG NUMBER
4. TITLE (and Subtitle) MECHANISMS OF MAGNETOPLASMA DYNAMIC ARC JET ACCELERATION PROCESSES		5. TYPE OF REPORT & PERIOD COVERED INTERIM May 1974 - May 1975 6. PERFORMING ORG. REPORT NUMBER Report No 2
7. AUTHOR(s) GORDON L CANN ADRIANO DUCATI		8. CONTRACT OR GRANT NUMBER(s) F44620-74-C-0017
9. PERFORMING ORGANIZATION NAME AND ADDRESS TECHNION INCORPORATED 17751 SKY PARK EAST/SUITE F IRVINE, CALIFORNIA 92707		10. PROGRAM ELEMENT, PROJECT, TASK AREA & WORK UNIT NUMBERS 681308 9752-02 61102F
11. CONTROLLING OFFICE NAME AND ADDRESS AIR FORCE OFFICE OF SCIENTIFIC RESEARCH/NA 1400 WILSON BOULEVARD ARLINGTON, VIRGINIA 22209		12. REPORT DATE Aug 1975 13. NUMBER OF PAGES 60
14. MONITORING AGENCY NAME & ADDRESS (if different from Controlling Office)		15. SECURITY CLASS. (of this report) UNCLASSIFIED 15a. DECLASSIFICATION/DOWNGRADING SCHEDULE

16. DISTRIBUTION STATEMENT (of this Report)

Approved for public release; distribution unlimited.

17. DISTRIBUTION STATEMENT (of the abstract entered in Block 20, if different from Report)

18. SUPPLEMENTARY NOTES

19. KEY WORDS (Continue on reverse side if necessary and identify by block number)

PLASMA ACCELERATOR
SATELLITE PROPULSION

20. ABSTRACT (Continue on reverse side if necessary and identify by block number)

An extensive series of tests have been conducted in a large (10'X20') vacuum chamber to investigate the feasibility of using the ambient air at a pressure level of 6×10^{-7} to 10^{-4} Torr as propellant in a Space Electric Ram Jet. During most of the tests, a low current discharge (.5 -.05 amps) was used, however performance was also measured under pulsed (high current) conditions. Unambiguous time of flight measurements indicate an exhaust beam velocity of about 40,000 ma/sec under pulsed operation. Beam ion flux rates of up to several milliamperes per square meter were detected 14 ft from the engine when the discharge operated

DD FORM 1 JAN 73 1473 EDITION OF 1 NOV 65 IS OBSOLETE

UNCLASSIFIED

SECURITY CLASSIFICATION OF THIS PAGE (When Data Entered) in the low current mode and probe measurements indicated that they had energies of close to 1000 volts (exhaust velocities 100,000 m/sec). No erosion could be detected on the electrodes after more than 300 firings over a period of 3 days.

TECHNION
INCORPORATED

INTERIM SCIENTIFIC REPORT NUMBER 2

Contract Number F44620-74-C-0017

Covering period May 1974 - May 1975

August 18, 1975

MECHANISMS OF MAGNETOPLASMADYNAMIC ARC JET ACCELERATION PROCESSES

Prepared for:

Air Force Office of Scientific Research
1400 Wilson Boulevard
Arlington, Virginia 22209
Attention: Darrell Blevins/PMD

Prepared by:

Gordon L. Cann, Ph.D.
President and Technical Director

Adriano Ducati
Consultant

TECHNION, INCORPORATED
17751 Sky Park East, Suite F
Irvine, California 92707

Approved by:

Gordon L. Cann

Gordon L. Cann, Ph.D.
President and Technical Director

INTERIM SCIENTIFIC REPORT NUMBER 2

ABSTRACT

An extensive series of tests have been conducted in a large (10' x 20') vacuum chamber to investigate the feasibility of using the ambient air at a pressure level of 6 x 10^{-7} to 10^{-4} Torr as propellant in a Space Electric Ram Jet. During most of the tests, a low current discharge (.5 - .05 amps) was used, however performance was also measured under pulsed (high current) conditions. Unambiguous time of flight measurements indicate an exhaust beam velocity of about 40,000 ma/sec under pulsed operation. Beam ion flux rates of up to several milli-amperes per square meter were detected 14 ft from the engine when the discharge operated in the low current mode and probe measurements indicated that they had energies of close to 1000 volts (exhaust velocities $\approx$100,000 m/sec). No erosion could be detected on the electrodes after more than 300 firings over a period of 3 days.

ic

LIST OF FIGURES

LIST OF FIGURES (continued)

TABLE OF CONTENTS

1. INTRODUCTION

The ability to use the ambient air as propellant in a Space Electric Ram Jet can have very great advantages for low orbit satellite propulsion systems. Experiments that are directed towards finding the best method of accomplishing this have been conducted under this contract over the past 18 months. During a series of tests in a small test cell evacuated to 10^{-8} Torr, a unique type of electrical discharge was obtained and some of its characteristics investigated. The electrodes consist of a cylindrical anode, about 1.3 inches in diameter and 1.3 inches long, a spiral grid, and a centrally located coated tungsten filament. The discharge is initiated by heating the cathode with a current pulse from a condenser bank. This releases the adsorbed mass from the filament as well as a flood of electrons. At potentials of under 1,500 volts between the anode and filament a space charge limited electron current flows that is usually under 20 milli-amperes. At higher potential drops a much higher current is observed (1/2 to 1 1/2 amperes). This current transitions discontinuously down to the space charge limited current at a critical potential difference, which depend primarily upon the initial ambient pressure. It is postulated that a significant fraction of this high current is carried by ions. These ions are produced by inelastic collisions of the high energy electrons with gas atoms released from the cathode as well as with atoms adsorbed on the anode surface.

Some cathode heating occurs from ion bombardment of the filament. However, this is not adequate to form a self-sustaining discharge, hence the discharge current decays to zero as the filament heating current falls off.

There appears to be a rough proportionality between current and voltage in the discharge, with

$$V/I = 3,400$$

when the applied magnetic field is zero.

When a solenoidal magnetic field is applied, several effects occur. The current level decreases as the magnetic field strength increases. This is in accordance with our understanding of current flow perpendicular to a magnetic field. The magnetic field causes the charged particles to spiral around the field lines and thus increases the impedance to current flow between the electrodes. The interaction observed among the discharge current, the filament heating current, and the magnetic field strength is complicated and, at present, not understood. Also, oscillations induced in the discharge current by the magnetic field have been observed and have not been identified.

The small size of the test cell raised the question as to whether the walls of the chamber affected the discharge. This is likely to be so especially when the magnetic field is applied. In order to study the discharge when the walls of the vacuum chamber were large enough to ensure that they could have only negligible influence upon the discharge, an experiment was conducted in a 10' x 20' vacuum chamber. The results of these experiments are reported here.

2. EXPERIMENTAL STUDIES

A series of tests were conducted earlier with an axisymmetric accelerator consisting of an NRC vacuum gauge with a solenoidal magnetic field mounted over it. These tests were conducted in a small evacuated glass chamber ($\approx$ 1 litre volume) and the results are reported in AFOSR-TR-75-0253.

Because of the small volume a strong possibility existed that some interaction could occur between the discharge and the walls of the vessel. Also, the chamber was so small that no accurate measurement of a time of flight could be made to obtain some estimate of the particle velocity in the exhaust beam. Accordingly, a series of tests were planned and conducted in a large volume facility, using the same engine configuration as in the earlier tests and covering the same range of operation parameters.

2.1 Experimental Equipment and Set-Up In the San Diego Tests

A vacuum chamber located at the Convair Aerospace Division of General Dynamics in San Diego was used for the tests. The specifications for the chamber "A" are given in Table I. Because of the time and cost involved in pumping down and repressurizing the chamber, it was decided to accomplish as many tests as possible with only one pumpdown. This required that special precautions be taken to ensure that no malfunction of any part of the electrical or mechanical equipment in the tank could occur.

Duplicate engines were mounted in the tank and four ion detectors were positioned downstream of the source. The placement of these components are shown in Figure 1. A photograph of the duplicate source (engine) is shown in Figure 2. The ion detectors were all identical and a photograph of one is shown in Figure 3.

A great deal of care was taken to maintain the noise level in the detector circuits at a very low level. All electrical connections between the tank and the instrumentation were made with #8 shielded amphenol cable. A special feed-through plate was designed and constructed which ensured that shielding continued through the tank walls and also that no ground loops could occur in the tank. A photograph of the feed-thru plate is shown in Figure 4.

All of the electrical and diagnostic equipment needed for the test was assembled in a mobile laboratory from which all tests were conducted on the site. A schematic of the electric circuit for the ion source (engine) is shown in Figure 5. All the shields for the cables, the chassis and the instrumentation were grounded on a common bus inside the mobile laboratory to minimize ground loop effects.

The circuits for the ion detectors were designed to measure accurately picoamperes of beam current impinging on the detector faces. The circuits used are shown schematically in Figure 6. The detector consisted of a thin wall outer cylindrical nickel electrode 3 cm in diameter by 2 cm long and a central solid copper electrode 1 cm in diameter and 2 cm long. These electrodes were rigidly mounted in a plexiglass plate and the electrical connections to the leads were buried in the plexiglass. The polarity was such that the outer electrode would collect ions and the inner one the electrons.

2.2 Experimental Results from San Diego Tests

During a period of 3 days over 300 data points were taken. The first series of tests were conducted to determine the relation between the discharge current and voltage when no mangetic field was applied. Typical current-voltage traces are shown in Figure 7, a,b,c.

In Figure 7b, picture 18, a breakdown is seen to occur when the capacitor was charged to only 2500 volts. Incipient breakdowns are also seen in Figure 7c. Originally, it was thought that these breakdowns were occurring at the high-voltage feedthroughs, since no breakdowns had been observed in the small volume device, even at potential differences of 8,000 volts. However, subsequent tests combined with a detailed examination of the current voltage traces lead to the conclusion that the breakdown is almost certainly occurring between the electrodes of the engine. It is tentatively assumed that this breakdown is associated with the formation of cathode spots.

A series of current voltage traces are presented next in Figure 8a,b,c,d for increasing magnetic field strength. As the field is increased in strength, the peak current is reduced and the length of the current pulse increased.

The signals from two ion current probes, numbers 3 and 4 are shown in Figure 9a,b,c, for different potential drops between the electrodes on the probe. A number of observations can be made.

a) For low potential drops the signal is negative.

b) The signal appears to last only during the time that the discharge current is increasing.

c) The signals appear to have come 60 hz. modulation in them.

d) The signal strength becomes assymtotic as the potential across the collector electrodes is increased.

The signals from two probes were monitored as the magnetic field strength was increased in the next series of tests. Representative signal traces are shown in Figure 10a,b,c. The signal strength continued to increase as the magnetic field strength was increased.

In the final test series the discharge current voltage traces as well as the probe traces were monitored as the ambient pressure was increased. Signal traces are shown in Figure 11a, b,c,d,e. for various pressures. At the higher pressure end, the discharge current and probe signals develop some high frequency oscillations. It is possible that these oscillations are associated with volume ionization processes. Also, it should be noted that the duration of the probe signals increases with the ambient pressure, so that atpressures of over 5 x 10^{-5} torr. the probe signals persist throughout the total time of the discharge. A high speed picture of the oscillations on the probe signals are shown in Figure 12. The frequency of the occillations is close to 6,000 hz.

Many attempts were made to obtain a time of flight measurement for the ions between two of the probes. The only time that unambiguous signals were obtained was when the discharge broke down. Two such traces are shown in Figure 13.

Although great care was exercised to ensure that the engine test configuration for the San Diego test be identical to that of the engine used in the small test cell, some differences did occur:

a) The long cables in the San Diego test had a significant resistance so that more energy was required in the filament capacitor to obtain the same filament temperature.

b) The connectors at the terminals of the pins from the NRC ionization gauge were potted in epoxy for the San Diego tests. This reduced the interelectrode resistance to 10^{9} ohms. Ordinarily, this should not have much influence upon the performance. However, some surprising differences were noted and they are investigated in the next section.

2.3 Experiments to Determine the Influence of the Grid Electrode

An NRC ionization gauge type 507 was used as the ion source in all of the experiments discussed in this and in the previous report AFOSR-TR-75-0253. This gauge consists of a thin nickel cylindrical electrode 1.4" in diameter and 1.4" long. A tungsten wire is wound into a 9 turn helix of .45" diameter to form a grid electrode. Near the centerline a V-type oxide coated filament is supported at one end from 2 posts and held taut by a spring wire at the other end.

During all of the tests reported the grid electrode was left floating. However, in the San Diego tests all of the electrode connections extending through the gauge tube were potted in epoxy, giving an interelectrode resistance in the order of 10^9 ohms.

In order to assess what role, if any, is played by the grid in determining the current-voltage characteristics of the discharge, a series of tests were conducted using the discharge tube in the one litre evacuated chamber. In the first series no magnetic field was used, the $4\mu f$ discharge capacitor was charged up to 4000V and the filament was heated with the .06 farad capacitor bank charged to 30 volts. The results are shown in Figure 14.

- on trace #8 the grid was left floating
- on trace #10, the grid was connected to the anode
- on trace #11, the grid was connected to the cathode

- on trace 12, the grid was connected to the cathode as in #11, but the current gain was increased and the sweepspeed reduced.

A second series of tests was conducted to investigate the influence upon the discharge of connection of an external resistance between the filament and the grid. All connections between the ion source and the laboratory equipment were made through the cables used at San Diego, including the feed through plate. This required that the filament capacitor bank be charged to about 36V instead of 30V to get comparable cathode heating. The results are shown in Figure 15.

- in picture #1 the grid was left floating
- in picture #2 the grid and one side of the filament at the discharge tube used in the San Diego tests was connected in parallel with the grid and filament of the discharge tube in the one litre chamber
- in picture #3, the connections were identical to those in picture #2, only the sweep speed was reduced. This picture also helps to indicate the reproducibility of the measurement
- in picture #4 a 10 resistor was connected externally between the grid and filament.

A third series of tests were conducted at a lower discharge voltage with the capacitor being charged to 2000V. All connections between the ion source and the laboratory equipment was made through the cables used at San Diego, including the feed-through plate. The filament capacitor bank was hence charged to 35 volts. The results are shown in Figure 16.

- on trace #1 the grid was left floating
- on trace #2 a 10^9 ohm resistor was connected between the grid and the filament
- on trace #3 the grid and one side of the filament from the discharge tube used in the San Diego tests were placed in parallel with the grid and filament of the discharge tube in the one litre chamber.
- on trace #4 a trace from the tests at San Diego fired under identical conditions is shown for comparison.

2.4 Data Correlation and Discussion of Results

Since the phenomena being investigated are novel, correlation parameters are not readily available. However, whenever possible we will attempt to present the data in such a form that it can be related to familiar physical phenomena.

2.4.1 Current-Voltage Characteristics vs Applied Magnetic Field

Typical current-voltage curves are plotted in Figure 17. The space-charge limited current curve, as determined from measurements on the small 1 litre device, is indicated. The current rises to a value 8-10 times as high as this current and then decays along a curve roughly parallel to the space charge curve. This can be expressed analytically as

$$I = 9 I_o \left(\frac{V}{V_o} \right)^{3/2}$$

$$= 9 \times .026 \left(\frac{V}{1000} \right)^{3/2} \qquad 2\text{-}1$$

$$= .234 \left(\frac{V}{1000} \right)^{3/2}$$

The peak current is not regular and can vary widely for the same initial conditions. This is probably due to the amount of air adsorbed on the anode being different from firing to firing. At times, breakdown occurred with the capacitor charged to only 2500 volts, at other times a 'normal' discharge would occur when the capacitor was charged to 4000V. The amount of scatter that occurs can be seen in Figure 18. Some reference curves are shown to indicate the relative magnitude of the impedance of the discharge.

Several major differences can be noted between these results and those obtained in the small test cell. The voltage at which the current discontinuity occurs here is 300-400 volts. In the small test cell it was 1400-2000 volts. After in the scope traces from this series of tests, oscillations in current occur at the current discontinuity, whereas none were observed in the tests in the small test cell. As noted earlier, breakdowns occurred fairly often at relatively low discharge potentials in the tests at San Diego; only rarely did breakdown occur in the small test cell.

The current is higher than the space charge limited current because of space charge neutralization by ions. It is assumed that these are ions of oxygen and nitrogen, produced on the anode surface by electron bombardment of the adsorbed layer. Depletion of the layer reduces the ion production rate and is responsible for the current peaking and then decaying. If the layer is dense and perhaps many atoms thick, then the current continues to build up and can lead to breakdown. Since the true breakdown current is hundreds of amperes, it is postulated that a cathode spot forms on the filament.

2.4.2 Current-Voltage Characteristics-Applied Magnetic Field

As can be seen from the scope traces in Figure 8, applying a solenoidal magnetic field profoundly affects the discharge current. The following effects are noted:

- the peak current continues to drop as the magnetic field strength is increased
- a time interval develops during which the current rises slowly even though the potential is dropping.

This time interval increases as the magnetic field strength is increased.

- the total time between discharge initiation and current cut-off increases as the magnetic field strength is increased
- some relatively low frequency, low amplitude oscillations develop during the period of slow current rise. The frequency is approximately 425 hz
- small bursts of much higher frequency oscillations occur at the higher magnetic field strengths
- the discontinuity in current becomes larger as the magnetic field strength is increased
- when the magnet capacitor is charged to over 45 volts (peak magnetic field of about .0750 Tesla)

a low current "breakdown" occurs, rather late in the discharge. The peak "breakdown" current increases as the magnetic field strength is increased

- the current rise rate before breakdown is much smaller than expected, indicating the onset of some new phenomenon at some critical magnetic field strength
- on the traces where the low current breakdown is observed the ion current measured on the downstream detectors decreased at least an order of magnitude. This, and the previous observation could be interpreted to mean that both ion production and acceleration downstream has ceased. If this is so, however, the low current "breakdown" must represent the onset of ion production with no downstream acceleration, since no signals were received on the downstream detectors at the time of the "breakdown".

Some of the gross effects of the magnetic field upon the discharge are summarized in Figure 19. The "average" impedance of the discharge is seen to rise about a factor of 3-4 over the range shown and the peak current is decreased about a factor of 5-6. The Δ t used in preparing Figure 19 was the time between the shoulder of the curve rise curve (at $\simeq$ 35m sec) and the current discontinuity.

The magnetic field strength was measured with a gaussmeter and found to be .00325 Tesla/amp. This combined with a measurement of the magnet current as a function of time permits the determination of the instantaneous magnetic field strength. This is presented in Figure 20.

The discharge impedance during current rise is shown in Figure 21 as a function of the magnetic field strength for various times from initiation of the discharges. While the impedance is seen to increase with the magnetic field strength, it also appears to decrease as a function of time. It should be noted that this cannot be due to the fact that the magnetic field strength is decreasing with time, since the instantaneous values of the magnetic field strength were used in plotting the data. A similar plot is shown in Figure 22 for the time when the current is decaying. Since some process dependent upon time appears to be important in determining the impedance of the discharge the time at which peak current occurs was investigated and its dependence upon the magnetic field strength is shown in Figure 23. A number of efforts were made to find correlation parameters. The best is shown in Figure 24. During current rise the quantity Vt/I is found to be a monatonic function of the applied magnetic field strength. During current decay, the quantity Vt_M/I is approximately the same monatonic function of the magnetic field. It should be emphasized that this is purely an empirical correlation and is only approximate. However, some speculation regarding the time dependent process occurring during current build-up cannot be avoided. Some candidates are:

- the filament temperature is increasing due to the combined effects of filament and discharge current. This provides more electron emission and consequently the current rises.
- the ion production rate is increasing with time and the current build-up is primarily ion current. In this regard, for reasonably strong magnetic field strengths (over 0.03 Tesla), the current starts out considerably below the space charge limited current at 35 milli-sec and increases to peak values several times greater than the space charge limited current.

2.4.3 Ion Current Detector Signals

The ion current probes were designed to measure the ion flux rate impinging on the detector cross-section. Instrumentation requirements necessitated, unfortunately, that the probes be connected, through the input impedance of the scope to the same ground point to which the cathode of the ion source was connected. If the plasma produced by the source was dense enough to permit a conducting path between the source and the detector, then signals could occur that need not be representative of the ion beam current. Signals could result from any one of the 4 following phenomena:

- a plasma beam impinges on the detector. The electrons are collected on the central electrode and the ions are collected on the outer cylindrical electrode. A positive signal results.
- the plasma is dense and is tied to ground potential, thus grounding both electrodes of the detector. A positive signal results.
- the plasma is dense and is tied to the anode potential of the source, thus raising the detector electrode to a high positive potential. A negative signal results.
- when the ion energy exceeds the potential across the detector electrodes, ions can bombard the central electrode and be neutralized by secondary electron emission. A negative signal results.

There are probably other sources of signals, such as noise, pick-up in the leads, etc.

Since the tank was grounded it is likely that the plasma would come closer to ground potential than any other. This would rule out negative signals resulting from a plasma at a high positive potential. On the other hand, any signals resulting from the plasma tending to ground the detector electrodes would not depend upon the magnitude of the resistance in the detector circuit. Since measurements indicated the signals were proportional to this resistance, we will tentatively assume that plasma shorting effects did not occur. This leads to the following interpretation:

- positive signals measure the plasma beam flux rate upon the detector.
- negative signals indicate bombardment of the central electrode by high energy ions.

Two detectors were monitored simultaneously on the scope. In order to get maximum sensitivity they were connected so that a positive signal deflected the upper trace downward and the lower trace upward.

A standard operating point was chosen and the signal measured on probes 3 and 4 as the potential between the electrodes was increased. The results are shown in Figure 25. For low potential differences the signals are negative, indicative of bombardment of the central electrode by high energy ions. As the potential difference is increased the signal reverses and its magnitude rises until it becomes asymtotic at about 1000V potential between the probe electrodes. It is not immediately clear why the signal from probe 4 is larger than that from probe 3 which is nearer to the source. This is probably because probe 2 is in the line of signt between the source and probe 3. An alternate explanation could be that the beam is denser off-axis. Because of the angular momentum in the beam this could be the case. The maximum signal on probe 4 is indicative of an ion flux of:

$$j = \frac{V_{probe}}{R\ A_{probe}}$$

$$= \frac{.32}{10^6 \times 707 \times 10^{-4}} \quad \frac{\text{amps}}{m^2}$$

$$= .45 \ \frac{\text{m.a.}}{m^2}$$

In Figure 26 the probe signal is shown as a function of the applied magnetic field strength. The signal is seen to rise rapidly as the strength of the magnetic field is increased. The maximum signal on probe 4 is indicative of an ion flux rate of

$$j = \frac{1.6 \times 10^{+3}}{10^6 \times 7.07 \times 10^{-4}} \quad \frac{\text{m.a.}}{m^2} \quad = \ 2.3 \ \frac{\text{m.a.}}{m^2}$$

Towards the end of the testing period the tank pressure was slowly increased and measurements taken every half decade in pressure. The current-voltage characteristics did not change significantly until a pressure of over 3 x 10^{-5} Torr was reached. At that point high amplitude, high frequency oscillations occurred in the discharge current. These oscillations were also observed in the probe signals. The magnitude of the probe signals increased with the pressure as is seen in Figure 27. The peak signal on probe 4 is indicative of an ion density of

$$j = \frac{6.5 \times 10^3}{7.07 \times 10^{-4} \times 10^6} \quad \frac{\text{m.a.}}{m^2} \quad = \ 9.2 \ \frac{\text{m.a.}}{m^2}$$

At the lowest pressure the signal on the probes lasted for only about 40-60 milliseconds after the initiation of the discharge currents whereas the discharge lasted for about 140 milliseconds. As the pressure was increased, the length of the signal, as well as its magnitude, increased. Once the high frequency oscillations started the probe signal lasted as long as the discharge current.

The significance of the 60 hz noise on the probe traces is not understood and is being investigated.

2.4.4 Time of Flight Measurement

Many efforts were made to make a time of flight measurement using the probe signals. Most of these were done using probes 1 and 4, which were separated by 4.27 meters. If the beam velocity were equivalent to ions with and energy of 1000 volts the velocity would be

$$v = \left(\frac{2|e|\,V}{m_I}\right)^{1/2}$$

$$= \left(\frac{2 \times 1.6 \times 10^{-19} \times 1000}{14 \times 1.67 \times 10^{-27}}\right)^{1/2}$$

$$= 117000\,\frac{m}{sec}$$

The time of flight would be

$$= \frac{4.27}{117000}$$

$$= 36.5\,\mu.\text{sec.}$$

When no breakdown occurred, there was never any sharp enough signal to use for a time of flight measurement. However, some fairly unambiguous signals were obtained when breakdown occurred. It should also be noted that these signals were of a very high amplitude (10^3 larger than without breakdown). A time of flight of about 100 μsec. is indicated on picture #93 of Figure 13.

$$v = \frac{4.27}{10^{-4}}$$

$$= 42{,}700 \ \frac{m}{sec}$$

This is equivalent to a specific impulse of 4360 sec. The particle energy (assuming a nitrogen ion) is

$$V = \frac{mv^2}{2|e|} = 133 \text{ volts.}$$

2.4.5 The Influence of the Grid Upon the Discharge Characteristics

The phenomena observed here are very puzzling and considerably more work is needed to clarify the physics. The observations can be summarized as follows:

- in the small test cell whenever the filament is connected to the grid through any resistance from 0 to 10^9 ohms, the discharge is suppressed and only the space charge limited current flows (See Figs. 14, 15, 16 and 17).
- when the filament and grid from the source used in San Diego are connected in parallel across the filament and grid of the sources in the small test cell, the discharge is suppressed and only space charge limited current flows, even at applied potentials of 4000V.
- when the grid is shorted to the anode the peak current is increased by about a factor of 2 and decays along a curve parallel to the space charge neutralized current but at a current level about 30 times higher (see Fig. 17).

No experiments were conducted during the San Diego tests with the grid. It was floating at all times, except for some high resistance path to the plate or filament through the epozy in which all leads were potted.

3. CONCLUSIONS

1. A discharge occurred without fail every time the filament was impulsively heated.
2. The impedance of the discharge was significantly lower than occurred during the tests in the small glass chamber at Technion.
3. Large ion and electron flow rates (beam plasma) were found to occur 15' downstream of the accelerator. From the measurements of detector (probe) current versus the probe potential difference, it was deduced that the particle energy in the beam exceeded several hundred electron volts.
4. Breakdown was observed to occur many times at San Diego, when either the discharge potential or the magnetic field strength was increased beyond rather modest values. A large pulse of plasma was accelerated downstream at a velocity of about 45,000 m/sec when breakdown occurred. The current that flows during breakdown has not been accurately measured.
5. Time of flight measurements made when breakdowns occurred indicated that the beam particles had an axial velocity of over 40,000 m/sec.
6. At the typical conditions chosen for many of the tests the discharge current flows for about 140 milliseconds. At an ambient pressure of 6×10^{-7}

Torr, the beam current, as measured by probe 4, 15 ft (4.27m) from the source, lasted only 40-60 milliseconds. As the pressure was increased to 10^{-4} Torr the duration of the beam current signal increased in length until it lasted as long as the discharge.

7. Considerable scatter in the current-voltage characteristics of the discharge occurred when all controllable electrical parameters were kept identical. This is attributed to the variability of the surface coverage of adsorbed air. For example, with an applied discharge potential of 3000V the peak current varied from .52 amperes to .85 amperes to breakdown. During the tests, no attempt was made to control or monitor the time between pulses hence large variations in surface coverage could occur from point to point.

A number of important differences in the discharge characteristics occurred between the tests conducted in San Diego and those conducted in the small chamber at Technion. These are listed below.

1. The impedance of the discharge, when no magnetic field was applied, was lower in the San Diego tests.
2. When a solenoidal magnetic field was applied, the impedance of the discharge increased much

more rapidly at San Diego than at Technion.

3. The critical voltage for discharge extinction was much lower at San Diego than at Technion.

4. Once the discharge extinguished at Technion a thermionic current of 10-25 m.a. continued to flow for many milliseconds at Technion. In San Diego, there appeared to be no current flow after discharge extinction.

5. The discharge tube was potted in epoxy for the San Diego tests. This resulted in an impedance of 10^9-10^{11} ohms between the filament and the grid of the discharge tube. At Technion the pins from the grid were exposed to air and the impedance between the filament and grid was probably several orders of magnitude higher.

6. When the grid to filament impedance of the San Diego discharge tube was connected in parallel to the grid and filament of the tube at Technion, the discharge was radically altered. The peak current was reduced by about a factor of 4-5 and no current discontinuity occurred. No condition could be found under which the discontinuity would occur although the discharge capacitor and charging voltage were varied over a wide range.

FIG. 1 EXPERIMENTAL ARRANGEMENT IN VACUUM CHAMBER AT CONVAIR

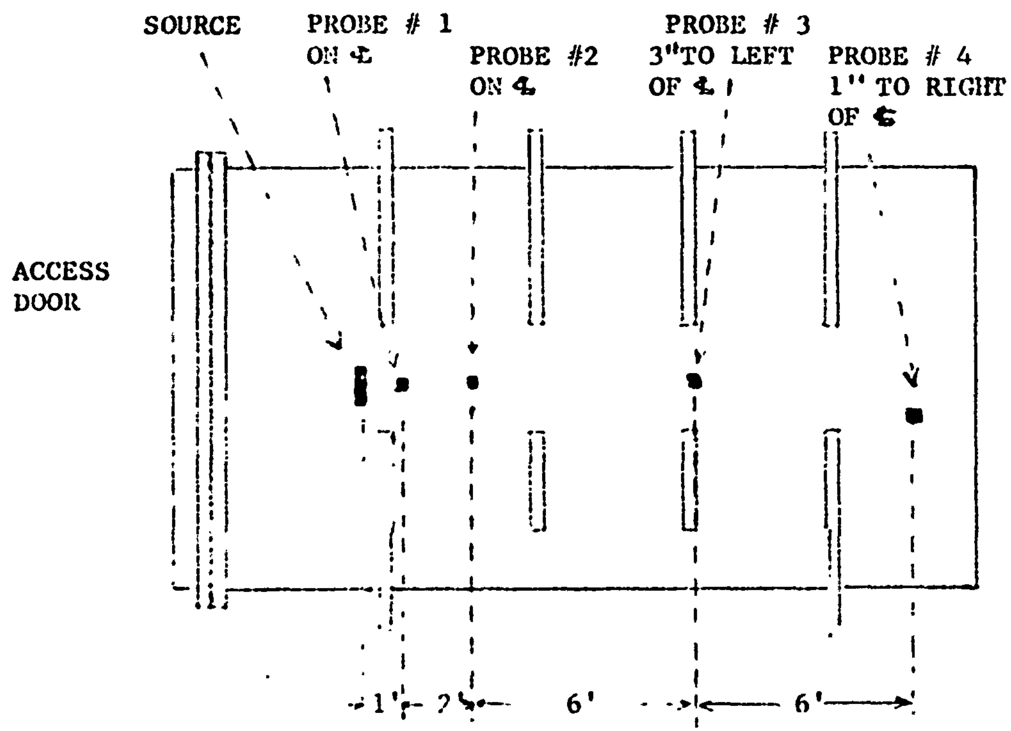

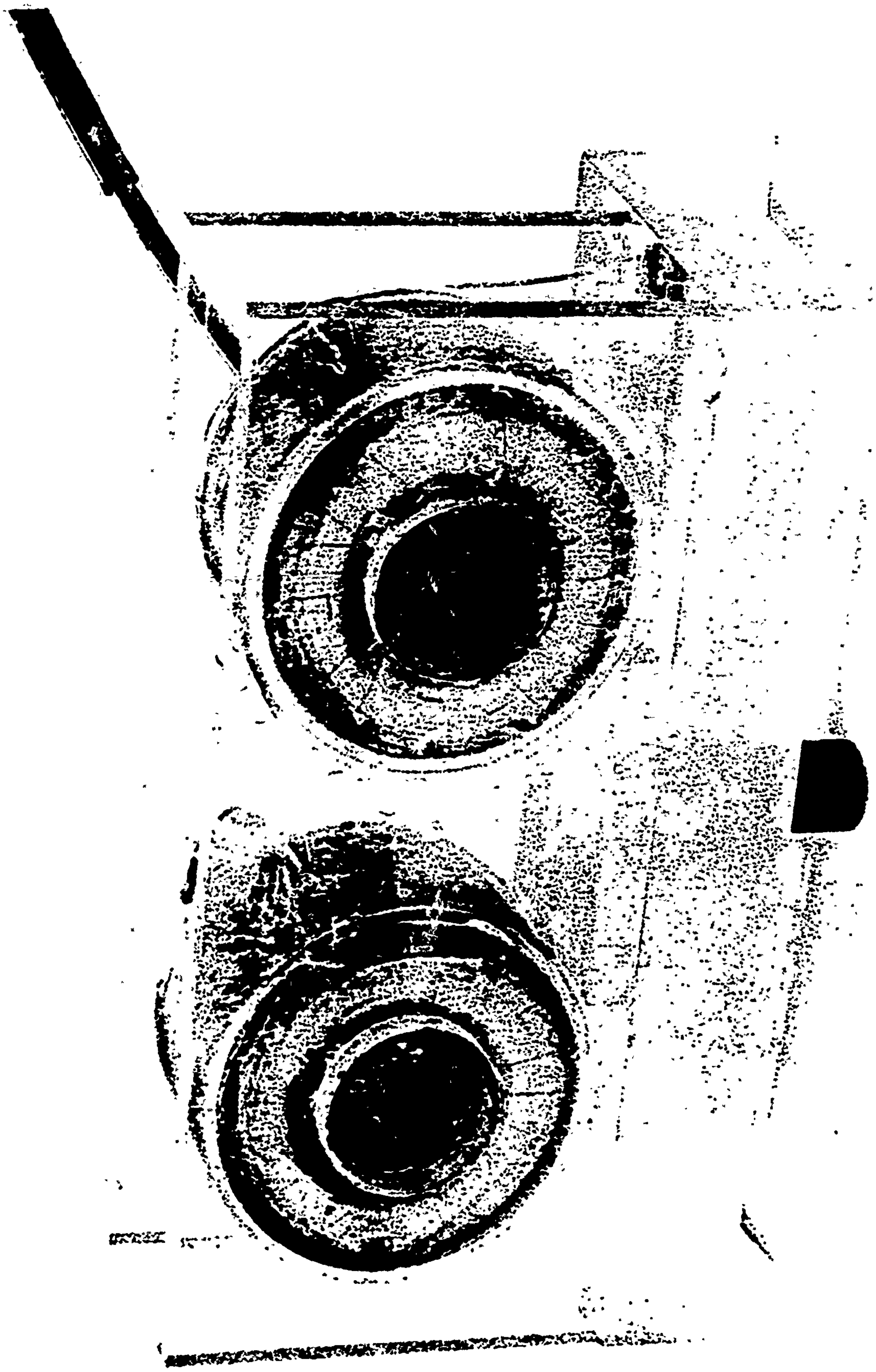

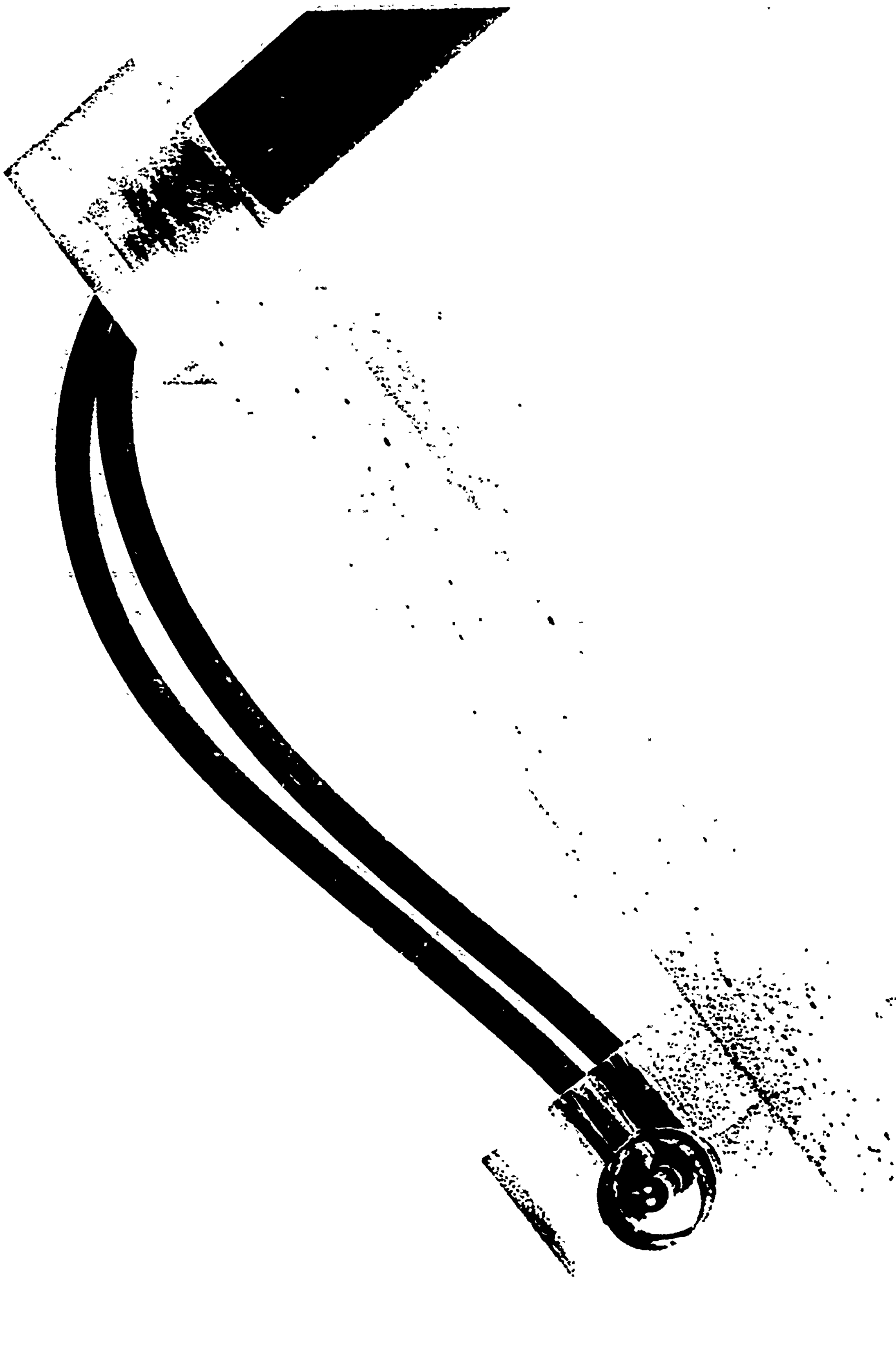

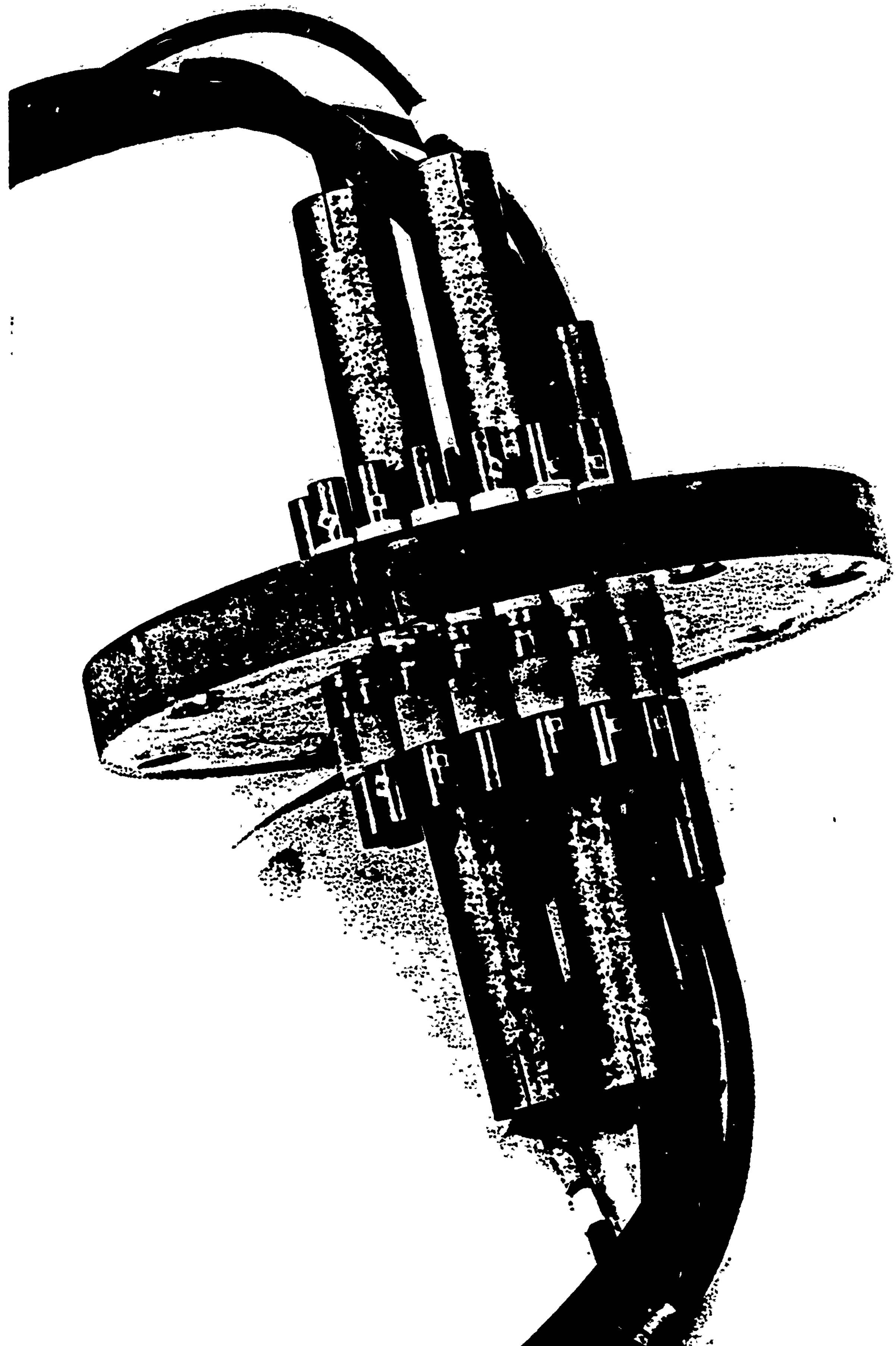

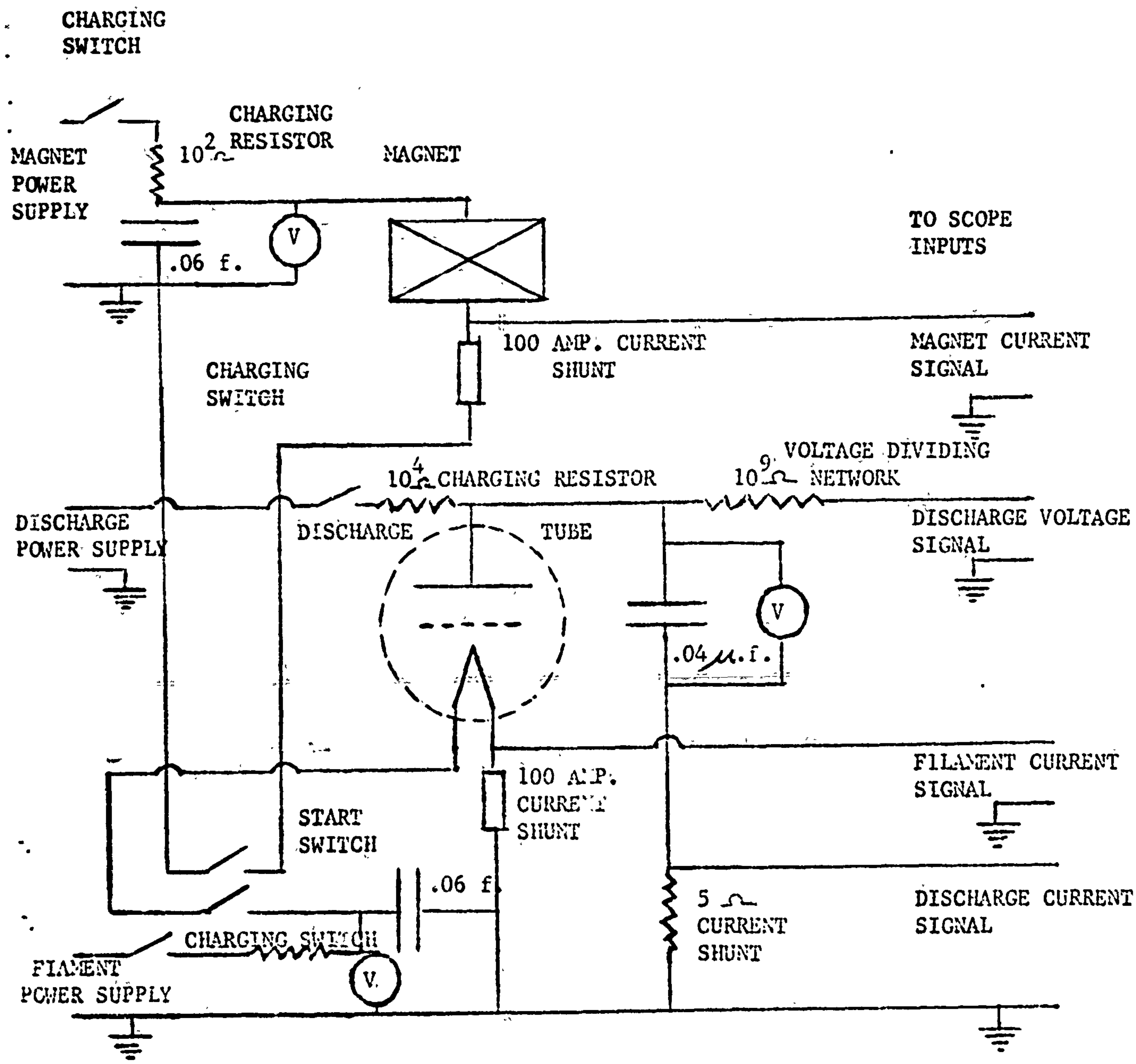

FIG. 5 SCHEMATIC OF DISCHARGE TUBE ELECTRIC CIRCUIT.

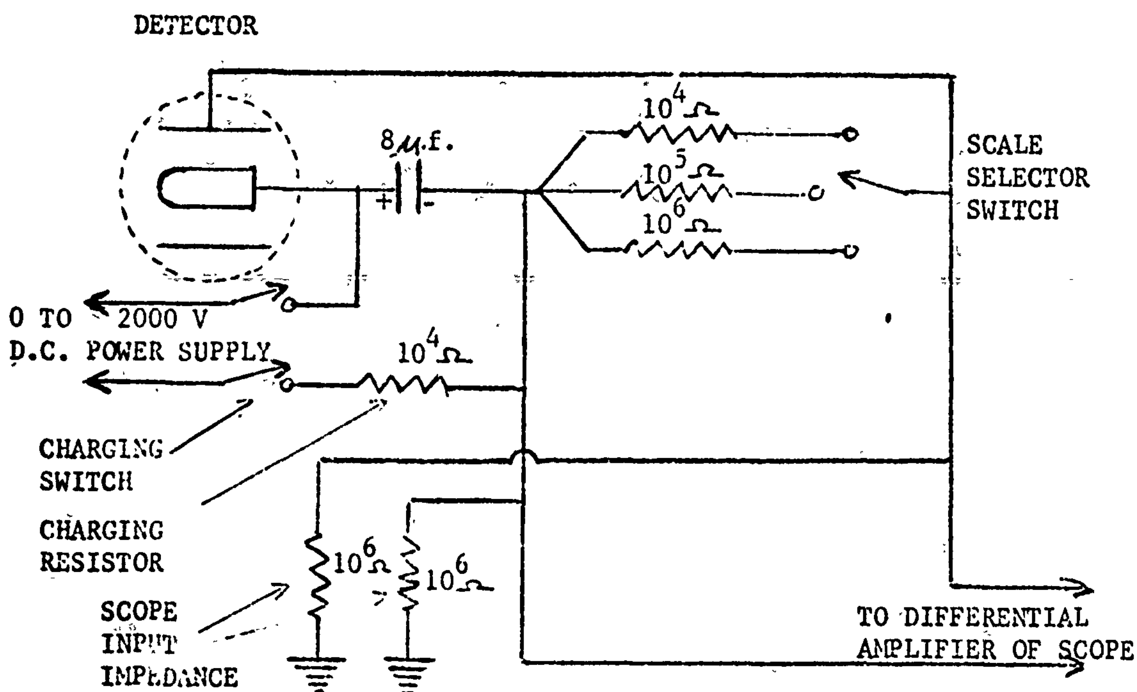

FIG. 6 SCHEMATIC OF DETECTOR CIRCUIT.

Date 1-28-75 Experiment ______

Picture # 15

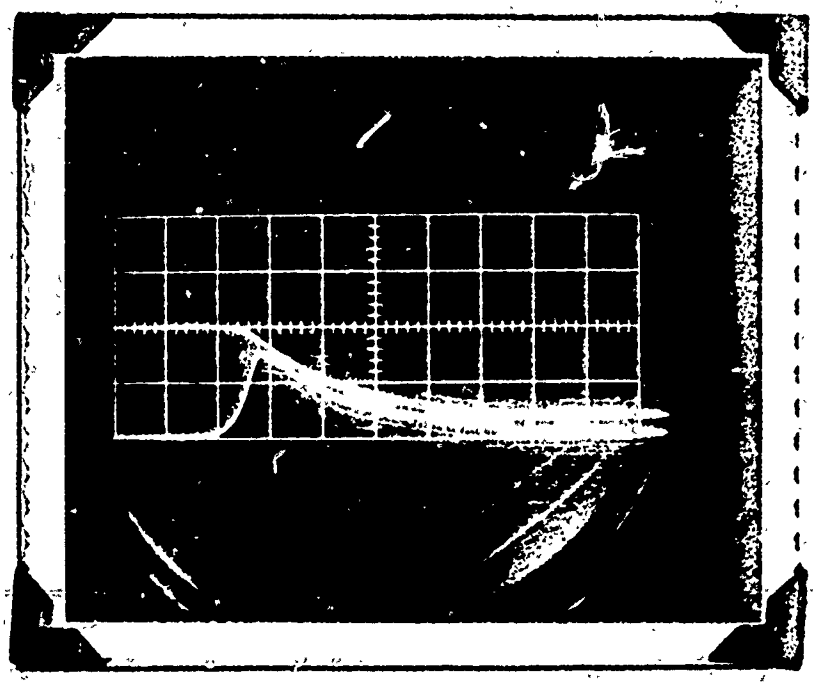

Capacitor
Charging
Voltages

Discharge 1,000 V
Filament 35 V
Magnet 0 V

Upper Trace

Signal Discharge Voltage
Ampl/cm. 500 V
Time/cm. 10 m. sec.

Lower Trace

Signal Discharge Current
Ampl/cm. 100 m.a.
Time/cm. 10 m. sec.

Discharge Capacitor 4 μf

Pressure = 4.6 x 10^{-7} Torr.

Picture # 16

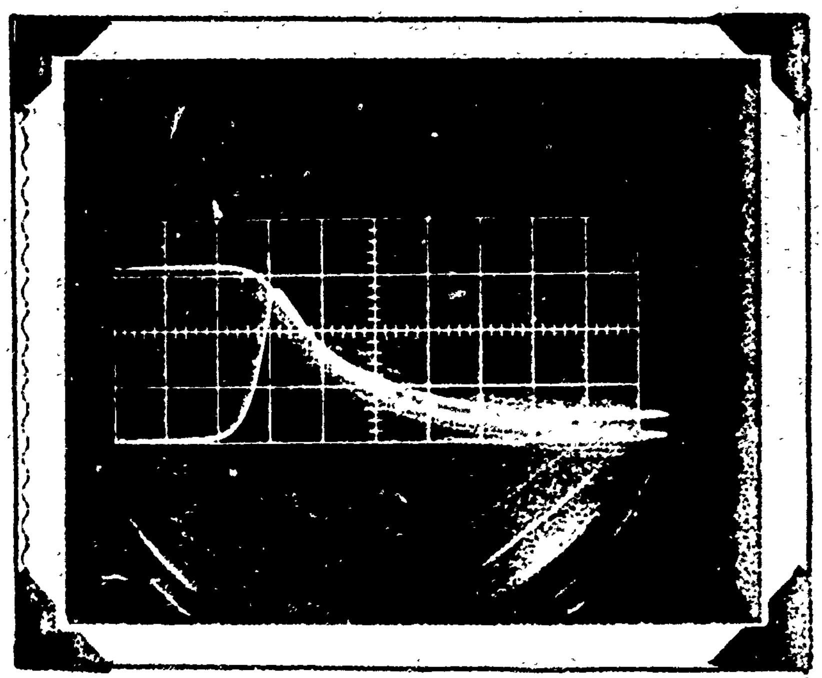

Capacitor
Charging
Voltages

Discharge 1,500 V
Filament 35 V
Magnet 0 V

Upper Trace

Signal Discharge Voltage
Ampl/cm. 500 V
Time/cm. 10 m. sec.

Lower Trace

Signal Discharge Current
Ampl/cm. 100 m.a.
Time/cm. 10 m. sec.

Discharge Capacitor 4 μf

Pressure = 4.6 x 10^{-7} Torr.

Figure 7a. Characteristic Current-Voltage Traces-
No Applies Magnetic Field.

Date 1-28-75 Experiment

Picture # 17

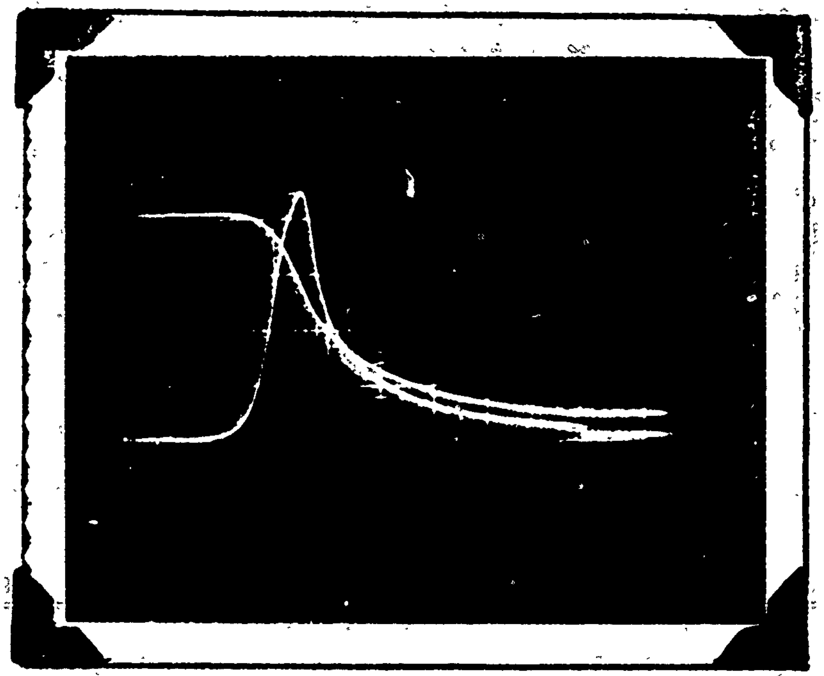

Capacitor Charging Voltages

Discharge 2,000 V
Filament 35 V
Magnet 0 V

Upper Trace

Signal Discharge Voltage
Ampl/cm. 500 V
Time/cm. 10 m. sec.

Lower Trace

Signal Discharge Current
Ampl/cm. 100 m.a.
Time/cm. 10 m. sec.

Discharge Capacitor 4 μf.

Pressure = 4.6×10^{-7} Torr.

Picture # 18

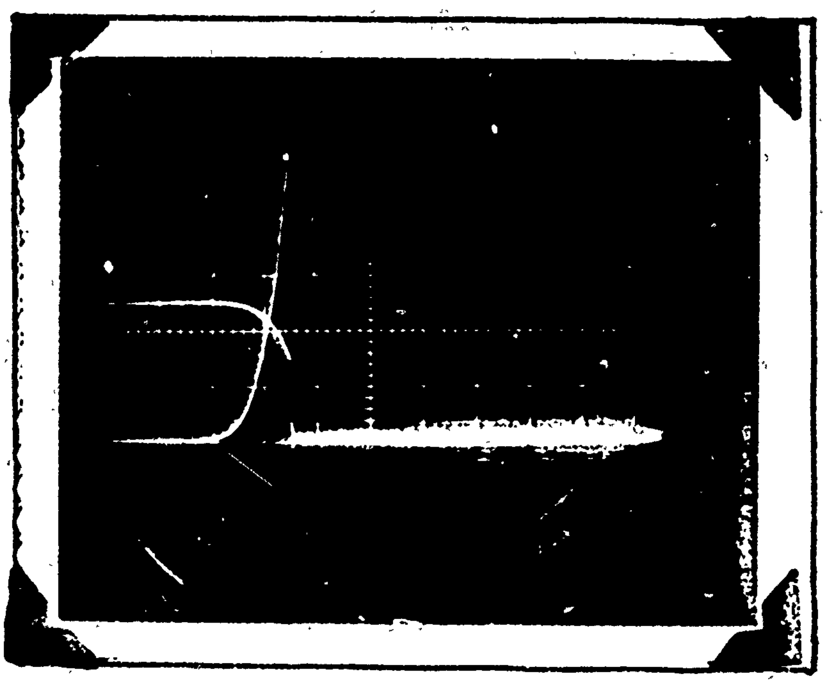

Capacitor Charging Voltages

Discharge 2,500 V
Filament 35 V
Magnet 0 V

Upper Trace

Signal Discharge Voltage
Ampl/cm. 1,000 V
Time/cm. 10 m. sec.

Lower Trace

Signal Discharge Current
Ampl/cm. 200 m.a.
Time/cm. 10 m. sec.

Discharge Capacitor 4 μf

Pressure = 4.6×10^{-7} Torr.

Figure 7b. (Continued)

Date 1-28-75 Experiment ____________

Picture # 41

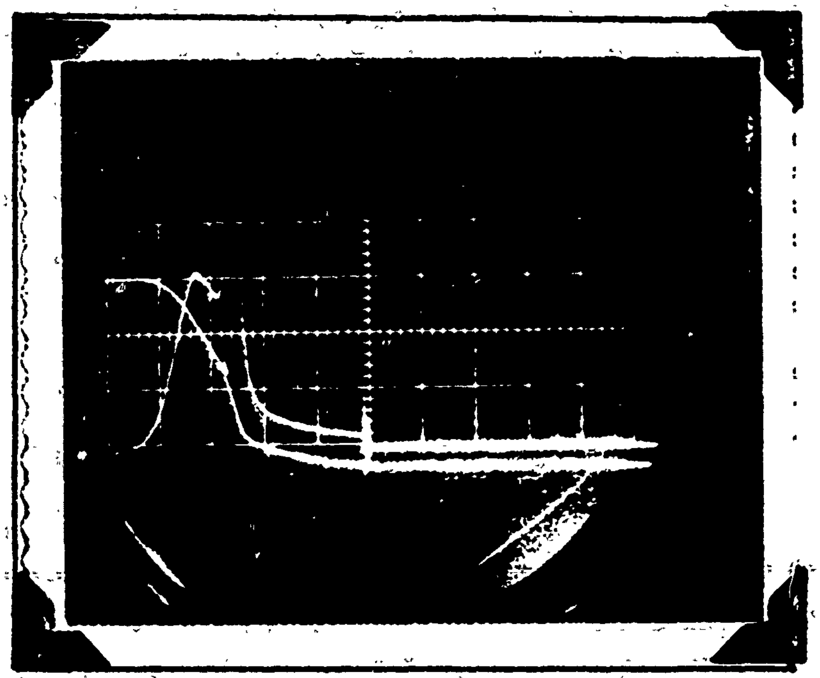

Capacitor
Charging
Voltages

Discharge 3,000 V
Filament 35 V
Magnet 0 V

Upper Trace

Signal Discharge Voltage
Ampl/cm. 1,000 V
Time/cm. 10 m. sec.

Lower Trace

Signal Discharge Current
Ampl/cm. 200 m.a.
Time/cm. 10 m. sec.

Discharge Capacitor 4 μf

Pressure = 4.6 x 10^{-7} Torr.

20 m. sec. delay

Picture # 42

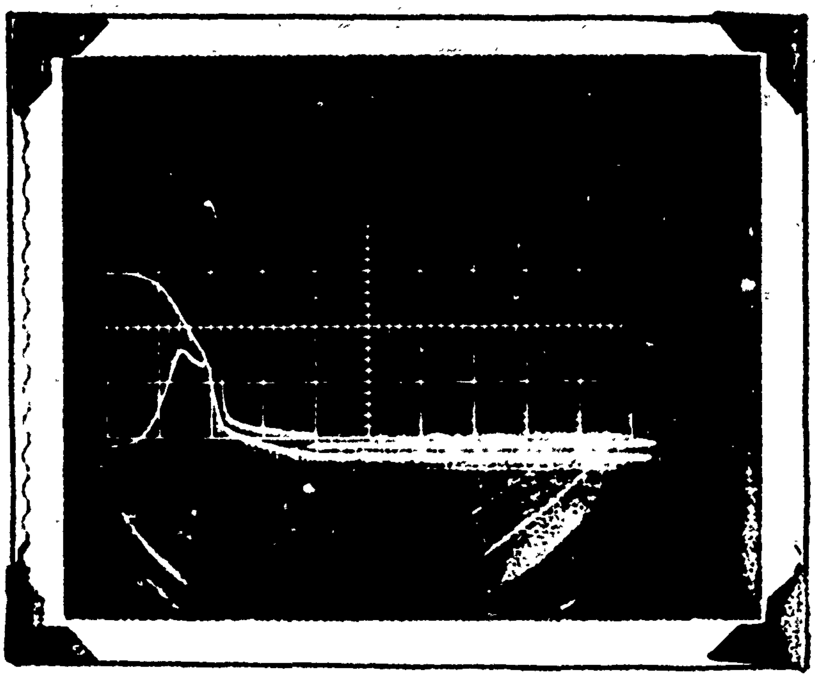

Capacitor
Charging
Voltages

Discharge 3,000 V
Filament 35 V
Magnet 0 V

Upper Trace

Signal Discharge Voltage
Ampl/cm. 1,000 V
Time/cm. 10 m. sec.

Lower Trace

Signal Discharge Current
Ampl/cm. 400 m.a.
Time/cm. 10 m. sec.

Discharge Capacitor 4 μf

Pressure = 4.6 x 10^{-7} Torr.

20 m. sec. delay

Figure 7c. (Continued)

Date 1-29-75 Experiment ______

Picture # 1

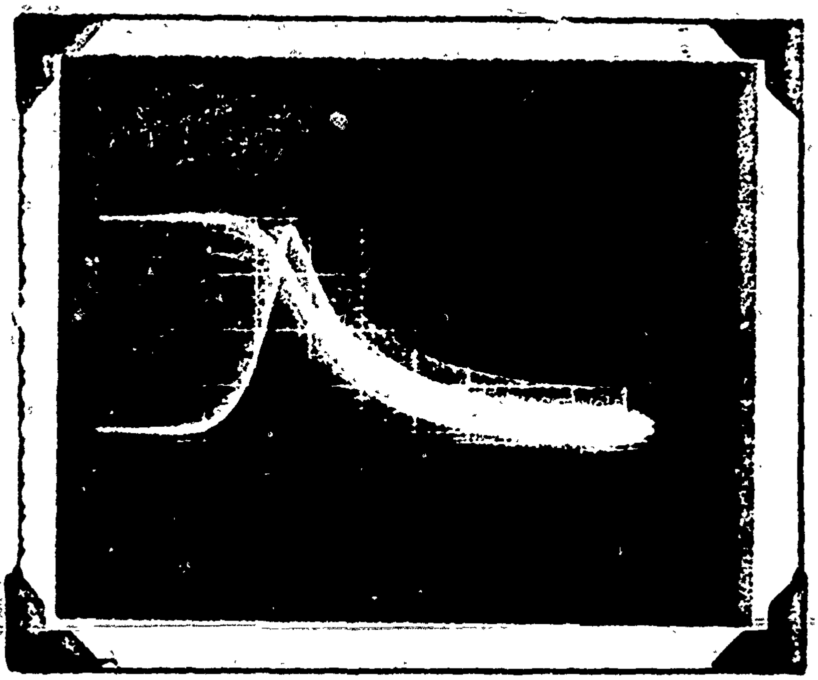

Capacitor Charging Voltages

Upper Detector ______ V
Lower Detector ______ V
Discharge 2,000 V
Filament 35 V
Magnet 0 V

Upper Trace

Signal Discharge Voltage
Ampl/cm. 500 V
Time/cm. 20 m. sec.

Lower Trace

Signal Discharge Current
Ampl/cm. 100 m.a.
Time/cm. 10 m. sec.

Discharge Capacitor 4 μf.
Pressure = 6.0×10^{-7} Torr.

Picture # 1

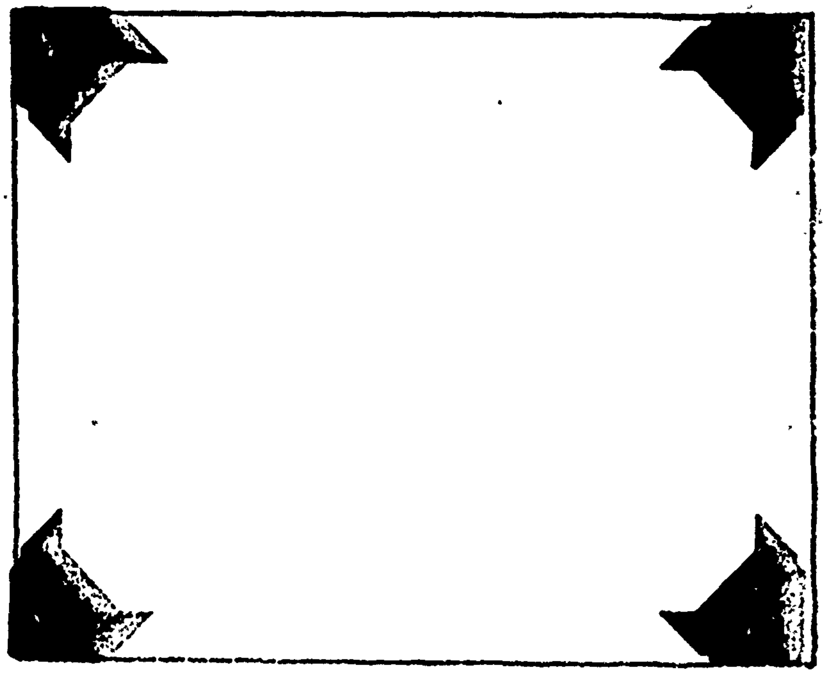

Capacitor Charging Voltages

Upper Detector ______ V
Lower Detector ______ V
Discharge 2,000 V
Filament 35 V
Magnet 0 V

Upper Trace

Signal Discharge Voltage
Ampl/cm. 500 V
Time/cm. 20 m. sec.

Lower Trace

Signal Discharge Current
Ampl/cm. 100 m.a.
Time/cm. 20 m. sec.

Discharge Capacitor 4 μf
Pressure = 6.0×10^{-7} Torr.

Figure 8a. Characteristic Current Voltage Traces - Applied Magnetic Field.

Date 1-29-75 Experiment ____________

Picture # 2

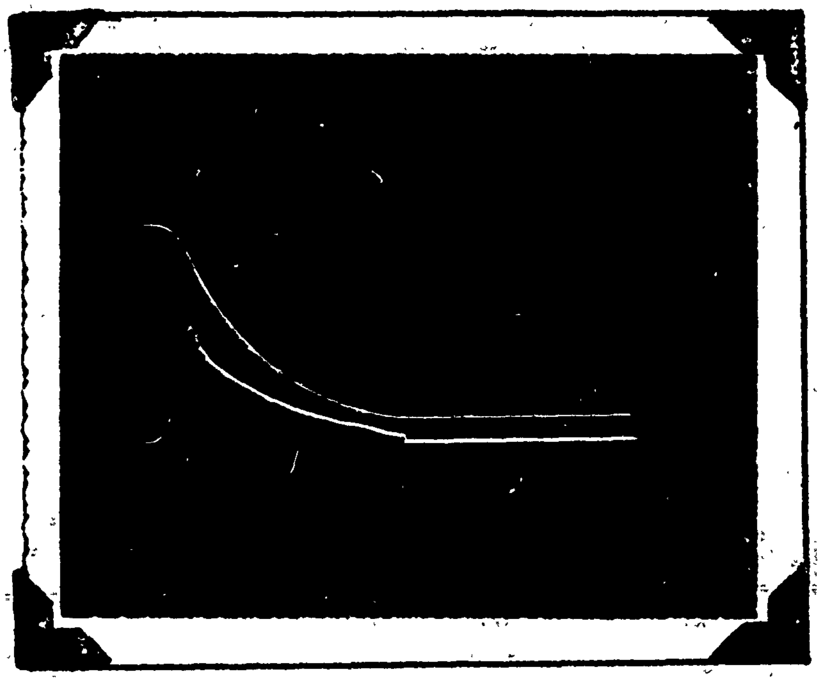

Capacitor Charging Voltages

Upper Detector ______ V
Lower Detector ______ V
Discharge 2,000 V
Filament 35 V
Magnet 10 V

Upper Trace

Signal Discharge Voltage
Ampl/cm. 500 V
Time/cm. 20 m. sec.

Lower Trace

Signal Discharge Current
Ampl/cm. 100 m.a.
Time/cm. 20 m. sec.

Discharge Capacitor 4 μf.
Pressure = 6.0×10^{-7} Torr.

Picture # 3

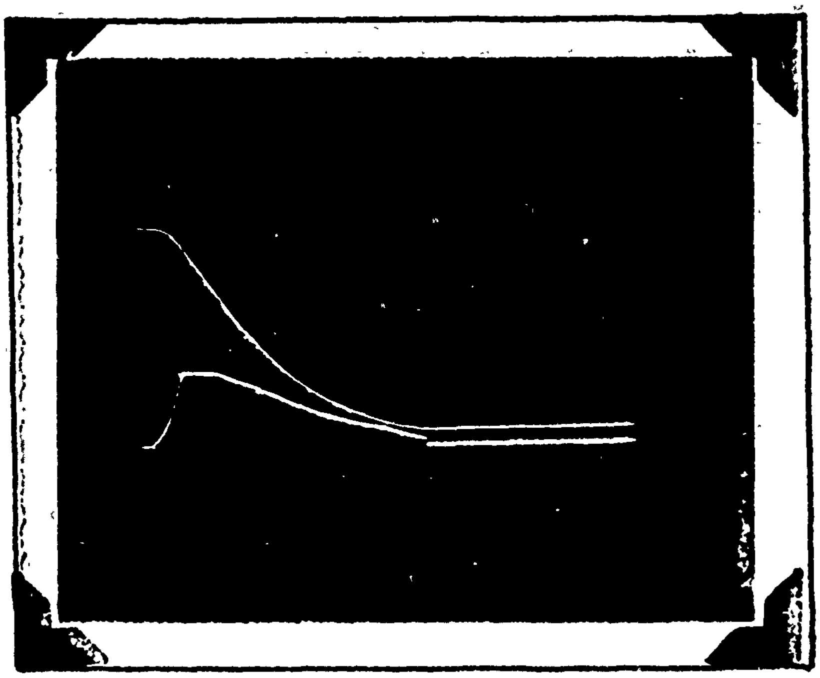

Capacitor Charging Voltages

Upper Detector ______ V
Lower Detector ______ V
Discharge 2,000 V
Filament 35 V
Magnet 12½ V

Upper Trace

Signal Discharge Voltage
Ampl/cm. 500 V
Time/cm. 20 m. sec.

Lower Trace

Signal Discharge Current
Ampl/cm. 100 m.a.
Time/cm. 20 m. sec.

Discharge Capacitor 4 μf.
Pressure = 6.0×10^{-7} Torr.

Figure 8b. (Continued)

Date 1-29-75 Experiment

Picture # 4

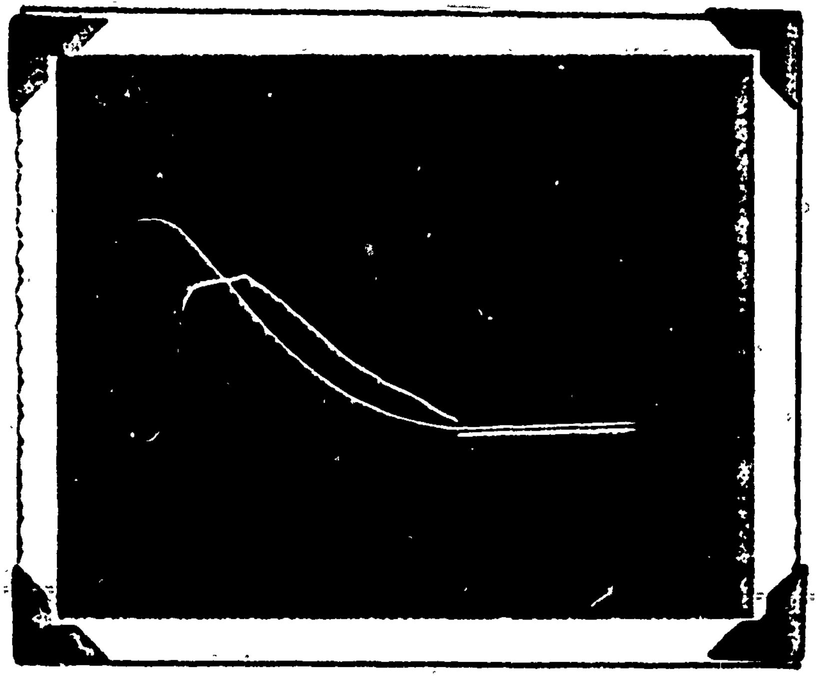

Capacitor Charging Voltages

Upper Detector		V
Lower Detector		V
Discharge	2,000	V
Filament	35	V
Magnet	15	V

Upper Trace

Signal	Discharge Voltage
Ampl/cm.	50 V
Time/cm.	20 m. sec.

Lower Trace

Signal	Discharge Current
Ampl/cm.	40 m.a.
Time/cm.	20 m. sec.

Discharge Capacitor 4 μf.

Pressure = 6.0×10^{-7} Torr.

Picture # 5

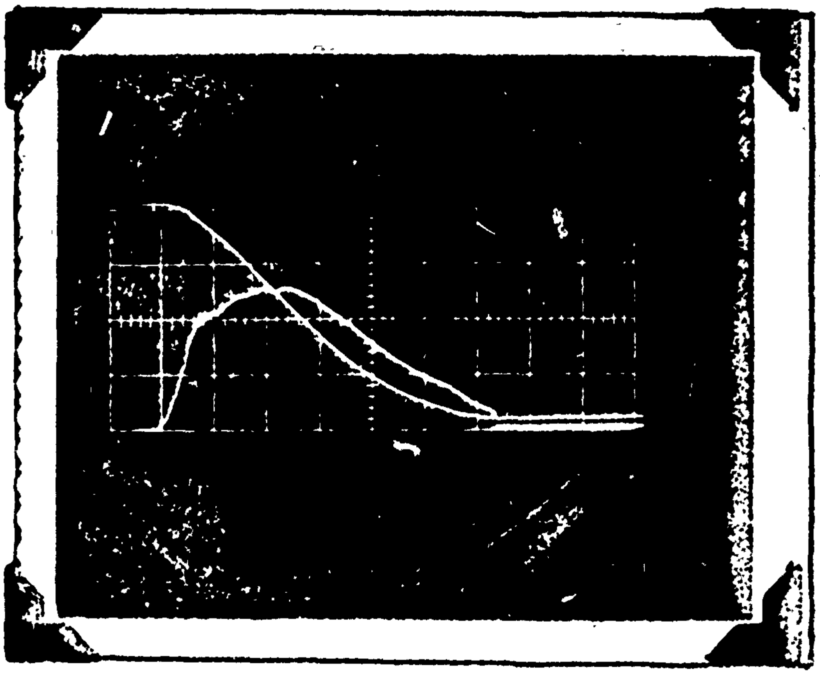

Capacitor Charging Voltages

Upper Detector		V
Lower Detector		V
Discharge	2,000	V
Filament	35	V
Magnet	17½	V

Upper Trace

Signal	Discharge Voltage
Ampl/cm.	500 V
Time/cm.	20 m. sec.

Lower Trace

Signal	Discharge Current
Ampl/cm.	40 m.a.
Time/cm.	20 m. sec.

Discharge Capacitor 4 μf.

Pressure = 6.0×10^{-7} Torr.

Figure 8c. (Continued)

Date 1-29-75 Experiment ______

Picture # 6

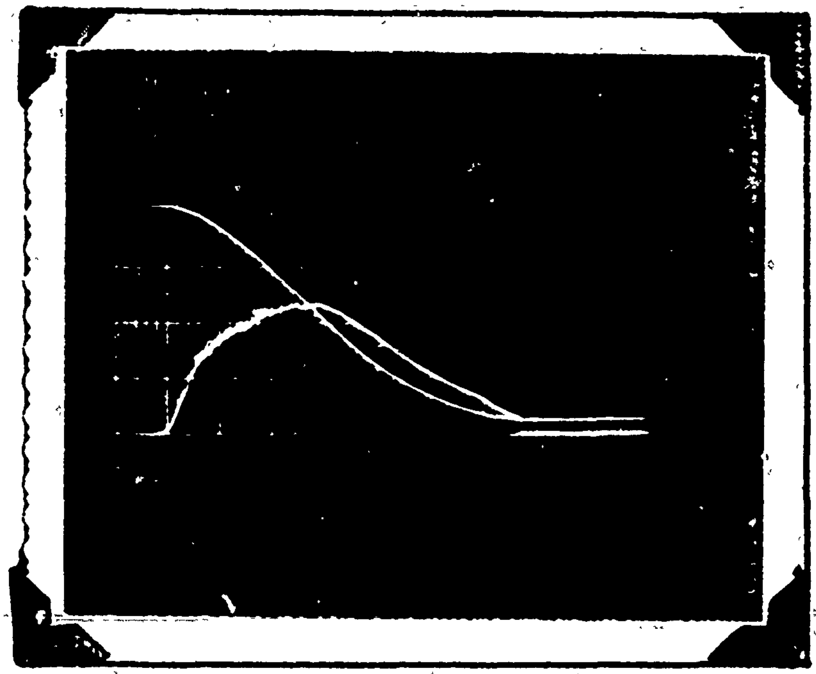

Capacitor Charging Voltages

Upper Detector	______	V
Lower Detector	______	V
Discharge	2,000	V
Filament	35	V
Magnet	20	V

Upper Trace

Signal	Discharge Voltage
Ampl/cm.	500 V
Time/cm.	20 m. sec.

Lower Trace

Signal	Discharge Current
Ampl/cm.	40 m.a.
Time/cm.	20 m. sec.

Discharge Capacitor 4 μf.

Pressure = 6.0×10^{-7} Torr.

Picture # 7

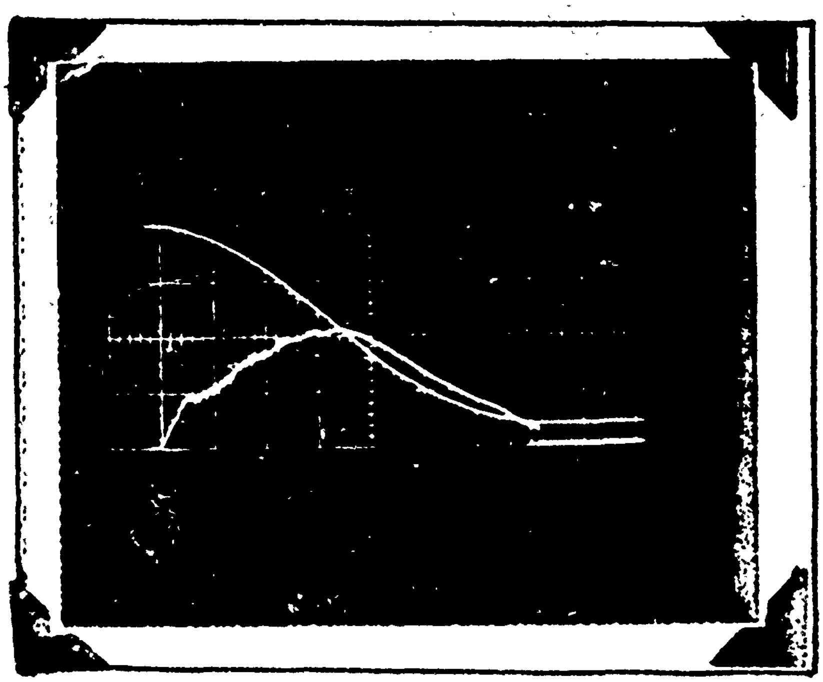

Capacitor Charging Voltages

Upper Detector	______	V
Lower Detector	______	V
Discharge	2,000	V
Filament	35	V
Magnet	22½	V

Upper Trace

Signal	Discharge Voltage
Ampl/cm.	500 V
Time/cm.	20 m. sec.

Lower Trace

Signal	Discharge Current
Ampl/cm.	40 m.a.
Time/cm.	20 m. sec.

Discharge Capacitor 4 μf.

Pressure = 6.0×10^{-7} Torr.

Figure 8d. (Continued)

Date 1-29-75 Experiment ______

Picture # 10

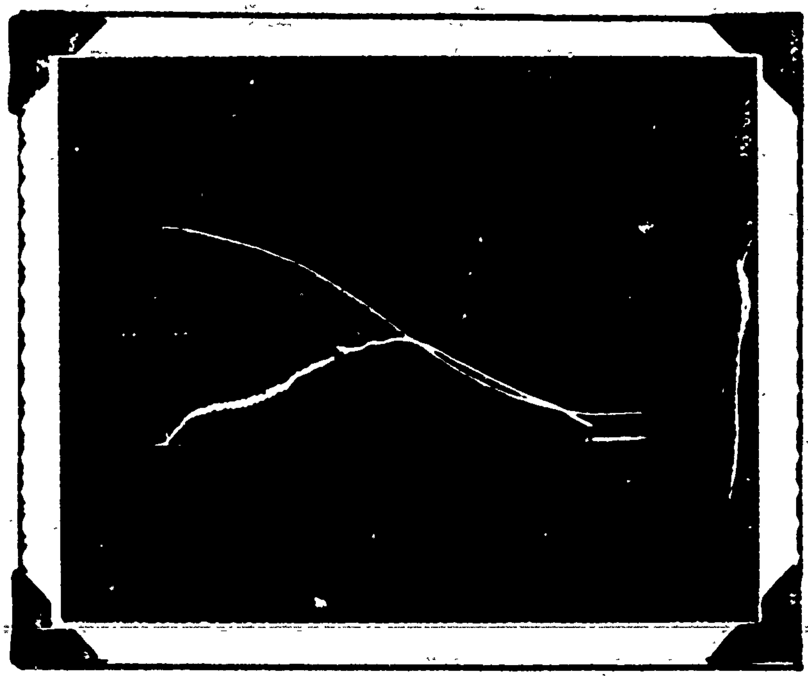

Capacitor Charging Voltages

Upper Detector ______ V
Lower Detector ______ V
Discharge 2,000 V
Filament 35 V
Magnet 30 V

Upper Trace

Signal Discharge Voltage
Ampl/cm. 500 V
Time/cm. 20 m. sec.

Lower Trace

Signal Discharge Current
Ampl/cm. 40 m.a.
Time/cm. 20 m. sec.

Discharge Capacitor 4 μf.
Pressure = 6.0×10^{-7} Torr.

Picture # 11

Capacitor Charging Voltages

Upper Detector ______ V
Lower Detector ______ V
Discharge 2,000 V
Filament 35 V
Magnet 32½ V

Upper Trace

Signal Discharge Voltage
Ampl/cm. 500 V
Time/cm. 20 m. sec.

Lower Trace

Signal Discharge Current
Ampl/cm. 40 m.a.
Time/cm. 20 m. sec.

Discharge Capacitor 4 μf.
Pressure = 6.0×10^{-7} Torr.

Figure 8e. (Continued)

Date 1-29-75 Experiment ____________

Picture # 62A

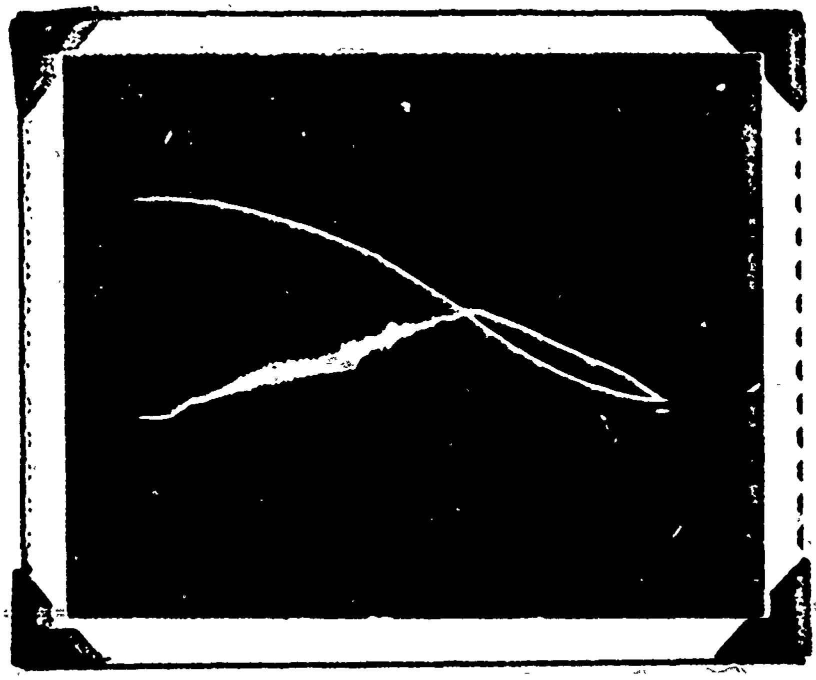

Capacitor Charging Voltages

Upper Detector ______ V
Lower Detector ______ V
Discharge 2,000 V
Filament 35 V
Magnet 45 V

Upper Trace

Signal Discharge Voltage
Ampl/cm. 500 V
Time/cm. 20 m. sec.

Lower Trace

Signal Discharge Current
Ampl/cm. 40 m a.
Time/cm. 20 m. sec

Discharge Capacitor 4 μf.
Pressure = 6.0×10^{-7} Torr.

Picture # 62B

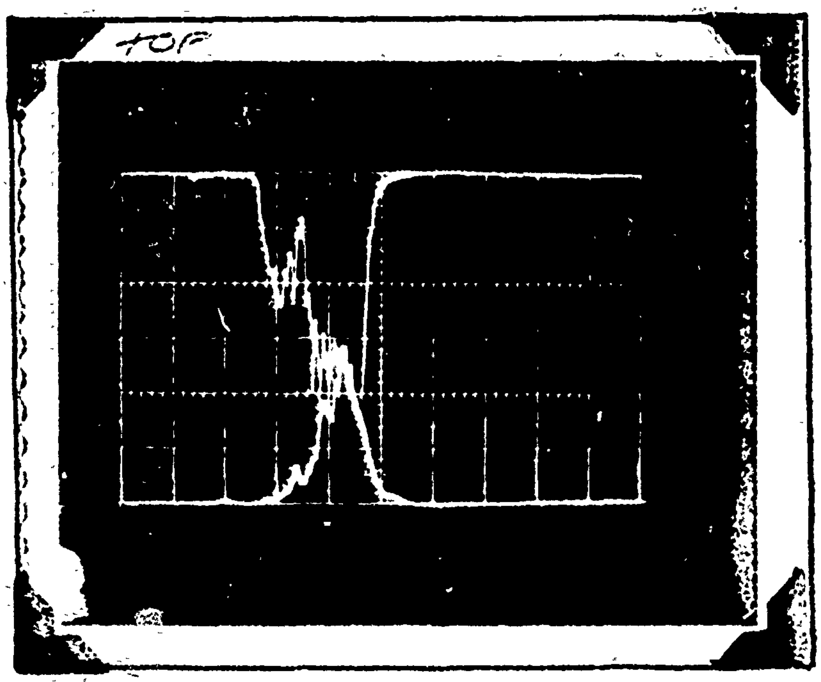

Capacitor Charging Voltages

Upper Detector 1,000 V
Lower Detector 1,000 V
Discharge 2,000 V
Filament 35 V
Magnet 45 V

Upper Trace

Signal Detector 3
Ampl/cm. 100 mV
Time/cm. 20 m. sec.

Lower Trace

Signal Detector 4
Ampl/cm. 500 mV
Time/cm. 20 m. sec.

Discharge Capacitor 4 μf.
Pressure = 6.0×10^{-7} Torr.

Figure 8f. (Continued)

Date 1-29-75 Experiment ______

Picture # 64 A

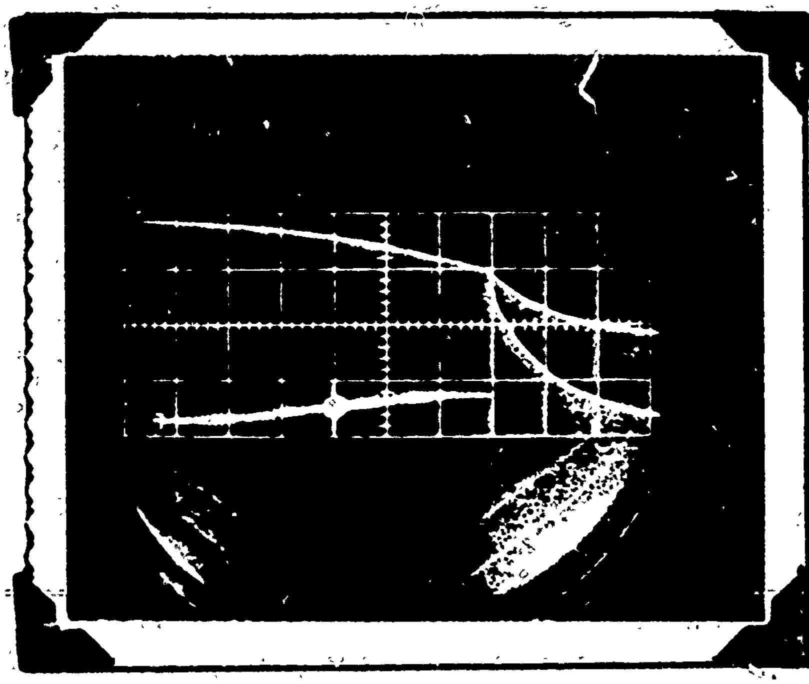

Capacitor Charging Voltages

Upper Detector ______ V
Lower Detector ______ V
Discharge 2,000 V
Filament 35 V
Magnet 47½ V

Upper Trace

Signal Discharge Voltage
Ampl/cm. 500 V
Time/cm. 20 m. sec.

Lower Trace

Signal Discharge Current
Ampl/cm. 40 m.a.
Time/cm. 20 m. sec.

Discharge Capacitor 4 μf
Pressure = 6.0 x 10^{-7} Torr.
40 m. sec. delay

Picture # 64 B

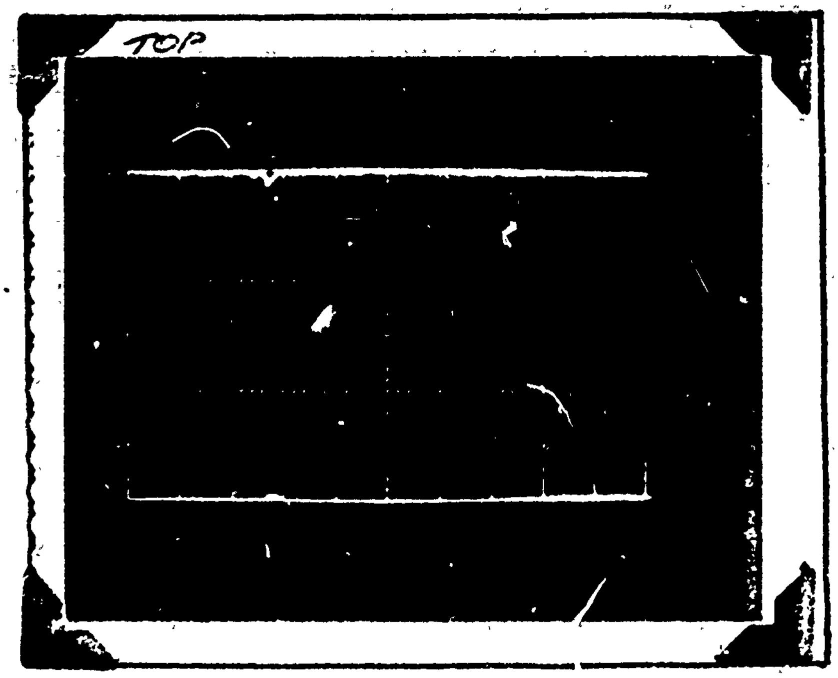

Capacitor Charging Voltages

Upper Detector 1,000 V
Lower Detector 1,000 V
Discharge 2,000 V
Filament 35 V
Magnet 47½ V

Upper Trace

Signal Detector 3
Ampl/cm. 100 mV
Time/cm. 20 m. sec.

Lower Trace

Signal Detector 4
Ampl/cm. 500 mV
Time/cm. 20 m. sec.

Discharge Capacitor 4 μf.
Pressure = 6.0 x 10^{-7} Torr.
40 m. sec. delay

Figure 8g. (Continued)

Date 1-29-75 Experiment ____________

Picture # 63A

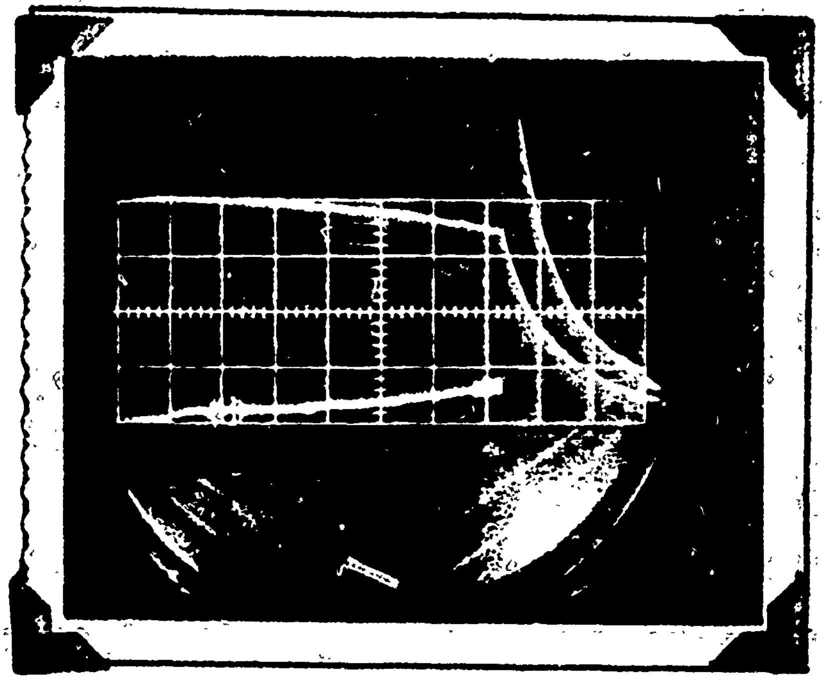

Capacitor Charging Voltages

Upper Detector		V
Lower Detector		V
Discharge	2,000	V
Filament	35	V
Magnet	50	V

Upper Trace

Signal	Discharge Voltage
Ampl/cm.	500 V
Time/cm.	20 m. sec.

Lower Trace

Signal	Discharge Current
Ampl/cm.	40 m.a.
Time/cm.	20 m. sec.

Discharge Capacitor 4 μf.

Pressure = 6.0×10^{-7} Torr.

Picture # 63 B

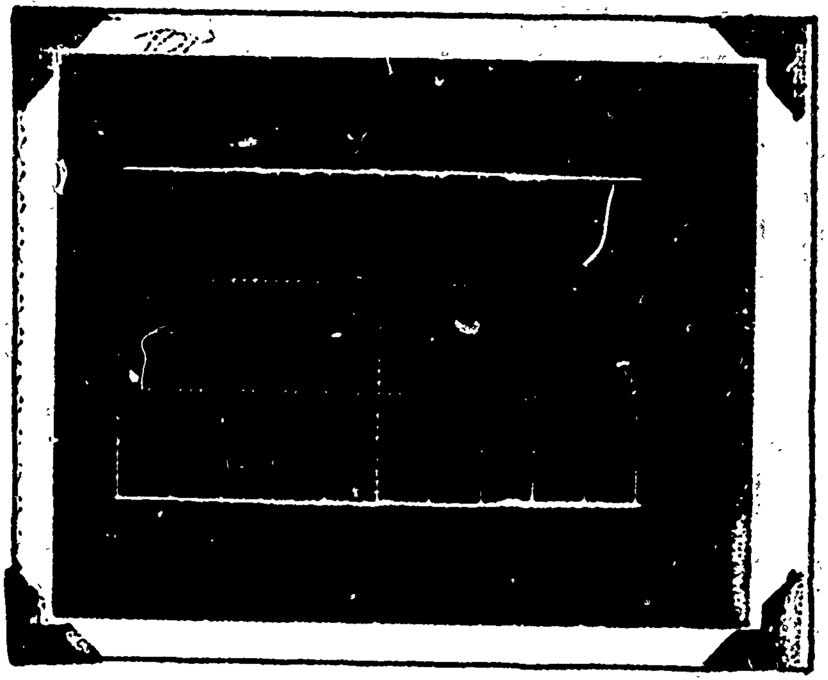

Capacitor Charging Voltages

Upper Detector	1,000	V
Lower Detector	1,000	V
Discharge	2,000	V
Filament	35	V
Magnet	50	V

Upper Trace

Signal	Detector 3
Ampl/cm.	100 mV
Time/cm.	20 m. sec.

Lower Trace

Signal	Detector 4
Ampl/cm.	500 mV
Time/cm.	20 m. sec.

Discharge Capacitor 4 μf.

Pressure = 6.0×10^{-7} Torr.

Figure 8h. (Continued)

Date 1-29-75 Experiment

Picture # 70

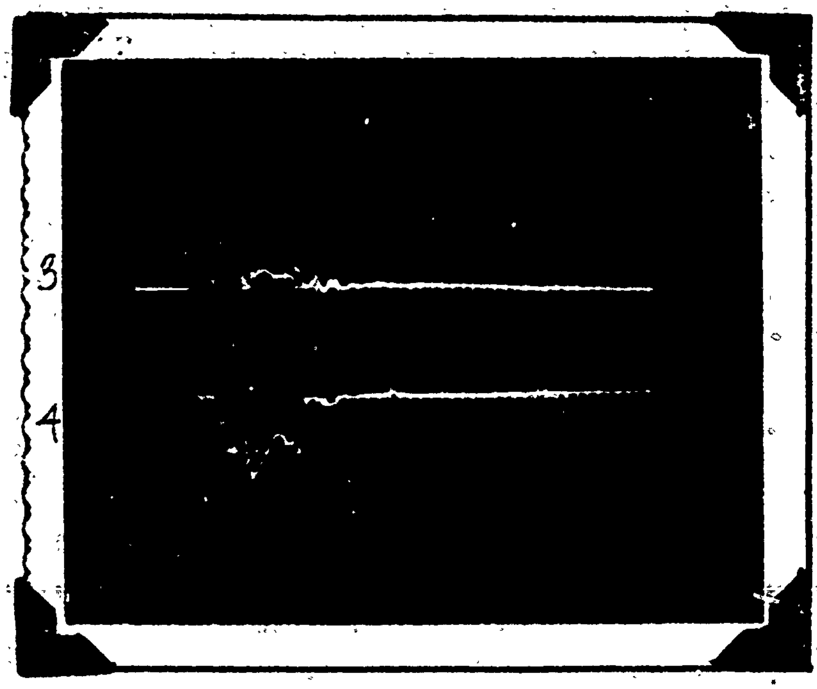

Capacitor Charging Voltages

Upper Detector	0	V
Lower Detector	0	V
Discharge	2,000	V
Filament	35	V
Magnet	30	V

Upper Trace

Signal	Detector 3
Ampl/cm.	10 mV $10^6\ \Omega$
Time/cm.	20 m. sec.

Lower Trace

Signal	Detector 4
Ampl/cm.	50 mV $10^6\ \Omega$
Time/cm.	20 m. sec.

Discharge Capacitor 4 μf.

Pressure = 6.0×10^{-7} Torr.

Picture # 71

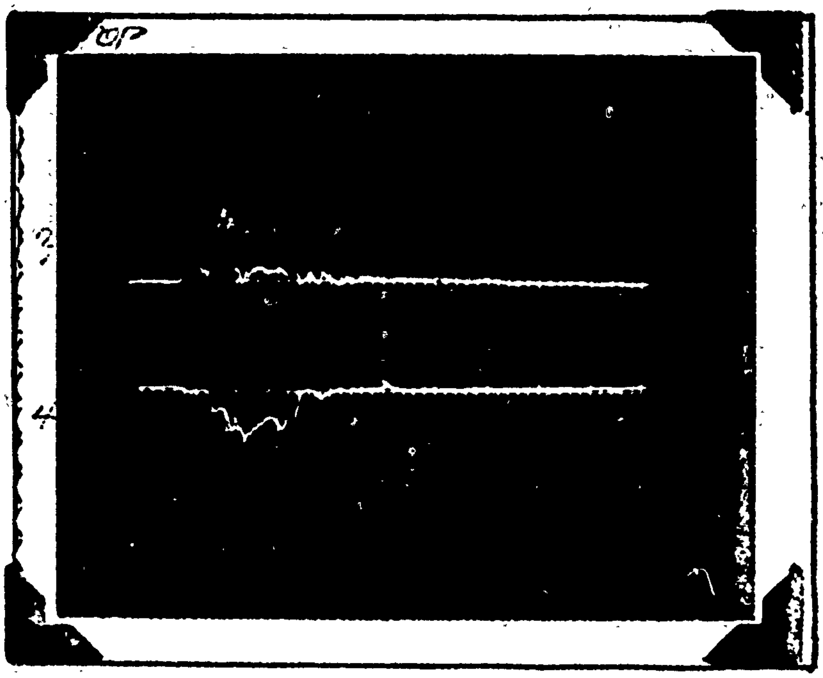

Capacitor Charging Voltages

Upper Detector	100	V
Lower Detector	100	V
Discharge	2,000	V
Filament	35	V
Magnet	30	V

Upper Trace

Signal	Detector 3
Ampl/cm.	10 mV $10^6\ \Omega$
Time/cm.	20 m. sec.

Lower Trace

Signal	Detector 4
Ampl/cm.	50 mV $10^6\ \Omega$
Time/cm.	20 m. sec.

Discharge Capacitor 4 μf.

Pressure = 6.0×10^{-7} Torr.

Figure 9a. Probe Signals for Various Potential Drops Across the Probe Electrodes.

Date 1-29-75 Experiment ______

Picture # 74

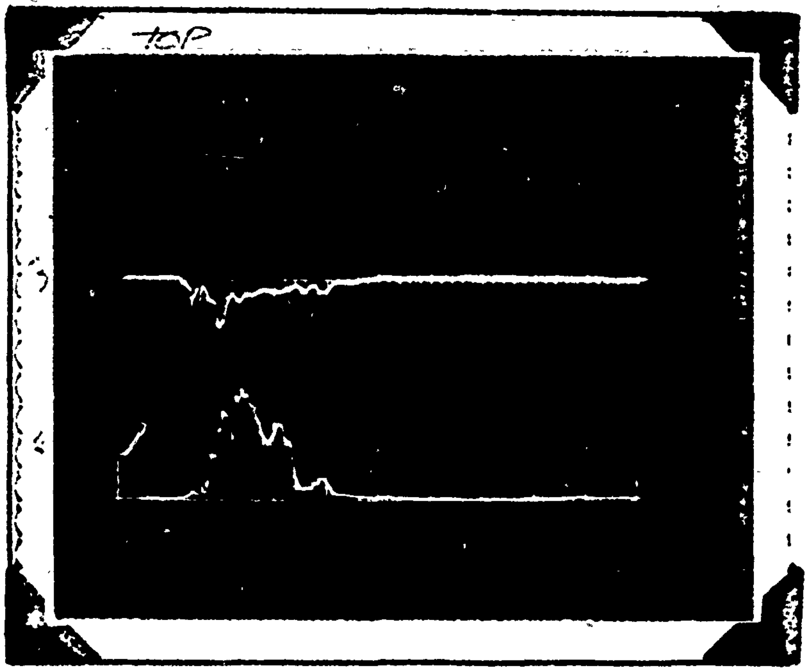

Capacitor Charging Voltages

Upper Detector 400 V
Lower Detector .400 V
Discharge 2,000 V
Filament 35 V
Magnet 30 V

Upper Trace

Signal Detector 3
Ampl/cm. 10 mV $10^6\Omega$
Time/cm. 20 m. sec.

Lower Trace

Signal Detector 4
Ampl/cm. 50 mV $10^6\Omega$
Time/cm. 20 m. sec.

Discharge Capacitor 4 μf.
Pressure = 6.0×10^{-7} Torr.

Picture # 75

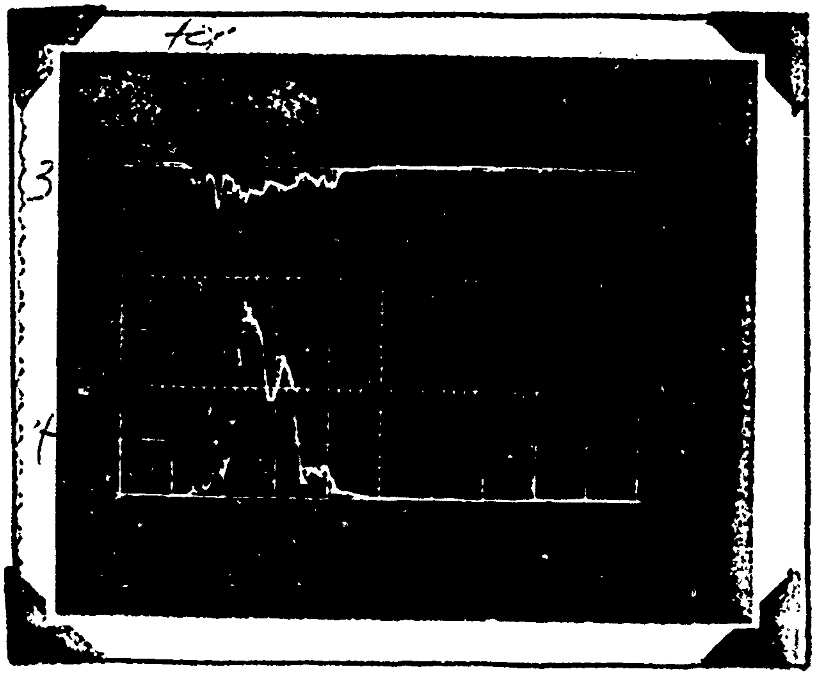

Capacitor Charging Voltages

Upper Detector 500 V
Lower Detector 500 V
Discharge 2,000 V
Filament 35 V
Magnet 30 V

Upper Trace

Signal Detector 3
Ampl/cm. 10 mV $10^6\Omega$
Time/cm. 20 m. sec.

Lower Trace

Signal Detector 4
Ampl/cm. 50 mV $10^6\Omega$
Time/cm. 20 m. sec.

Discharge Capacitor 4 μf.
Pressure = 6.0×10^{-7} Torr.

Figure 9b. (Continued)

Date 1-29-75 Experiment ______

Picture # 80

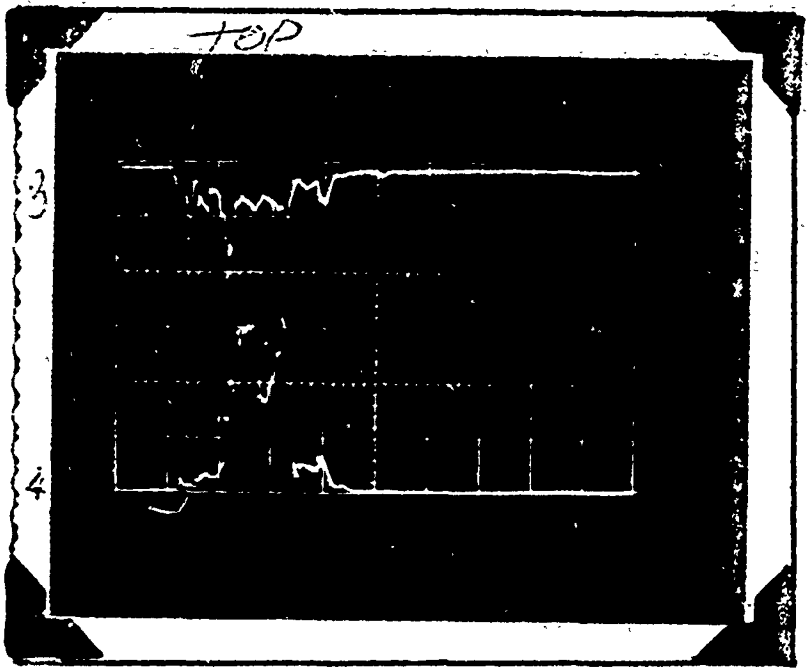

Capacitor Charging Voltages

Upper Detector	1,000	V
Lower Detector	1,000	V
Discharge	2,000	V
Filament	35	V
Magnet	30	V

Upper Trace

Signal	Detector 3
Ampl/cm.	20 mV $10^6\,\Omega$
Time/cm.	20 m. sec.

Lower Trace

Signal	Detector 4
Ampl/cm.	100 mV $10^6\,\Omega$
Time/cm.	20 m. sec.

Discharge Capacitor 4 μf.

Pressure = 6.0×10^{-7} Torr.

Picture # 81

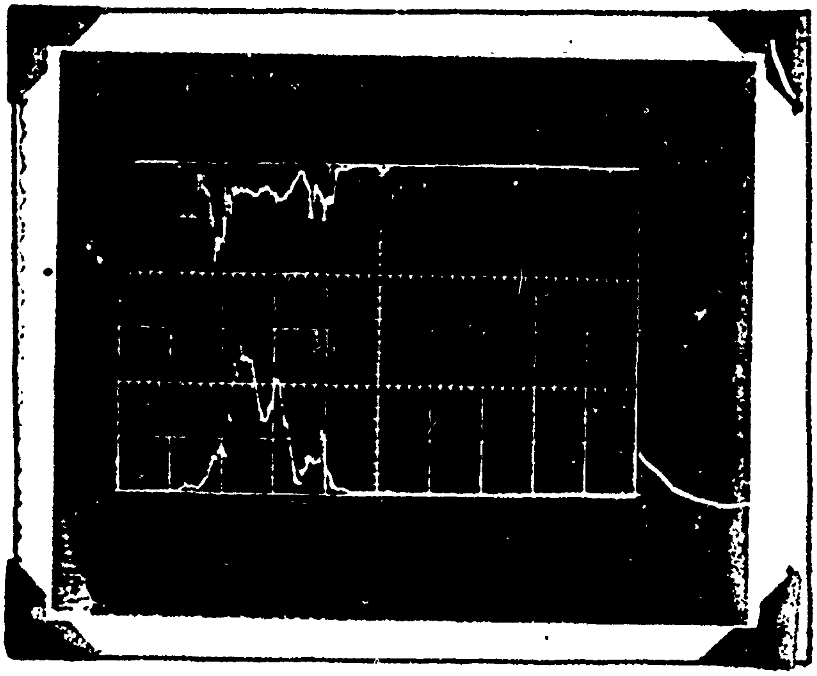

Capacitor Charging Voltages

Upper Detector	1,100	V
Lower Detector	1,100	V
Discharge	2,000	V
Filament	35	V
Magnet	30	V

Upper Trace

Signal	Detector 3
Ampl/cm.	20 mV $10^6\,\Omega$
Time/cm.	20 m. sec.

Lower Trace

Signal	Detector 4
Ampl/cm.	100 mV $10^6\,\Omega$
Time/cm.	20 m. sec.

Discharge Capacitor 4 μf.

Pressure = 6.0×10^{-7} Torr.

Figure 9c. (Continued)

Date 1-29-75 Experiment ____________

Picture # 51

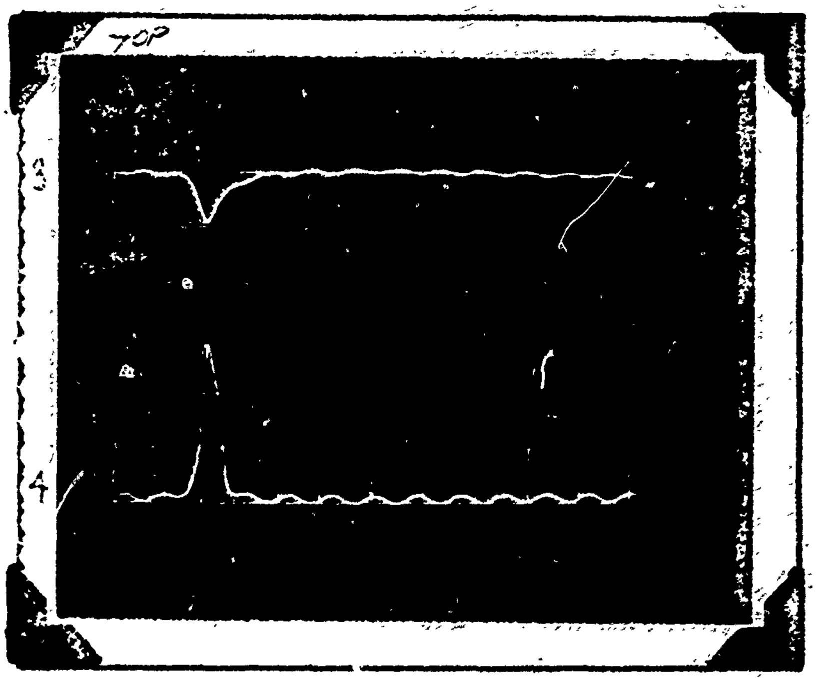

Capacitor Charging Voltages

Upper Detector 1,000 V
Lower Detector 1,000 V
Discharge 2,000 V
Filament 35 V
Magnet 0 V

Upper Trace

Signal Detector 3
Ampl/cm. 2 mV
Time/cm. 20 m. sec.

Lower Trace

Signal Detector 4
Ampl/cm. 5 mV
Time/cm. 20 m. sec.

Discharge Capacitor 4 μf.
Pressure = 6.0 x 10^{-7} Torr.

Picture # 52

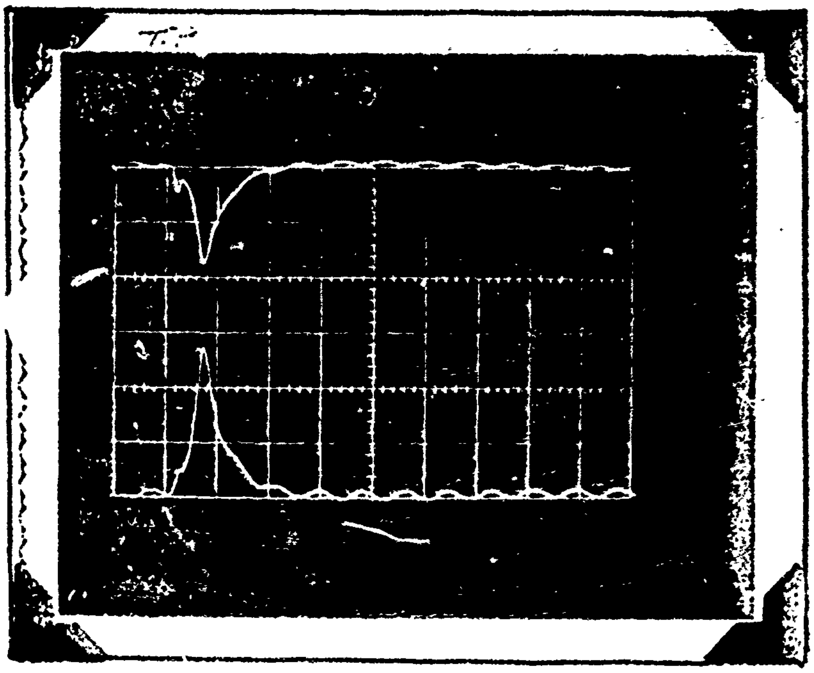

Capacitor Charging Voltages

Upper Detector 1,000 V
Lower Detector 1,000 V
Discharge 2,000 V
Filament 35 V
Magnet 5 V

Upper Trace

Signal Detector 3
Ampl/cm. 2 mV
Time/cm. 20 m. sec.

Lower Trace

Signal Detector 4
Ampl/cm. 5 mV
Time/cm. 20 m. sec.

Discharge Capacitor 4 μf.
Pressure = 6.0 x 10^{-7} Torr.

Figure 10a. Probe Signals for Various Magnetic Field Strengths.

Date 1-29-75 Experiment ____________

Picture # 56

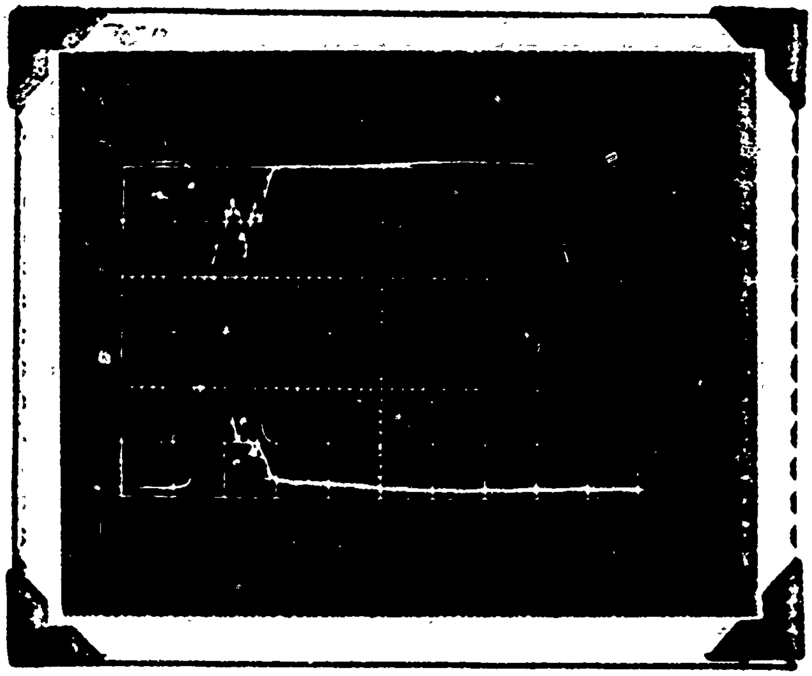

Capacitor Charging Voltages

Upper Detector 1,000 V
Lower Detector 1,000 V
Discharge 2,000 V
Filament 35 V
Magnet 20 V

Upper Trace

Signal Detector 3
Ampl/cm. 20 mV
Time/cm. 20 m. sec.

Lower Trace

Signal Detector 4
Ampl/cm. 50 mV
Time/cm. 20 m. sec.

Discharge Capacitor 4 μf.
Pressure = 6.0 x 10^{-7} Torr.

Picture # 57

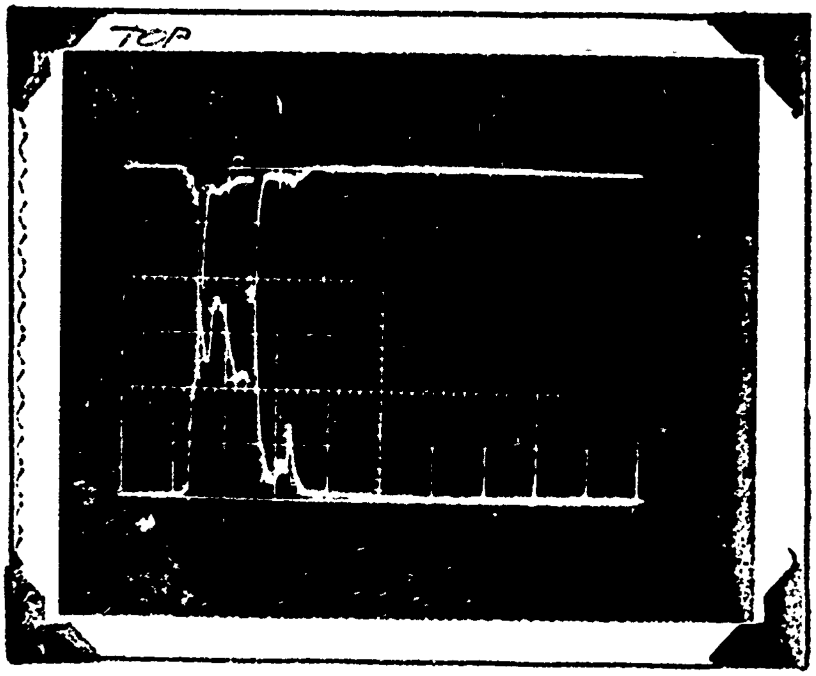

Capacitor Charging Voltages

Upper Detector 1,000 V
Lower Detector 1,000 V
Discharge 2,000 V
Filament 35 V
Magnet 25 V

Upper Trace

Signal Detector 3
Ampl/cm. 50 mV
Time/cm. 20 m. sec.

Lower Trace

Signal Detector 4
Ampl/cm. 100 mV
Time/cm. 20 m. sec.

Discharge Capacitor 4 μf.
Pressure = 6.0 x 10^{-7} Torr.

Figure 10b. (Continued)

Date 1-29-75 Experiment ________

Picture # 60

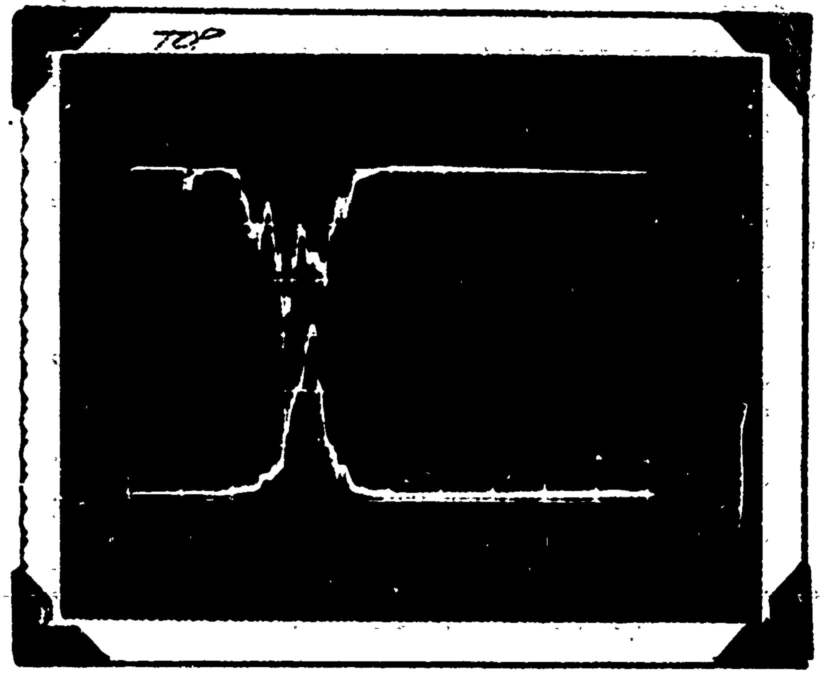

Capacitor Charging Voltages

Upper Detector 1,000 V
Lower Detector 1,000 V
Discharge 2,000 V
Filament 35 V
Magnet 35 V

Upper Trace

Signal Detector 3
Ampl/cm. 100 mV
Time/cm. 20 m. sec.

Lower Trace

Signal Detector 4
Ampl/cm. 500 mV
Time/cm. 20 m.sec.

Discharge Capacitor 4 μf.

Pressure = 6.0×10^{-7} Torr.

Picture #____

Capacitor Charging Voltages

Upper Detector ________ V
Lower Detector ________ V
Discharge ________ V
Filament ________ V
Magnet ________ V

Upper Trace

Signal ________
Ampl/cm. ________
Time/cm. ________

Lower Trace

Signal ________
Ampl/cm. ________
Time/cm. ________

Discharge Capacitor ______

Pressure = ________ Torr.

Figure 10c. (Continued)

Date 1-30-75 Experiment ______

Picture # 54 A

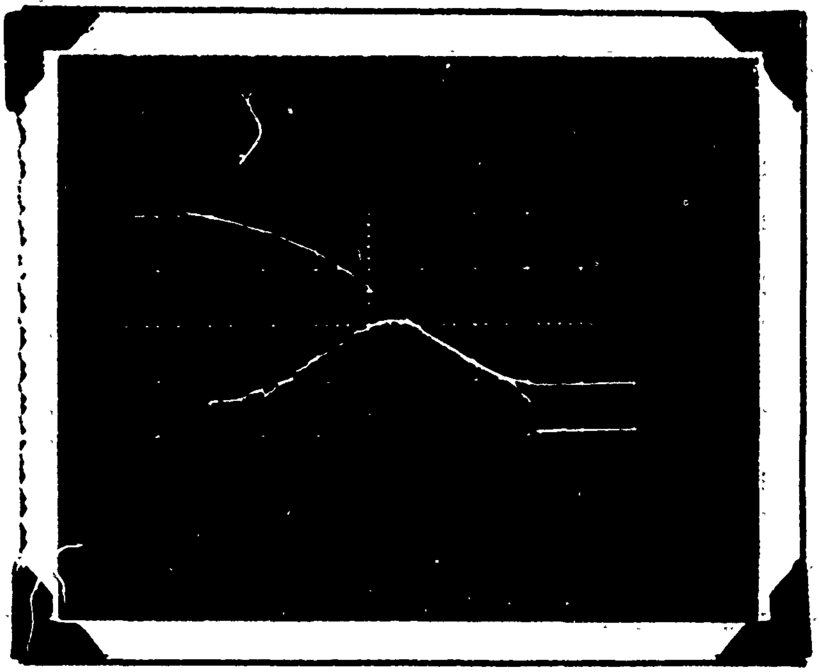

Capacitor Charging Voltages

Upper Detector ______ V
Lower Detector ______ V
Discharge 2,000 V
Filament 35 V
Magnet 30 V

Upper Trace

Signal Discharge Voltage
Ampl/cm. 500 V
Time/cm. 20 m. sec.

Lower Trace

Signal Discharge Current
Ampl/cm. 40 m.a.
Time/cm. 20 m. sec.

Discharge Capacitor 4 μf.
Pressure = 1×10^{-6} Torr.

Picture # 54 B

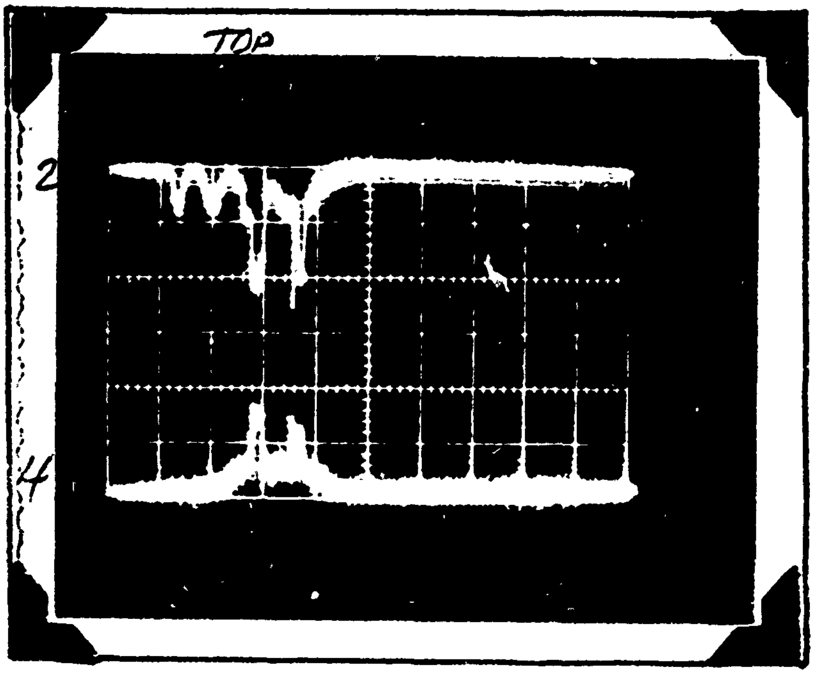

Capacitor Charging Voltages

Upper Detector 500 V
Lower Detector 500 V
Discharge 2,000 V
Filament 35 V
Magnet 30 V

Upper Trace

Signal Detector 2
Ampl/cm. 500 mV $10^6\,\Omega$
Time/cm. 20 m. sec.

Lower Trace

Signal Detector 4
Ampl/cm. 100 mV $10^6\,\Omega$
Time/cm. 20 m. sec.

Discharge Capacitor 4 μf.
Pressure = 1×10^{-6} Torr.

Figure 11a. Probe Signals for Various Ambient Pressures.

Date 1-30-75 Experiment ____________

Picture # 57 A

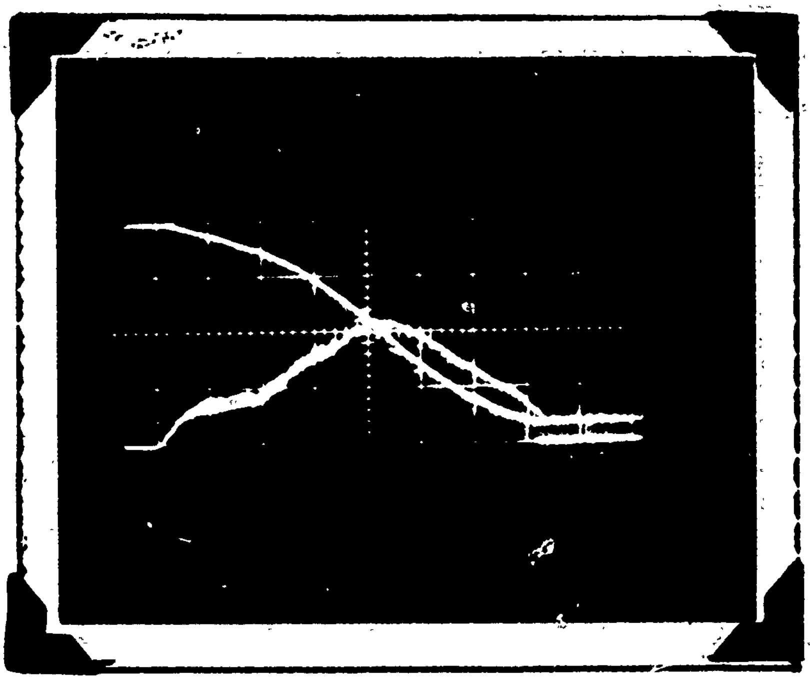

Capacitor Charging Voltages

Upper Detector	______	V
Lower Detector	______	V
Discharge	2,000	V
Filament	35	V
Magnet	30	V

Upper Trace

Signal	Discharge Voltage
Ampl/cm.	500 V
Time/cm.	20 m. sec.

Lower Trace

Signal	Discharge Current
Ampl/cm.	40 m.a.
Time/cm.	20 m. sec.

Discharge Capacitor 4 μf.

Pressure = 3×10^{-6} Torr.

Picture # 57 B

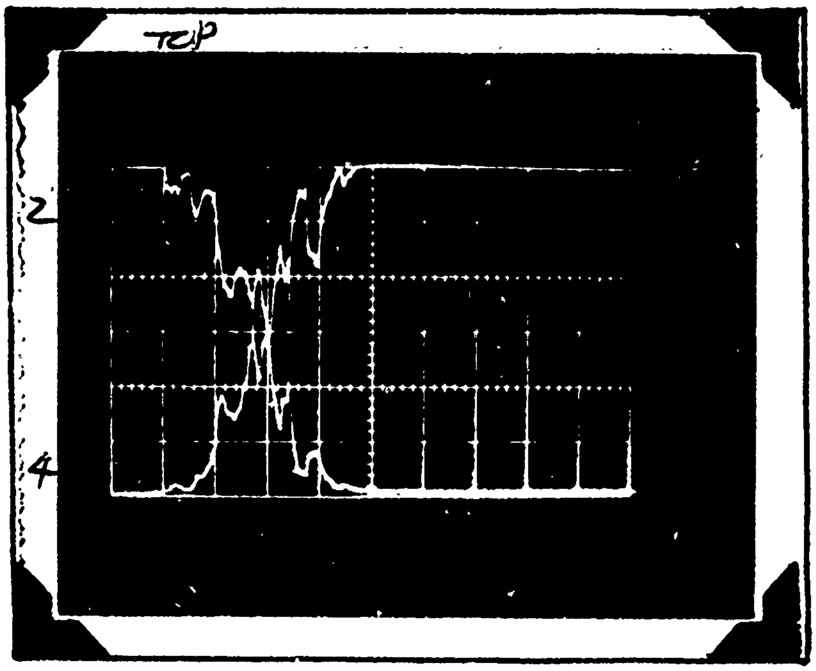

Capacitor Charging Voltages

Upper Detector	500	V
Lower Detector	500	V
Discharge	2,000	V
Filament	35	V
Magnet	30	V

Upper Trace

Signal	Detector 2
Ampl/cm.	2 V $10^6 \Omega$
Time/cm.	20 m. sec.

Lower Trace

Signal	Detector 4
Ampl/cm.	100 mV $10^6 \Omega$
Time/cm.	20 m. sec.

Discharge Capacitor 4 μf.

Pressure = 3×10^{-6} Torr.

Figure 11b. (Continued)

Date 1-30-75 Experiment ______

Picture # 59 A

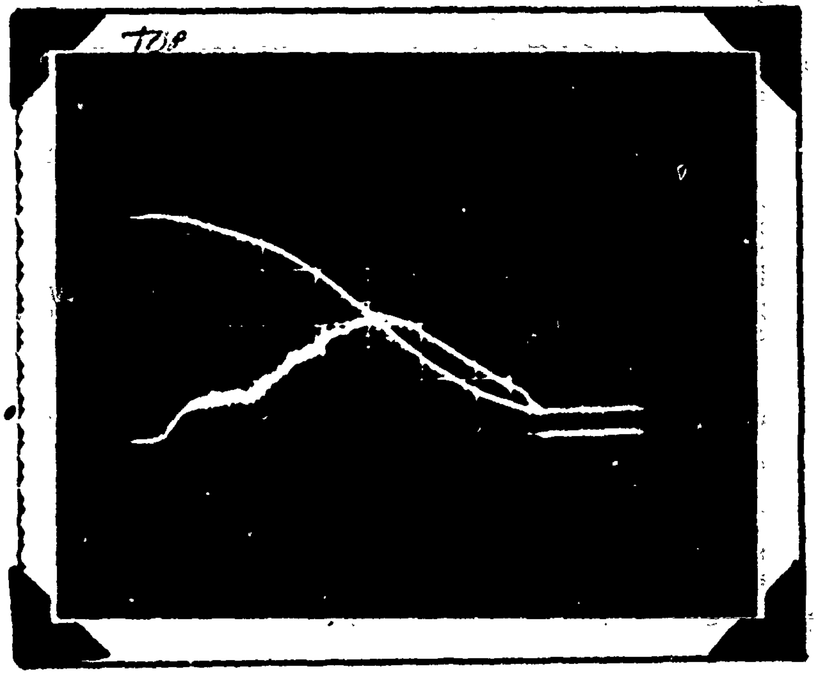

Capacitor Charging Voltages

Upper Detector ______ V
Lower Detector ______ V
Discharge 2,000 V
Filament 35 V
Magnet 30 V

Upper Trace

Signal Discharge Voltage
Ampl/cm. 500 V
Time/cm. 20 m. sec.

Lower Trace

Signal Discharge Current
Ampl/cm. 40 m.a.
Time/cm. 20 m. sec.

Discharge Capacitor 4 μf
Pressure = 1 x 10^{-5} Torr

Picture # 59 B

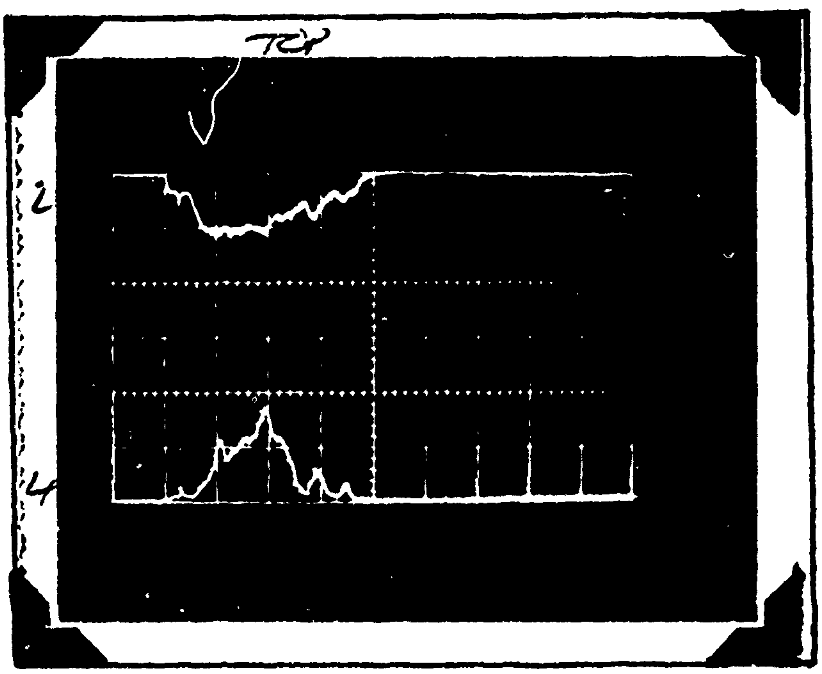

Capacitor Charging Voltages

Upper Detector 500 V
Lower Detector 500 V
Discharge 2,000 V
Filament 35 V
Magnet 30 V

Upper Trace

Signal Detector 2
Ampl/cm. 20 V $10^6 \Omega$
Time/cm. 20 m. sec.

Lower Trace

Signal Detector 4
Ampl/cm. 1 V $10^6 \Omega$
Time/cm. 20 m. sec.

Discharge Capacitor 4 μf
Pressure = 1 x 10^{-5} Torr

Figure 11c. (Continued)

Date 1-30-75 Experiment ____________

Picture # 62 A

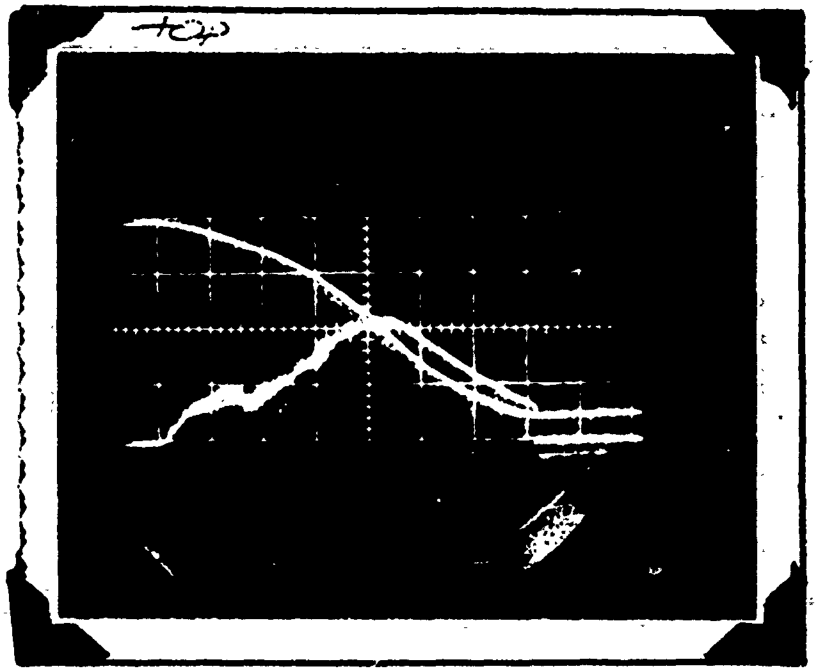

Capacitor Charging Voltages

Upper Detector ______ V
Lower Detector ______ V
Discharge 2,000 V
Filament 35 V
Magnet 30 V

Upper Trace

Signal Discharge Voltage
Ampl/cm. 500 V
Time/cm. 20 m. sec.

Lower Trace

Signal Discharge Current
Ampl/cm. 40 m.a.
Time/cm. 20 m. sec.

Discharge Capacitor 4 μf.
Pressure = 3×10^{-5} Torr.

Picture # 62 B

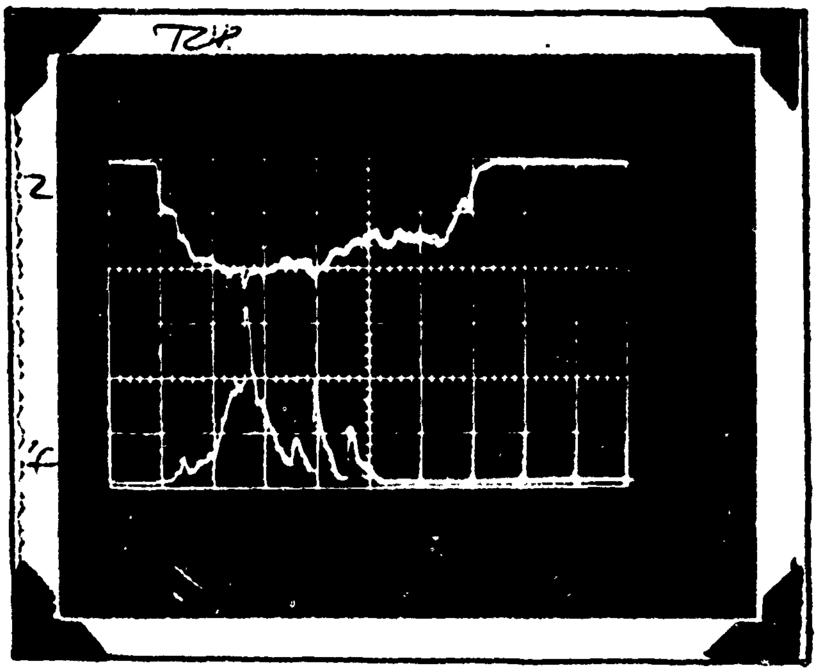

Capacitor Charging Voltages

Upper Detector 500 V
Lower Detector 500 V
Discharge 2,000 V
Filament 35 V
Magnet 30 V

Upper Trace

Signal Detector 2 10^6 Ω
Ampl/cm. 20 V
Time/cm. 20 m. sec.

Lower Trace

Signal Detector 4 10^6 Ω
Ampl/cm. 2 V
Time/cm. 20 m. sec.

Discharge Capacitor 4 μf.
Pressure = 3×10^{-5} Torr.

Figure 11d. (Continued)

Date 1-30-75 Experiment ____________

Picture # 67 A

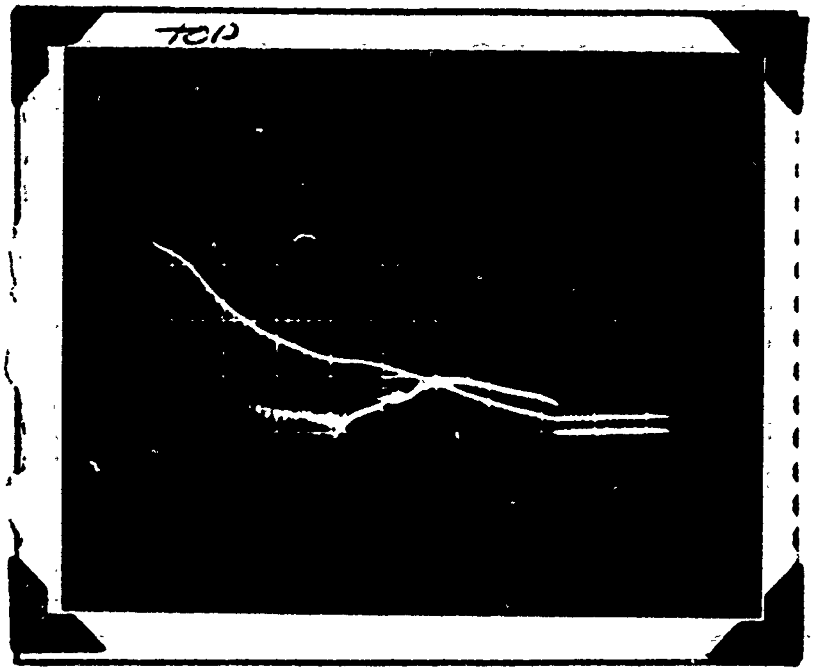

Capacitor Charging Voltages

Upper Detector ______ V
Lower Detector ______ V
Discharge 2,000 V
Filament 35 V
Magnet 30 V

Upper Trace

Signal Discharge Voltage
Ampl/cm. 500 V
Time/cm. 20 m. sec.

Lower Trace

Signal Discharge Current
Ampl/cm. 40 m.a.
Time/cm. 20 m. sec.

Discharge Capacitor 4 μf.
Pressure = 1×10^{-4} Torr.

Picture # 67 B

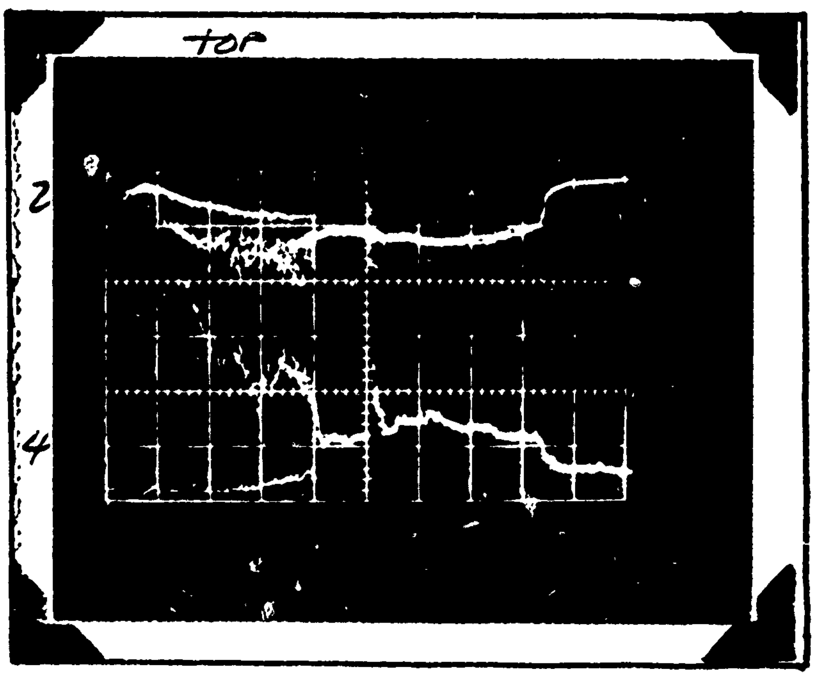

Capacitor Charging Voltages

Upper Detector 500 V
Lower Detector 500 V
Discharge 2,000 V
Filament 35 V
Magnet 30 V

Upper Trace

Signal Detector 2
Ampl/cm. 5 V $10^4 \Omega$
Time/cm. 20 m. sec.

Lower Trace

Signal Detector 4
Ampl/cm. 0.5 V $10^4 \Omega$
Time/cm. 20 m. sec.

Discharge Capacitor 4 μf.
Pressure = 1×10^{-4} Torr.

Figure 11e. (Continued)

Date 1-30-75 Experiment ______

Picture # 68

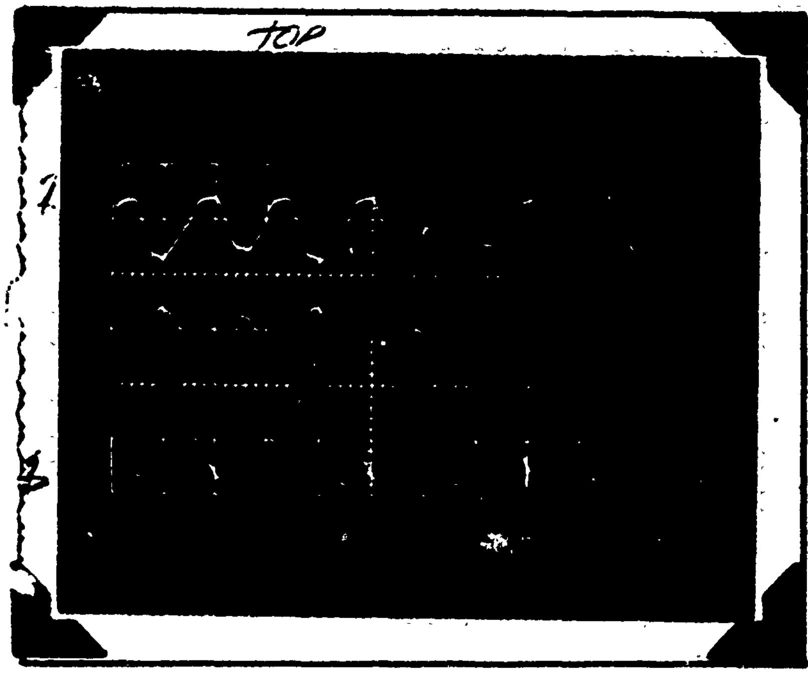

Capacitor Charging Voltages

Upper Detector 500 V
Lower Detector 500 V
Discharge 2,000 V
Filament 35 V
Magnet 30 V

Upper Trace

Signal Detector 2
Ampl/cm. 5 V 10:1
Time/cm. .1 m. sec.

Lower Trace

Signal Detector 4
Ampl/cm. 0.5 V 10:1
Time/cm. .1 m. sec.

Discharge Capacitor 4 μf.
Pressure = 1×10^{-4} Torr.
40 m. sec. delay

Picture # 69

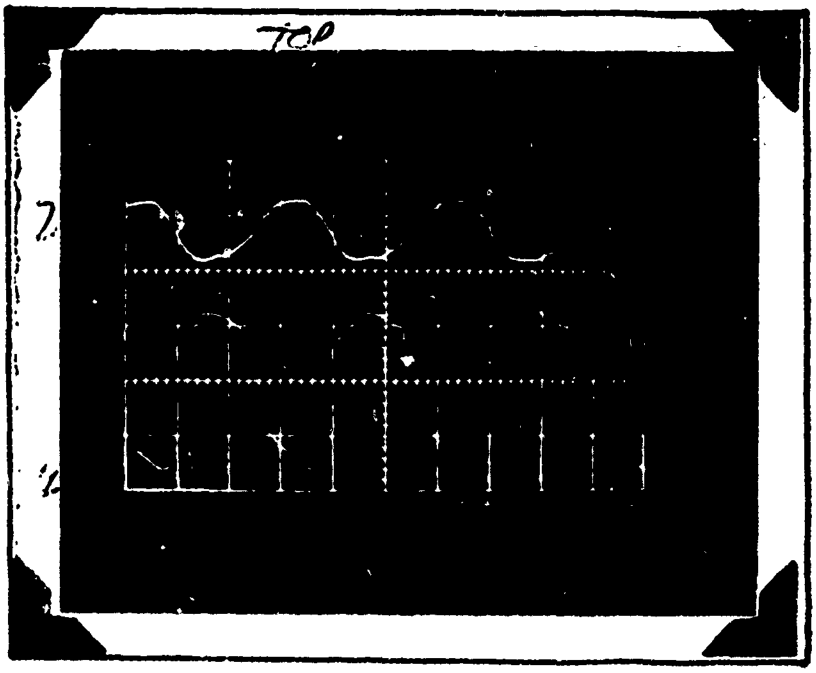

Capacitor Charging Voltages

Upper Detector 500 V
Lower Detector 500 V
Discharge 2,000 V
Filament 35 V
Magnet 30 V

Upper Trace

Signal Detector 2
Ampl/cm. 5 V 10:1
Time/cm. 50 μ. sec.

Lower Trace

Signal Detector 4
Ampl/cm. 0.5 V 10:1
Time/cm. 50 μ. sec.

Discharge Capacitor 4 μf.
Pressure = 1×10^{-4} Torr.
40 m. sec. delay

Figure 12. High Frequency Oscillations in the Probe Signal at High Ambient Pressure.

Date 1-28-75 Experiment ________

Picture # 92

Capacitor Charging Voltages

Upper Detector	500	V
Lower Detector	500	V
Discharge	3000	V
Filament	35	V
Magnet	20	V

Upper Trace

Signal	Detector 1
Ampl/cm.	300 V $10^4 \Omega$
Time/cm.	0.2 m. sec.

Lower Trace

Signal	Detector 4
Ampl/cm.	1 V $10^4 \Omega$
Time/cm.	0.2 m. sec.

Discharge Capacitor 4 μf

Pressure = 4.6×10^{-7} Torr.

Picture # 93

Capacitor Charging Voltages

Upper Detector	500	V
Lower Detector	500	V
Discharge	3000	V
Filament	35	V
Magnet	20	V

Upper Trace

Signal	Detector 1
Ampl/cm.	50 V $10^4 \Omega$
Time/cm.	100 .. sec.

Lower Trace

Signal	Detector 4
Ampl/cm.	50 V $10^4 \Omega$
Time/cm.	100 .. sec.

Discharge Capacitor 4 μf

Pressure = 4.6×10^{-7} Torr.

Figure 13. Probe Traces For Determining Time of Flight.

Date 3-14-75 Experiment Grid Influence on Discharge

Picture # 8 Grid Floating.

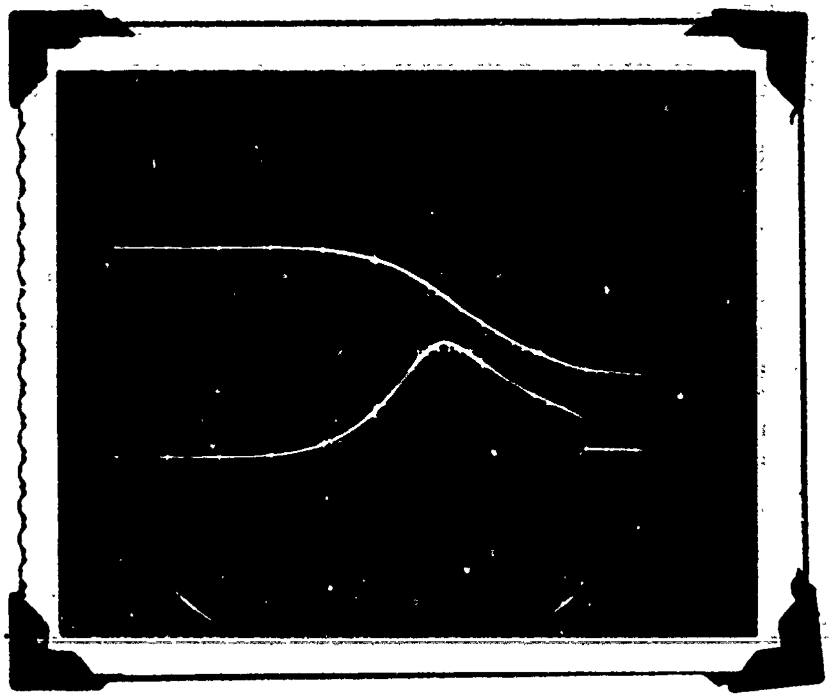

Capacitor Charging Voltages

Discharge 4000 V 4 μ.f.
Filament 30 V
Magnet 0 V

Upper Trace

Signal Voltage
Ampl/cm. 1000 V
Time/cm. 5 m.sec.

Lower Trace

Signal Current
Ampl/cm. 286 m.a.
Time/cm. 5 m.sec.

Picture # 10 Grid Shorted to Plate (Anode)

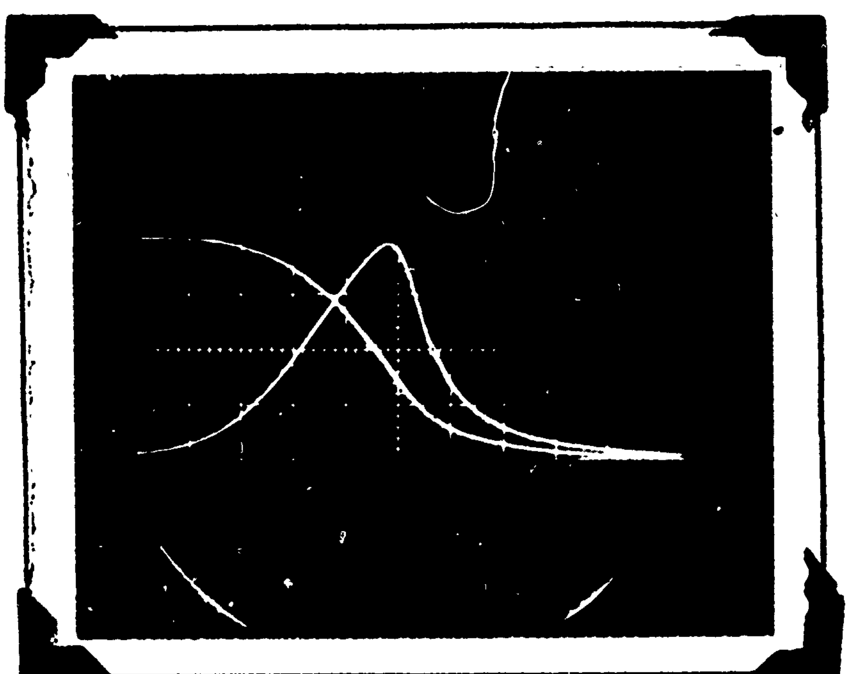

Capacitor Charging Voltages

Discharge 4000 V 4 μ.f.
Filament 30 V
Magnet 0 V

Upper Trace

Signal Voltage
Ampl/cm. 1000 V
Time/cm. 5 m.sec.

Lower Trace

Signal Current
Ampl/cm. 286 m.a.
Time/cm. 5 m.sec.

Figure 14a. Influence of Grid Potential on the Discharge Characteristics.

Date 3-14-75 Experiment Grid Influence on Discharge

Picture # 11 Grid Shorted to Filament

Capacitor Charging Voltages

Discharge	4000	V 4μf.
Filament	30	V
Magnet	0	V

Upper Trace

Signal	Voltage
Ampl/cm.	1000 V
Time/cm.	5 m.sec.

Lower Trace

Signal	Current
Ampl/cm.	286 m.a.
Time/cm.	.5 m.sec.

Picture # 12 Grid Shorted to Filament

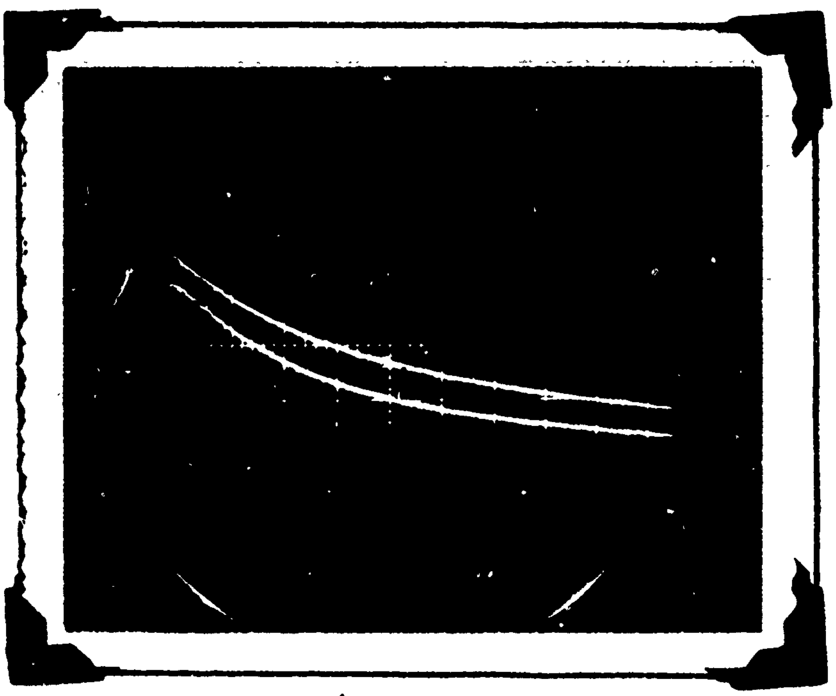

Capacitor Charging Voltages

Discharge	4000	V 4μf.
Filament	30	V
Magnet	0	V

Upper Trace

Signal	Voltage
Ampl/cm.	1000 V
Time/cm.	20 m.sec.

Lower Trace

Signal	Current
Ampl/cm.	57.2 m.a.
Time/cm.	20 m.sec.

Figure 14b. (Continued)

Date 3-15-75 Experiment Grid Influence on Discharge

Picture # 1

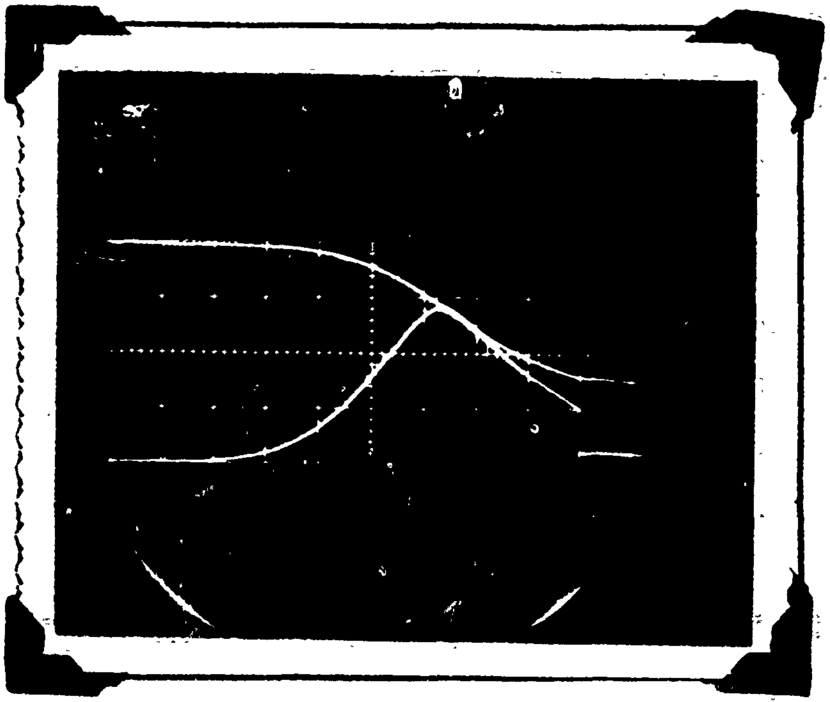

Capacitor Charging Voltages

Discharge 4000 V 4 μ.f.
Filament 36 V .06f.
Magnet 0 V

Upper Trace

Signal Voltage
Ampl/cm. 1000 Volts
Time/cm. 5 m.sec.

Lower Trace

Signal Current
Ampl/cm. 200 m.a.
Time/cm. 5 m.sec.

GRID FLOATING

Picture # 2

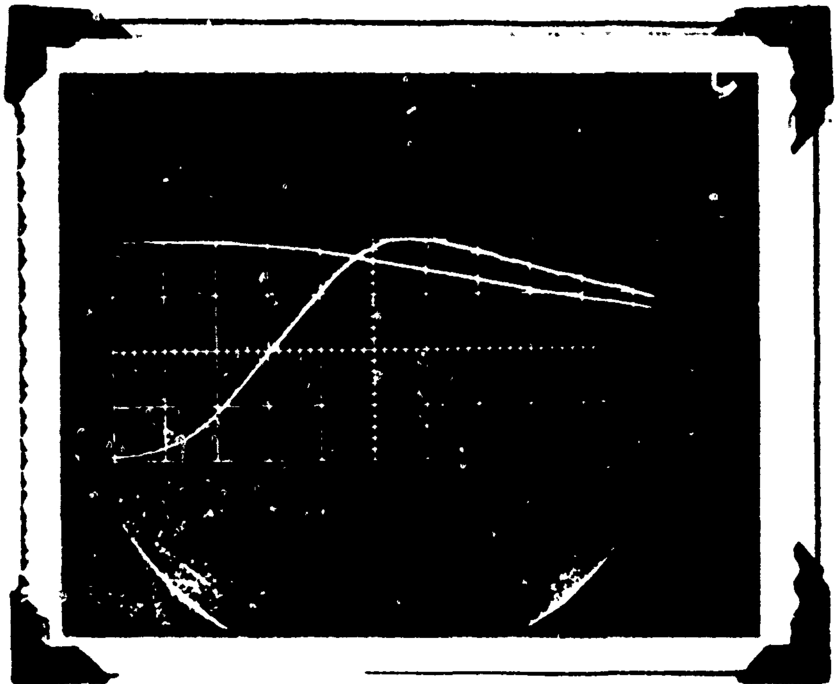

Capacitor Charging Voltages

Discharge 4000 V 4 μ.f.
Filament 36 V .06f.
Magnet 0 V

Upper Trace

Signal Voltage
Ampl/cm. 1000 Volts
Time/cm. 5 m.sec.

Lower Trace

Signal Current
Ampl/cm. 40 m.a.
Time/cm. 5 m.sec.

GRID-FILAMENT FROM SAN DIEGO DISCHARGE TUBE CONNECTED IN PARALLEL WITH GRID-FILAMENT OF DISCHARGE TUBE.

Figure 15a. Influence of the Grid to Filament Resistance on the Discharge Characteristics.

Date 3-15-75 Experiment Grid Influence on Discharge

Picture # 3

Capacitor Charging Voltages

Discharge	4000	V 4 μf.
Filament	36	V .06f.
Magnet	0	V

Upper Trace

Signal	Voltage
Ampl/cm.	1000 Volts
Time/cm.	

Lower Trace

Signal	Current
Ampl/cm.	40 m.a.
Time/cm.	20 m.sec.

GRID-FILAMENT FROM SAN DIEGO DISCHARGE TUBE CONNECTED IN PARALLEL WITH GRID-FILAMENT OF DISCHARGE TUBE

Picture # 4

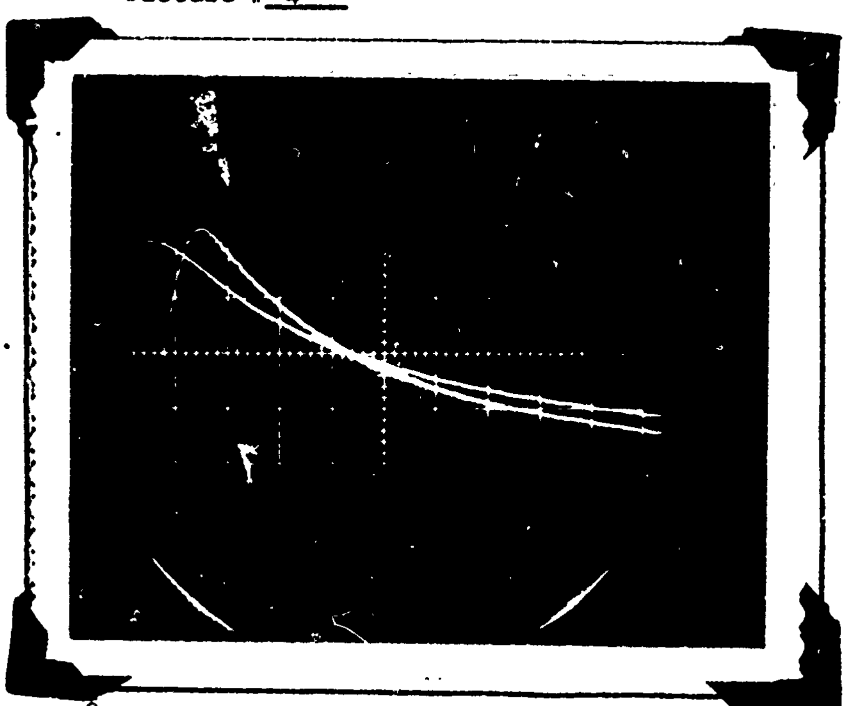

Capacitor Charging Voltages

Discharge	4000	V 4 f.
Filament	36	V .06f.
Magnet	0	V

Upper Trace

Signal	Voltage
Ampl/cm.	1000 Volts
Time/cm.	20 m.sec.

Lower Trace

Signal	Current
Ampl/cm.	40 m.a.
Time/cm.	20 m.sec.

10^9 OHMS ACROSS GRID-FILAMENT

Figure 15b. (Continued)

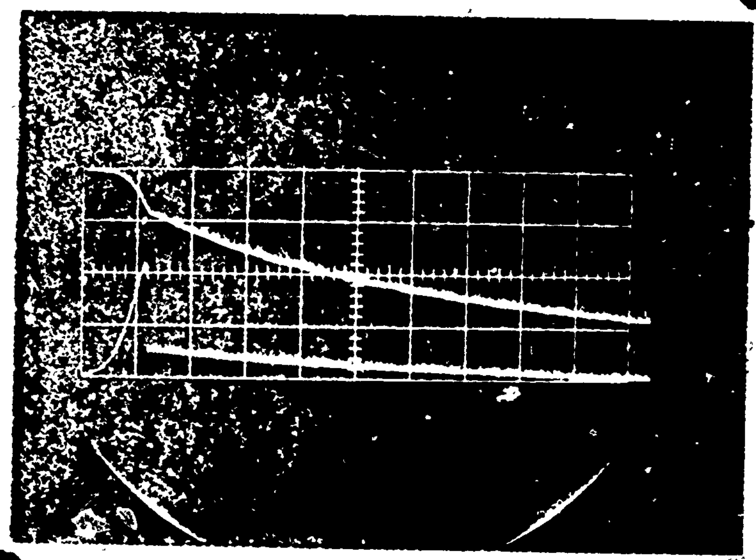

Signal Disch. Voltage
Ampl/cm 500 volts
Time/cm 20 m.sec.

Signal Disch.Current
Ampl/cm 100 m.a.
Time/cm 20 m.sec.

DISCHARGE IN GLASS TUBE

PRESSURE
5×10^{-7} Torr.

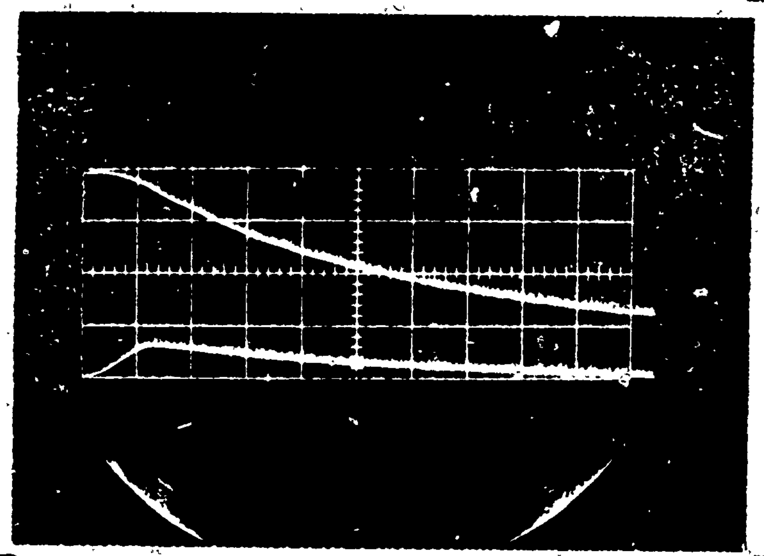

Signal Disch.Voltage
Ampl/cm 500 volts
Time/cm 20 m.sec.

Signal Disch.Current
Ampl/cm 100 m.a.
Time/cm 20 m. sec.

DISCHARGE IN GLASS TUBE 10^9 OHMS GRID-FIL.

Figure 16. Comparison of Discharge Characteristics with Different Grid to Cathode Resistances

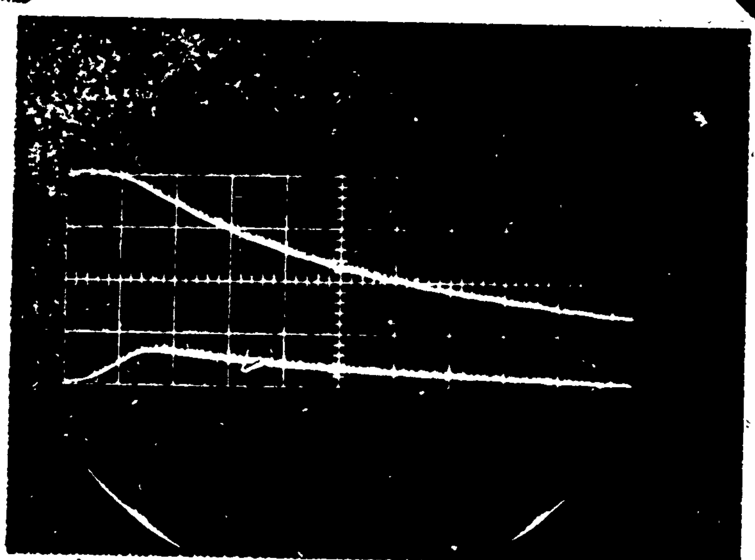

Signal Disch.Voltage
Ampl/cm 500 volts
Time cm 20 m.sec.

Signal Disch.Current
Ampl cm 100 m.a.
Time/cm 20 m.sec.

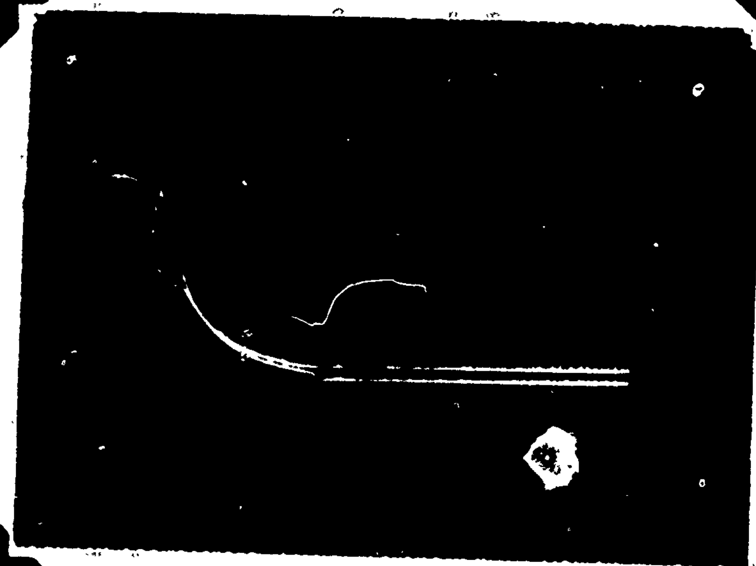

Signal Disch.Voltage
Ampl cm 500 volts
Time cm 20 m.sec.

Signal Disch.Current
Ampl/cm 100 m.a.
Time cm 20 m.sec.

DISCHARGE IN GLASS

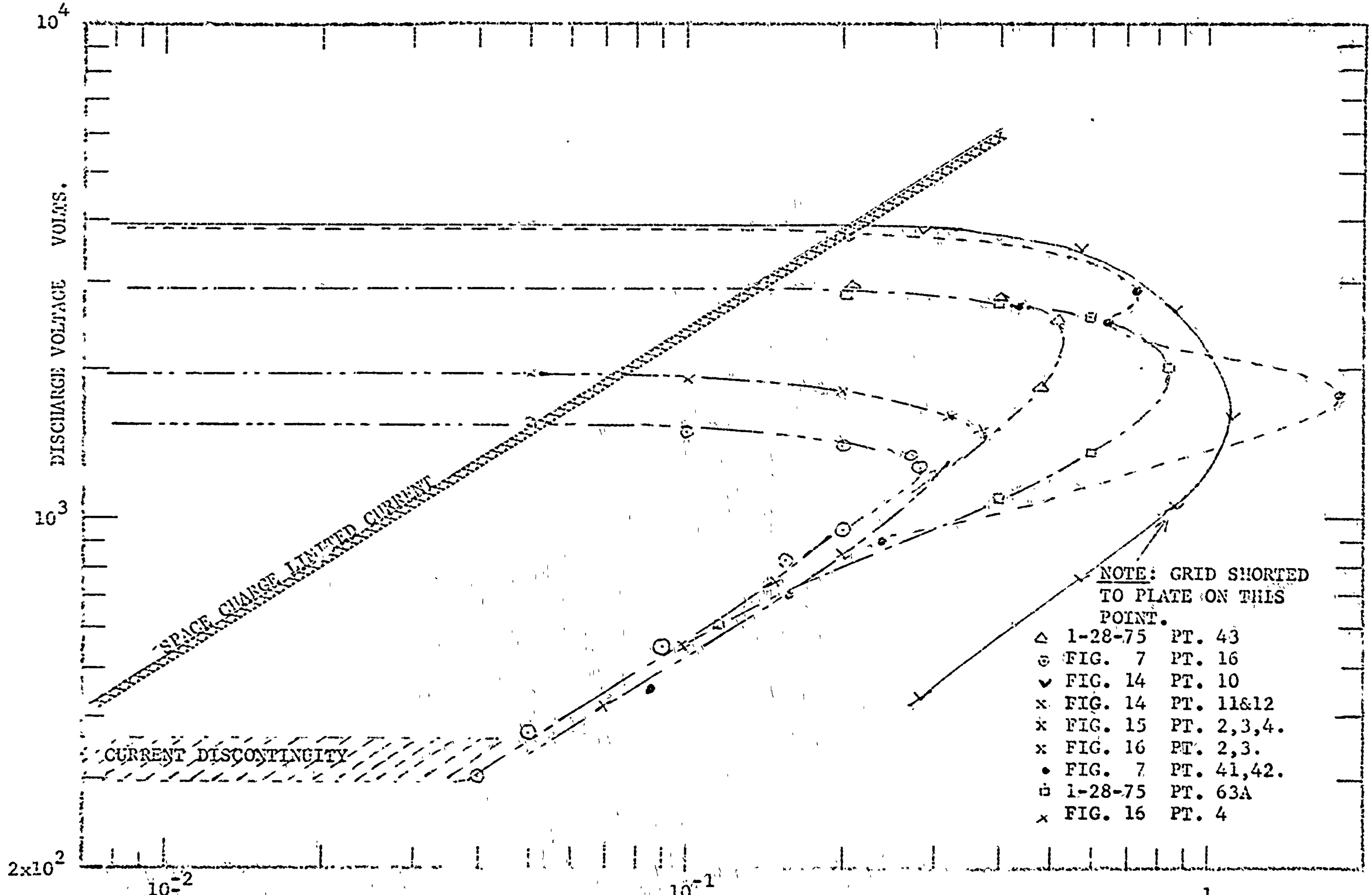

FIGURE 17. DISCHARGE CHARACTERISTICS - NO MAGNETIC FIELD

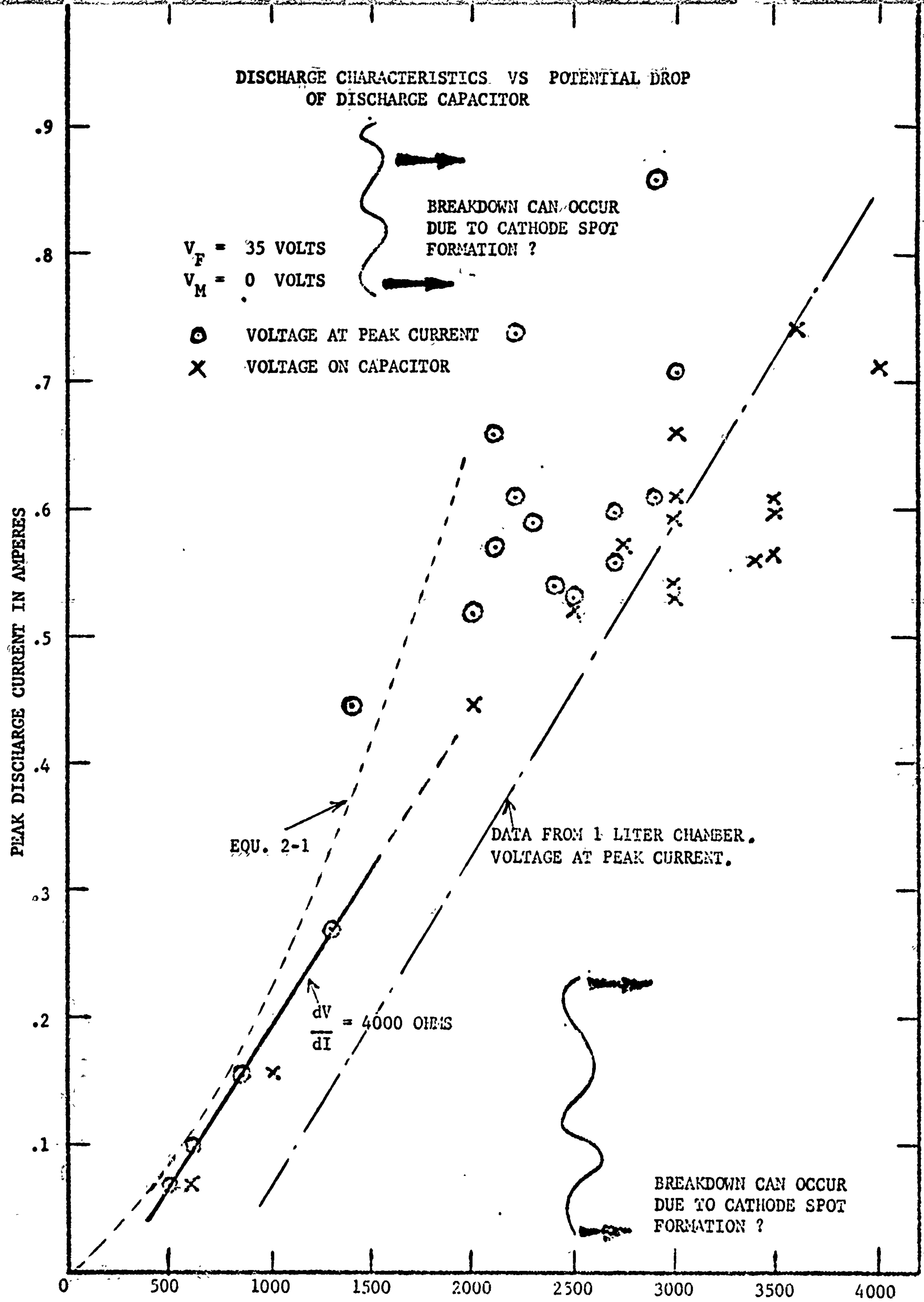

Figure 18. VOLTAGE ON DISCHARGE CAPACITOR IN VOLTS

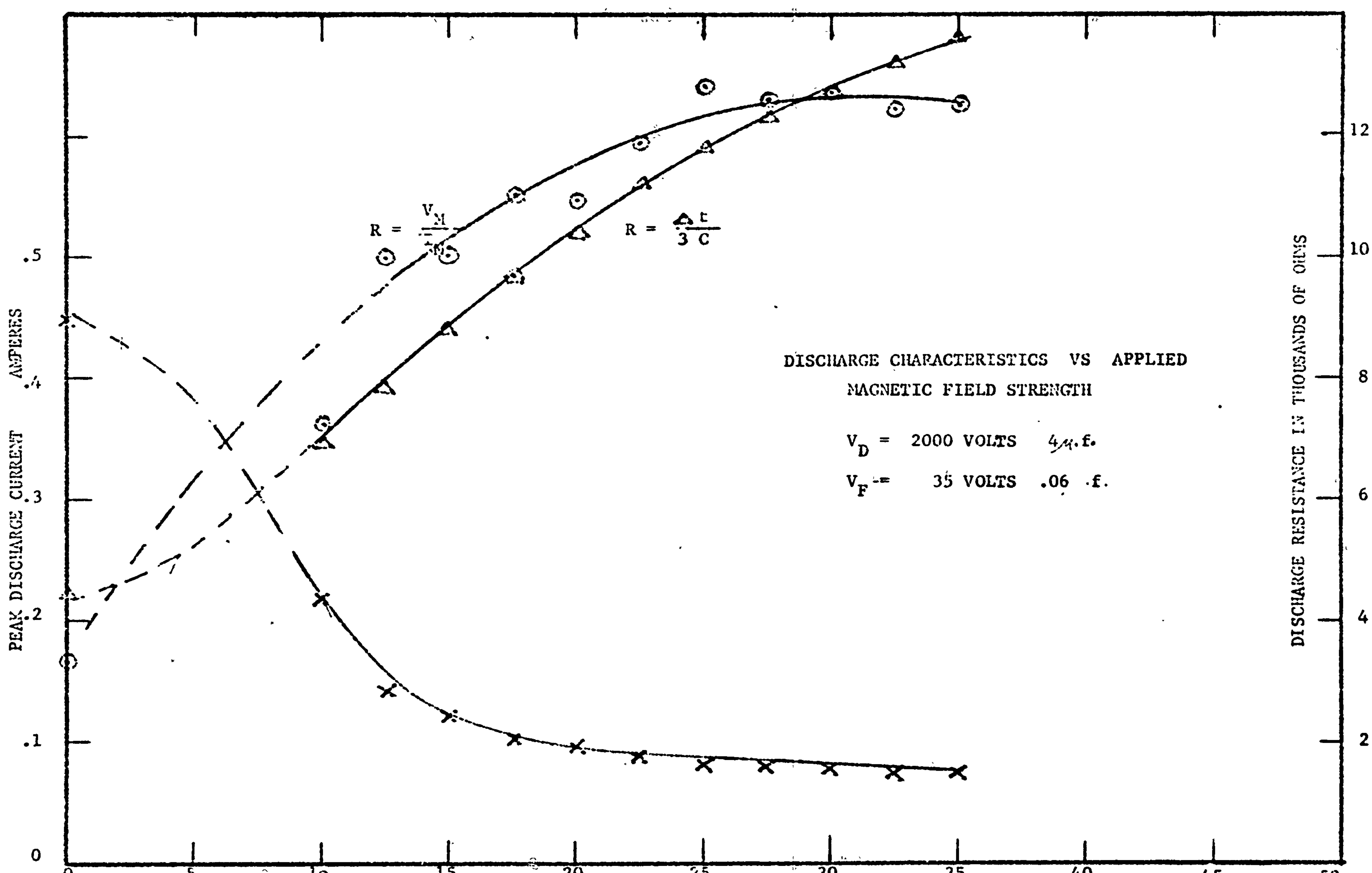

Figure 19. VOLTAGE ON MAGNETIC FIELD CAPACITOR

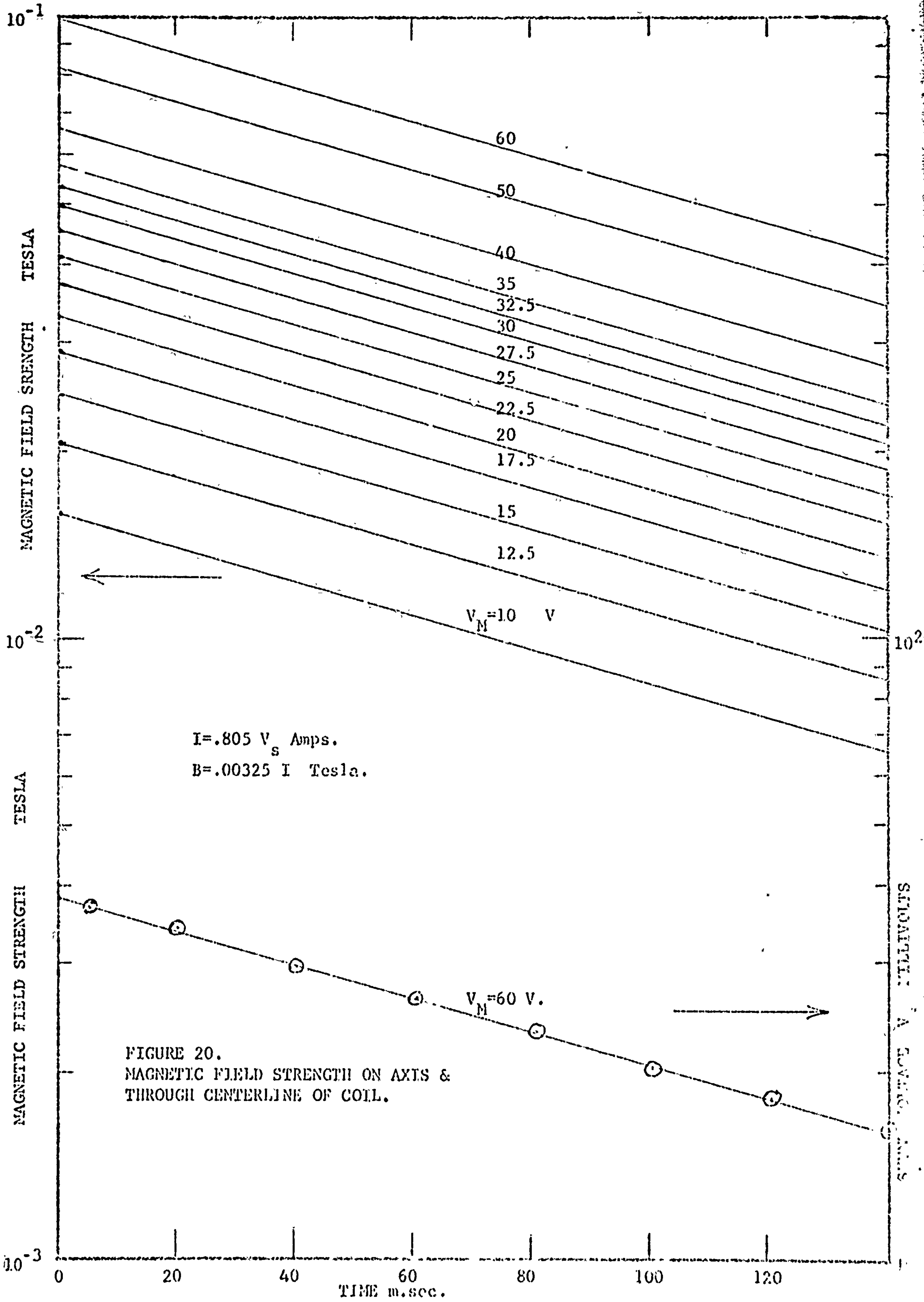

FIGURE 20.
MAGNETIC FIELD STRENGTH ON AXIS & THROUGH CENTERLINE OF COIL.

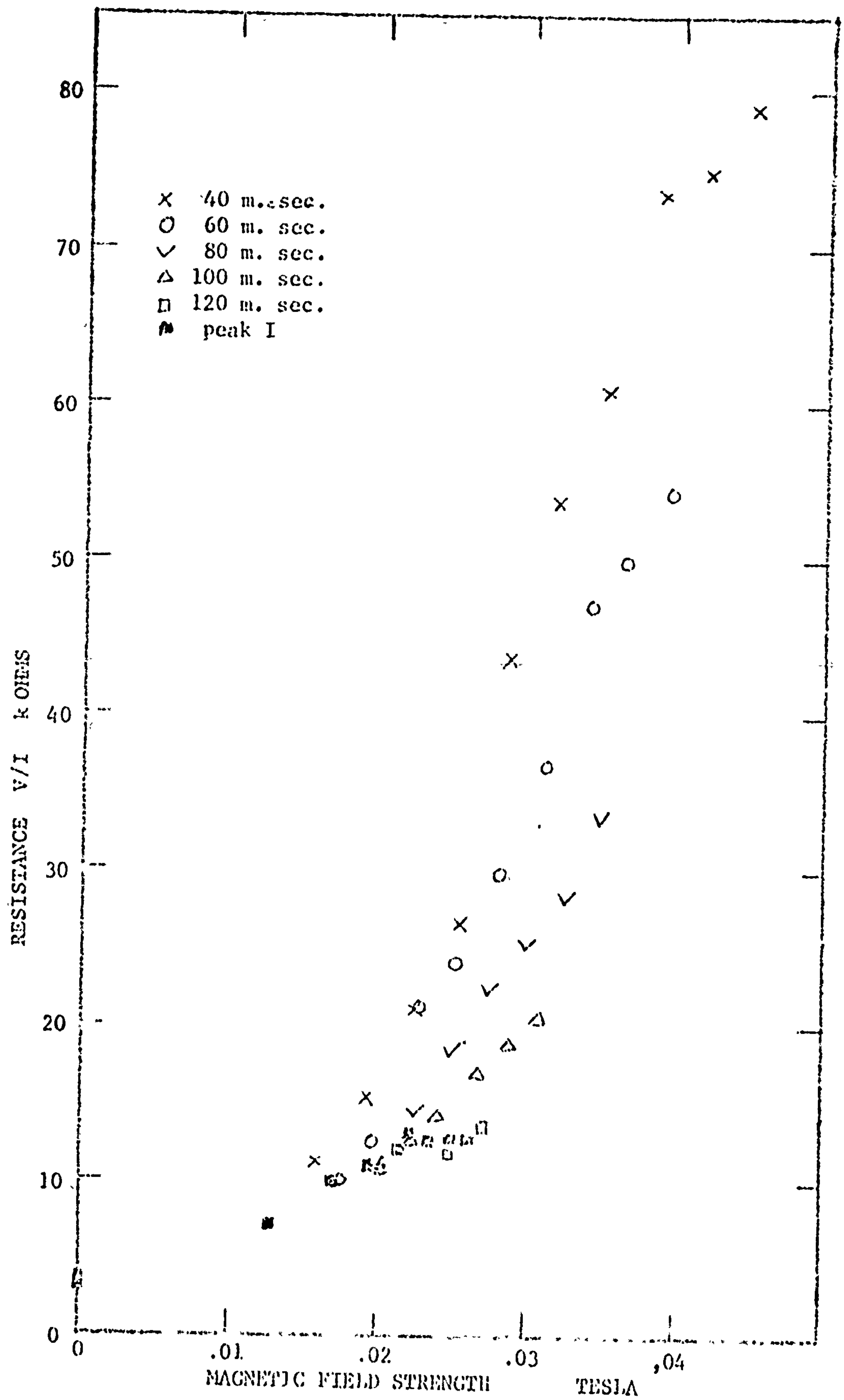

FIGURE 21. RESISTANCE OF DISCHARGE DURING CURRENT RISE.

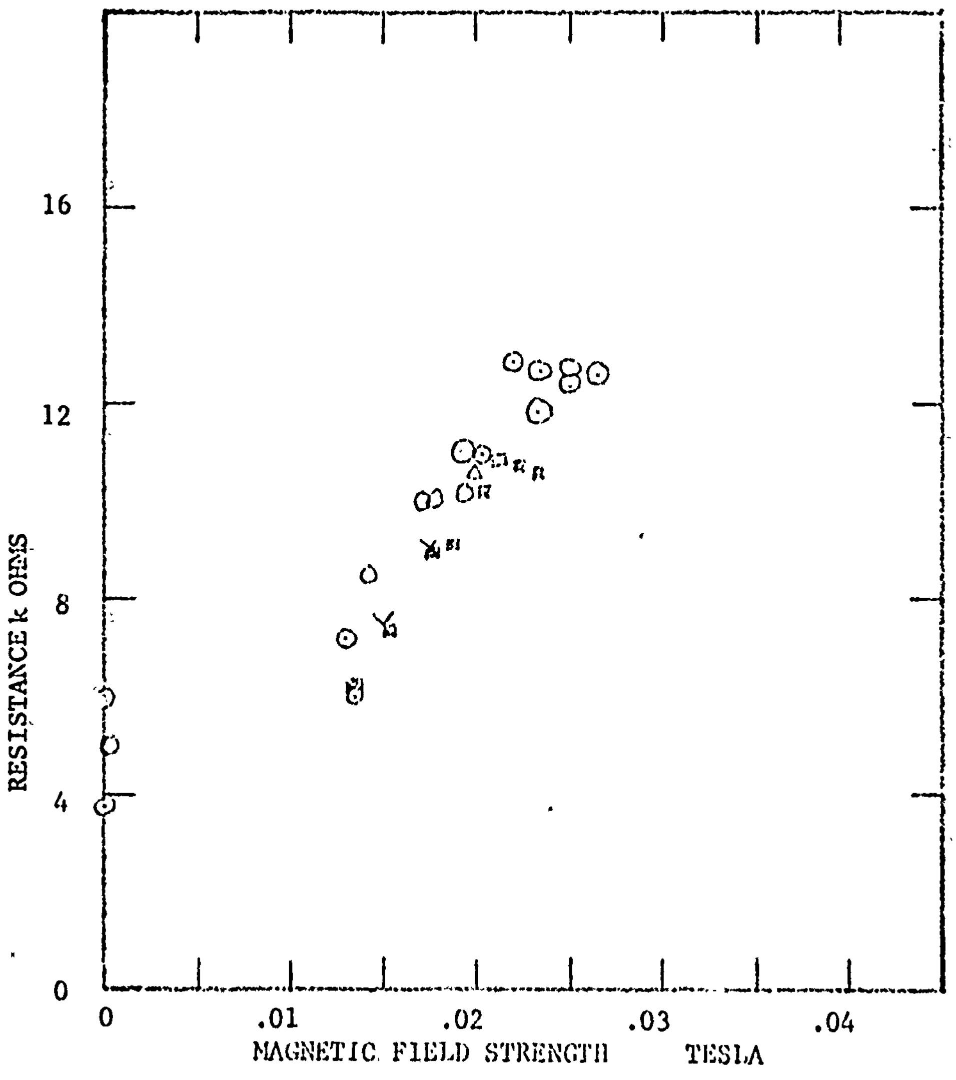

FIGURE 22. RESISTANCE OF DISCHARGE DURING CURRENT DECAY

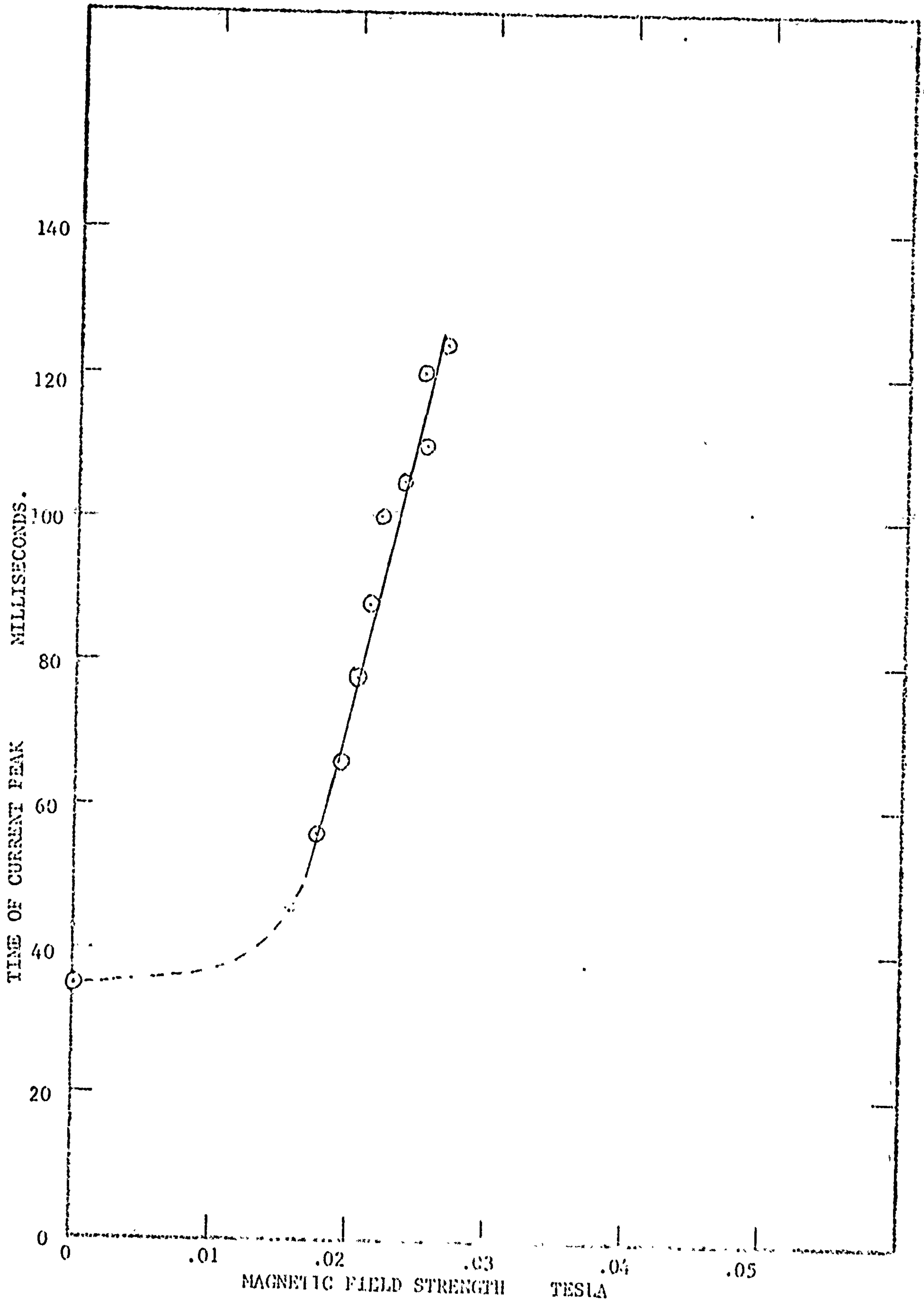

FIGURE 23. TIME OF PEAK DISCHARG CURRENT.

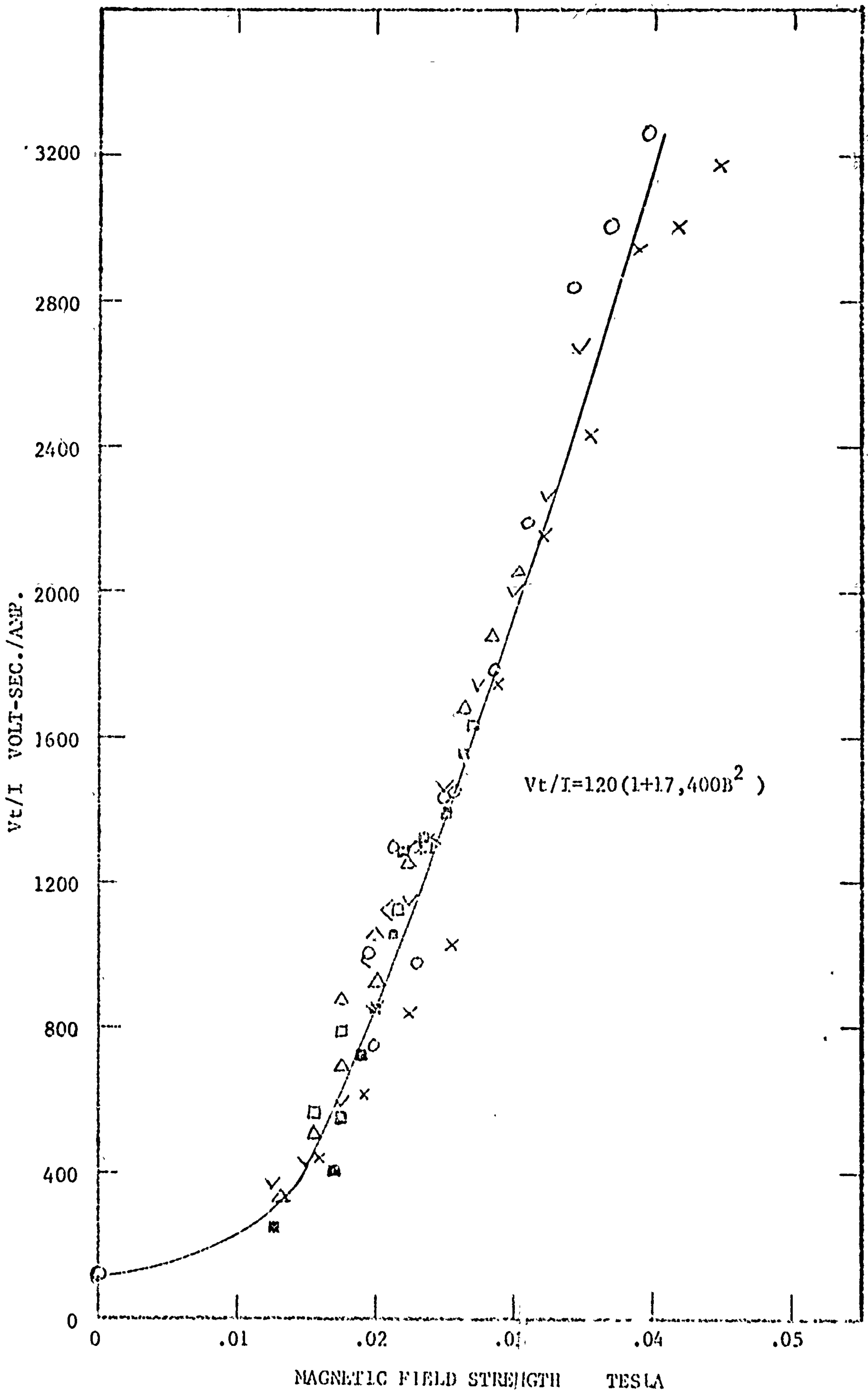

FIGURE 24. CORRELATION OF DISCHARGE CHARACTERISTICS-MAGNETIC FIELD

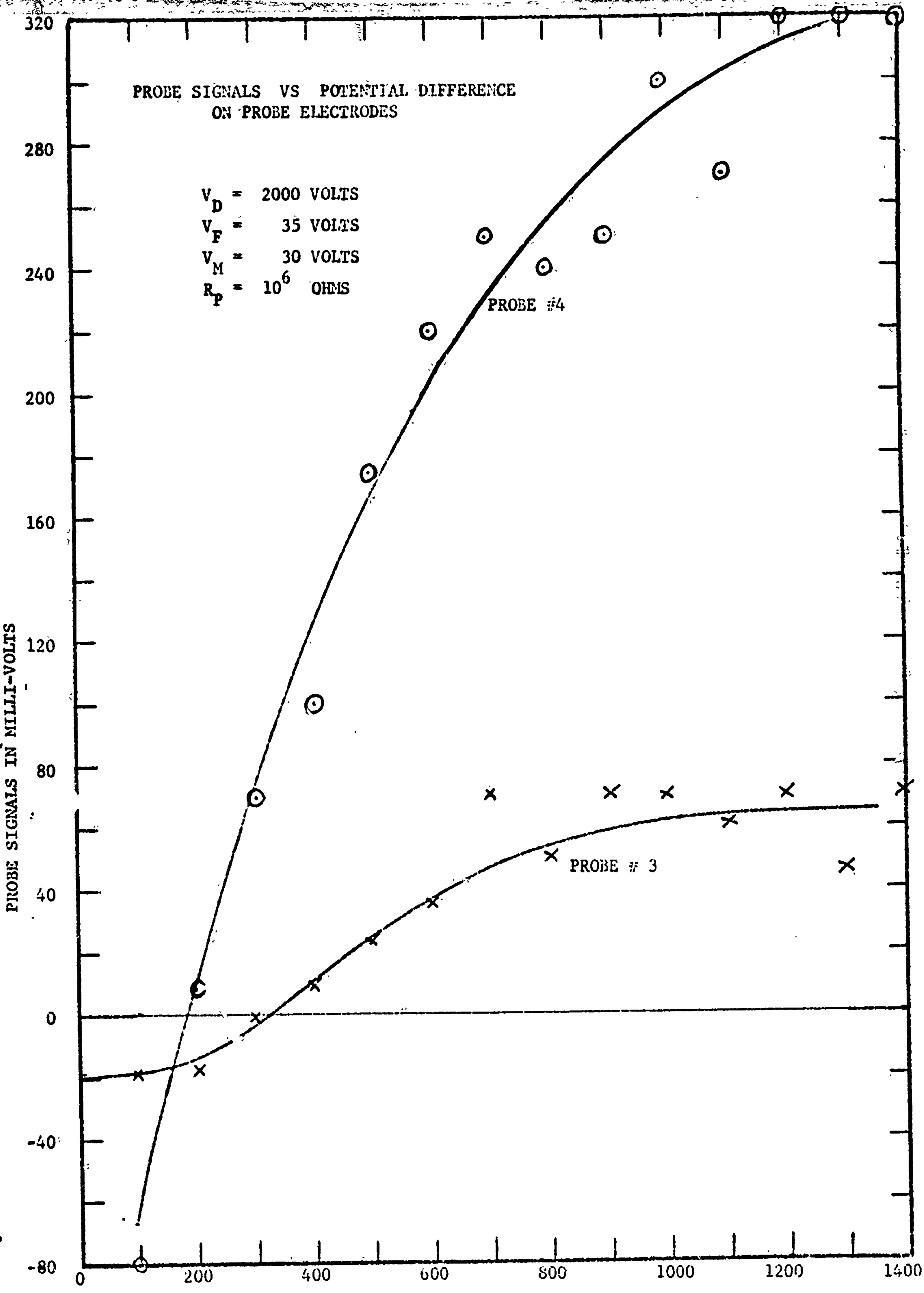

Figure 25. POTENTIAL ACROSS PROBE ELECTRODES VOLTS

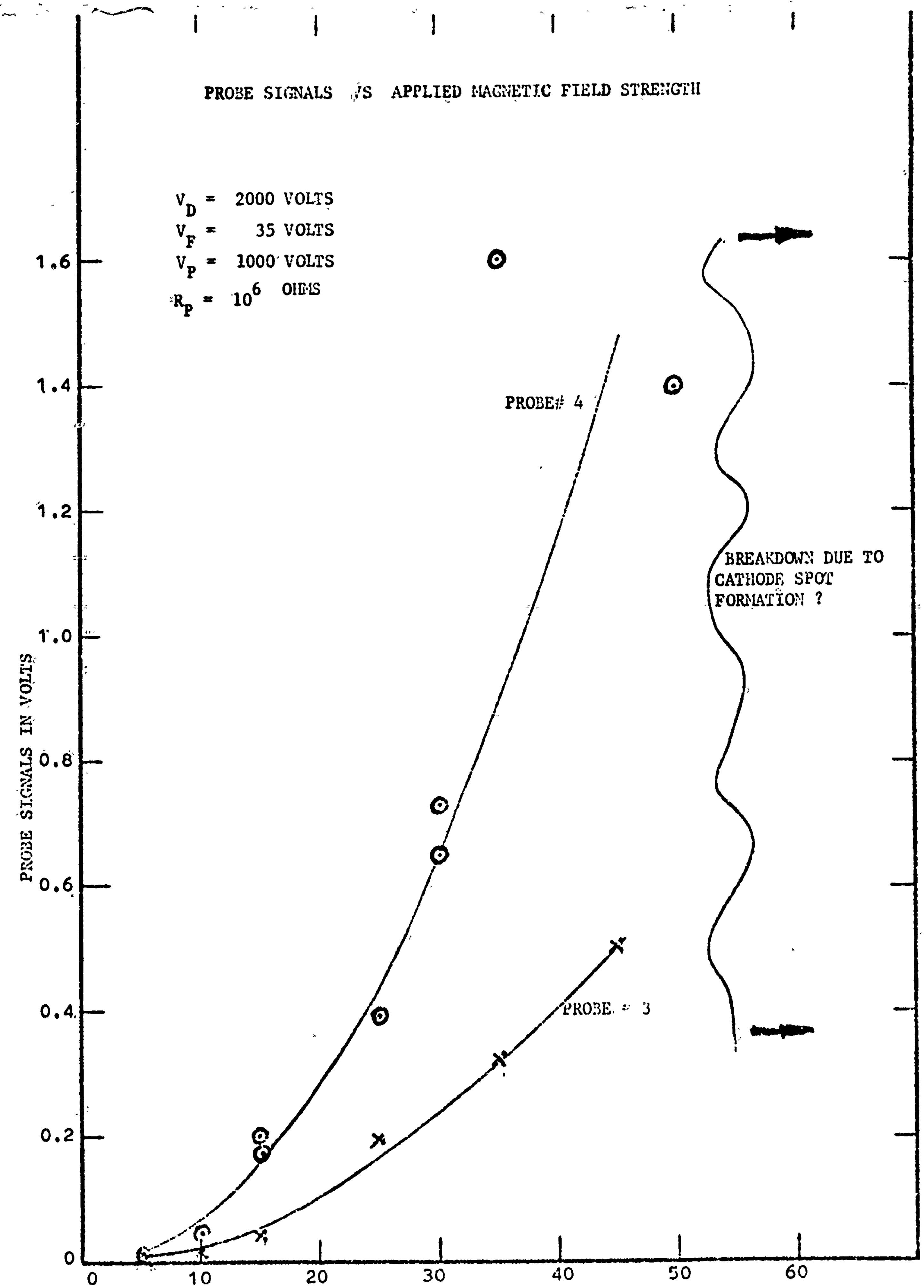

Figure 26. VOLTAGE ON MAGNETIC FIELD CAPACITOR

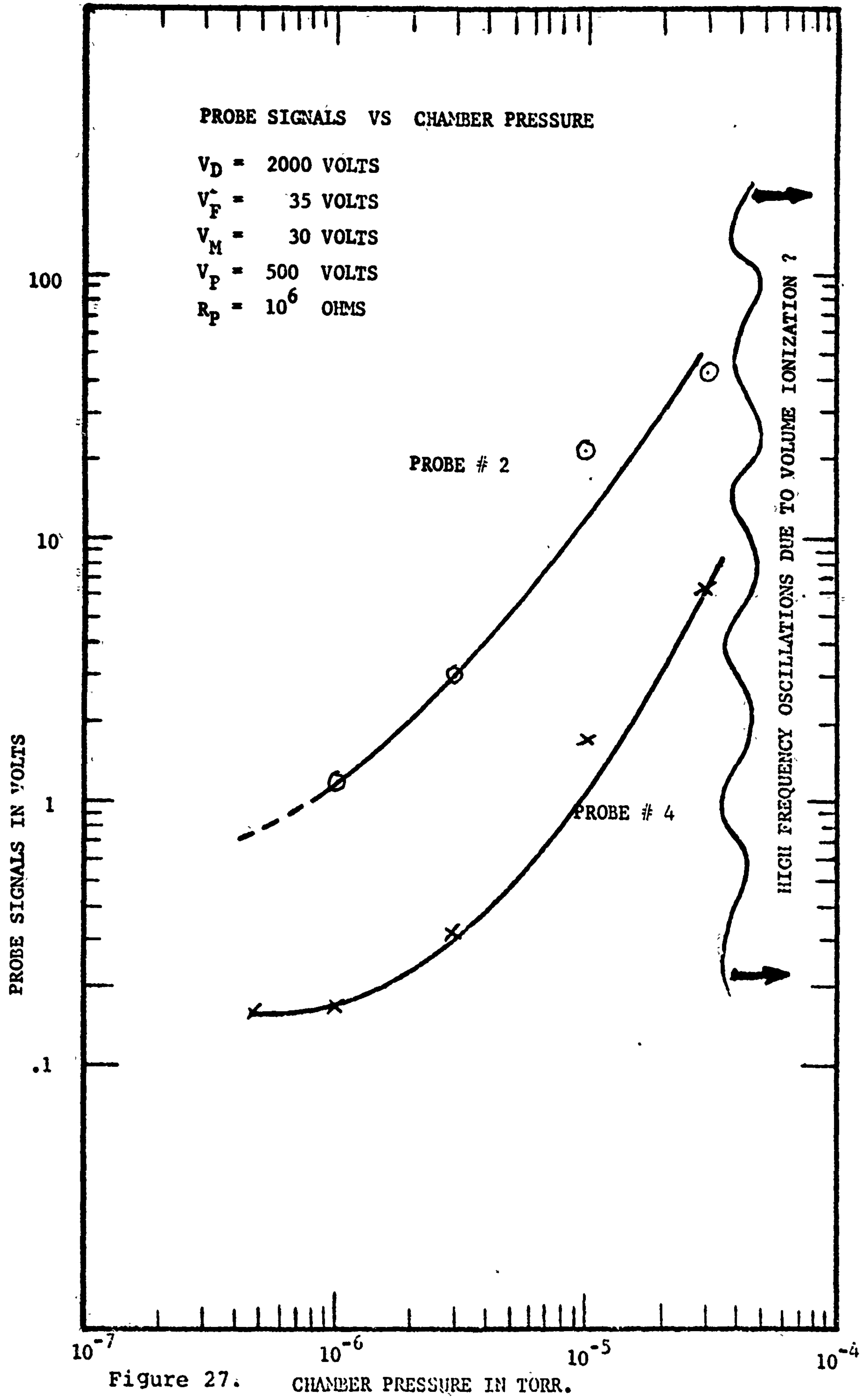

PROBE SIGNALS VS CHAMBER PRESSURE
V_D = 2000 VOLTS
V_F^- = 35 VOLTS
V_M = 30 VOLTS
V_P = 500 VOLTS
R_P = 10^6 OHMS
PROBE # 2
PROBE # 4
HIGH FREQUENCY OSCILLATIONS DUE TO VOLUME IONIZATION ?
PROBE SIGNALS IN VOLTS
100
10
1
.1
10^{-7}
10^{-6}
10^{-5}
10^{-4}
CHAMBER PRESSURE IN TORR.

Figure 27.

TABLE I

Chamber B was used

DESCRIPTION
SPACE SIMULATOR, SPACECRAFT TEST LABORATORY

General Dynamics Convair Aerospace Division
San Diego, California

Internal Dimensions	Chamber "A"	12 ft. diam, 19 ft. long horizontal cylinder.
	Chamber "B"	11 ft. diam, 22 ft. long horizontal cylinder.
Pumps		
Mechanical	3 to 6, 280 CFM each	
Diffusion	Chamber "A"	3-15,000 l/s, mercury diffusion
	Chamber "B"	2-95,000 l/s, oil diffusion
		1-9500 CFM, oil diffusion (booster)
Traps	Chamber "A"	-40°F freon plus LN_2 Chevron
	Chamber "B"	chilled H_2O manifold plus LN_2 Chevron
Net Speed (from chamber)	Chamber "A"	6000 l/s
	Chamber "B"	80,000 to 95,000 l/s
Chamber Air Conditioning	500 CFM, -10°F dewpoint, 60-70°F, absolute filters.	
Vacuum	Chamber "A"	1×10^{-5} Torr ultimate pressure
	Chamber "B"	$<1 \times 10^{-7}$ Torr ultimate pressure with cold wall

---

Data

A 200 guarded-channel data system is capable of recording on either or both punched tape and printed tape at 5 points per second. Computers and plotters are available for data reduction. Guarding and isolation of instrumentation provides high accuracy acquisition of millivolt signals from thermocouples, etc. 100 guarded copper constantan and an additional 100 copper wire passthroughs are available.

Thirty land lines to the Analog and Digital Computer Laboratories provide system control or additional data handling.

Location

General Dynamics Convair Aerospace, Spacecraft Test Laboratory, Bldg. 28, San Diego, California, Telephone 277-8900, Ext. 2221.